



**Energy Generation from Exhaust of an Engine and Simulation of Turbine using
CFD Analysis**

Roman Kalvin

**A Thesis Submitted in Fulfillment of the Requirements for the
Degree of Doctor of Philosophy in Energy Technology**

Prince of Songkla University

2021

Copyright of Prince of Songkla University

Thesis Title Energy generation from exhaust of an engine and simulation of turbine using CFD analysis

Author Mr. Roman Calvin

Major Program Energy Technology

Major Advisor

.....
 (Asst. Prof. Dr. Juntakan Taweekun)

Co-Advisor

.....
 (Dr. Kitinan Maliwan)

Examining Committee:

.....Chairperson
 (Prof. Madya Dr.Mohammad Kamil Bin Abdullah)

.....Committee
 (Asst.Prof. Dr.Juntakan Taweekun)

.....Committee
 (Dr. Kitinan Maliwan)

.....Committee
 (Dr.Somchai Saeung)

.....Committee
 (Dr.Thanansak Theppaya)

The Graduate School, Prince of Songkla University, has approved this thesis as fulfillment of the requirements for the Doctor of Philosophy Degree in Energy Technology

.....
 (Prof. Dr. Damrongsak Faroongsarng)
 Dean of Graduate School

This is to certify that the work here submitted is the result of the candidate's own investigations. Due acknowledgement has been made of any assistance received.

.....Signature
(Asst.Prof. Juntakan Taweekun)

Major Advisor

.....Signature
(Mr. Roman Kalvin)

Candidate

I hereby certify that this work has not been accepted in substance for any degree, and is not being currently submitted in candidature for any degree.

..... Signature

(Mr. Roman Kalvin)

Candidate

Thesis Title	Energy generation from exhaust of an engine and simulation of turbine using CFD analysis
Author	Mr. Roman Kalvin
Major Program	Energy Technology
Academic Year	2021

ABSTRACT

The aim of this research is modification of internal combustion engine for producing power from exhaust gases. Energy is extracted by placing turbine in exhaust gas passage. Two-third of the energy from combustion in a vehicle is lost as waste heat, out of which 40% is in the form of exhaust gases. Turbine was installed in the exhaust passage to generate power which would be utilized to run the electrical accessories of the engine. SOLIDWORKS were used for 3D CAD modeling and flow analysis of turbine with radial inlet-axial outlet. In addition to that ANSYS was used for stress-strain analysis. In addition, research has been carried out to check catalytic activity of catalysts made from salts/metal precursors; Cerium Sulphate Tetra hydrate, Manganese Sulphate Mono hydrate and Copper Sulphate Penta hydrate that are not expensive and could be replaced by the noble metals as they are very expensive and absolutely not abundant on Earth. Test sample catalysts were prepared through co-precipitation method having different molar concentration and then tested the conversion efficiency by applying the catalysts on ceramic plates by using Flue Gas Analyzer. On basis of results, final catalysts was prepared and applied on monolithic ceramic plate and then tested concerning the resulting conversion rate of pollutants as compared to already installed Catalytic Converter. During the experimentation work it was observed that base metals catalyst have low thermal stability at higher temperature and it adversely altered the performance of the catalyst greatly. Future study can be done to do research on increasing the thermal stability of catalysts with different molar ratios.

KEY WORDS: Catalytic Converter, Noble Metals, Flue Gas Analyzer, Pollutants, SOLIDWORKS, ANSYS

ACKNOWLEDGEMENTS

This research work was carried out at Faculty of Engineering, Prince of Songkla University, HatYai Campus. I also pay my gratitude to the Almighty for enabling me to complete this Research Report within due course of time.

I would like to express my sincere gratitude to Asst. Prof Juntakan Taweekun for her consistent guidance, support and patience in last three years. She always trusted and encouraged me during the ups and downs of my research duration. In addition, I spent three years of my PhD study in Energy Department of PSU where I performed core of my research work under the supervision of Asst. Prof Juntakan Taweekun. She has always believed in me, and has been boosting me during all research activities.

I want to pay special gratitude to Dr. Kittinan Maliwan for his continuous supporting my research.

I also want to pay special gratitude to Prof. Madya Dr.Mohammad Kamil Bin Abdullah for being external examiner in my thesis examination.

I would also like to thank my all colleagues and friends at PSU, especially Yosita. Who always supported me technically and morally on every step of my research.

At last, Words are very few to express enormous humble obligations to my affectionate Parents for their prayers and strong determination to enabling me to achieve this goal. Moreover, I am truly thankful to my wife without whom I couldn't complete my thesis.

Roman Kalvin

Contents

ABSTRACT.....	v
ACKNOWLEDGEMENTS.....	vi
CHAPTER 01	1
1.1. Introduction.....	1
1.2. Classification of Internal Combustion Engine (ICE).....	1
1.2.1. Reciprocating Engine.....	1
1.2.2. Rotary Engine	1
1.3. Problem Statement.....	1
1.4. Aims and Objectives	2
1.5. Scope of Research.....	2
1.6. Significance of Study.....	2
1.7. Motivation.....	3
Thesis Outline	3
CHAPTER 02	5
2.1. Literature Review.....	5
2.2. Heat Energy Analyzation	7
2.3. Review of Turbocharger	8
2.4. CFD Analysis of Turbo-charged Turbine	10
2.5. Recovery of Energy from Exhaust.....	14
2.6. Way to Reduce Toxic Gases and Catalytic Convertor.....	18
2.7. Research Gap.....	19
CHAPTER 03	20
3.1. Research Methodology	20
3.1.1. Fabrication of Engine Test Bench	20
3.1.2. Turbine Selection.....	20
3.1.3. 3D Modeling of Turbine.....	20
3.1.4. CFD Analysis of Turbine.....	20
3.1.5. Install Catalytic Converter with an Engine.....	20
3.1.6. Calculation of Emissions produce from Engine	20
3.2. Engine Specification and Fabrication of Test Bench.....	21
3.3. Solid Work Model of Test Frame	22
3.4. Dimension of the Test Frame.....	22
3.5. Material Properties.....	23
3.6. Stress Analysis of Frame	24
3.7. Displacement Analysis.....	24
3.8. Strain Analysis.....	25
3.9. Fabrication of Engine Test Bench.....	25
3.10. Coordinates Extraction, Modeling of Turbine	27
3.11. Mesh Independent Study.....	29
3.11.1. System specifications and Software.....	30
3.11.2. Boundry Conditions	30

3.12. Strain Analysis of Turbine	31
3.13. Stress Analysis of Turbine	31
3.14. Pressure and Velocity Contours of Turbine	32
CHAPTER 04	34
4.1. Results and Discussions	34
4.2. Power Generated from Turbine.....	34
4.3. Catalytic Converter:	34
4.4. Preparation of Sample Catalysts	36
4.5. Preparation of Test Samples	38
4.6. Testing and Analyzing	38
4.7. Preparation of new Catalytic Converter:.....	39
4.8. Infrared Spectroscopy of Synthesized Materials:	40
4.9. Final Testing and Comparison with Old installed Catalytic Converter	41
4.10. Conversion Comparison of Exhaust gases produced by both Catalytic Converter:	42
CHAPTER 05	44
5.1. Conclusions:.....	44
5.2. Future Recommendations	44
REFERENCES.....	45
APPENDICES	50
Vitae.....	90

List of Tables

3.1. Engine Specification.....	22
3.2. Material Properties.....	23
4.1. Turbine Speed.....	34
4.2. Power Generated from Turbine.....	35
4.3. Molar Ratios for Base Metals.....	36
4.4. Results without Catalytic Converter and with different Ratios of Materials.....	39
4.5. Ratios used in preparation of Catalytic Converter.....	39
4.6. Old Catalytic Converter Results.....	42
4.7. Upgraded Catalytic Converter Results.....	42

List of Figures

1.1. Energy Split in Gasoline Internal Combustion Engine	2
2.1. Vehicle Model developed for Volvo V-60	5
2.2. Pyrolysis Setup.....	6
2.3. Schematic Diagram of thermoelectric generator.....	8
2.4. Schematic Diagram of turbo-compounding.....	11
2.5. Typical diagram of turbocharger.....	15
2.6. Typical diagram of catalytic converter	18
3.1. Flow Chart of Research Methodology.....	21
3.2. 3D View of Test Frame.....	22
3.3. Dimensions of Test Frame	23
3.4. Stress Anlaysis of Frame	24
3.5. Displacement Analysis of Frame	24
3.6. Strain Analysis of Test Frame.....	25
3.7. Engine Frame.....	26
3.8. Engine mounted on Frame.....	26
3.9. Engine Test Bench with all Accessories.....	26
3.10. Turbine.....	27
3.11. Coordinatnes Extraction of Turbine by using CMM	27
3.12.. Dimension of Turbine	28
3.13. 2D and isometric views of Turbine.....	28
3.14. Import Turbine on ANSYS.....	29
3.15. Mesh Independent Study.....	29
3.16.. Meshing of Turbine and Shaft	30
3.17. Views of Turbine and Shaft	30
3.18. Strain Anlaysis of Turbine.....	31
3.19. Stress Analysis of Turbine.....	32
3.20. Pressure Contours of Turbine	32
3.21. Velocity Contours of Turbine	33
4.1. Power Generated from Turbine.....	36
4.2. Metal Weight on Electronic Balance	37
4.3. Metal Salts Solution.....	37
4.4. Comparison of Conversion of all Pollutants by each Cataysts	39
4.5. Spectroscopy of Cerium Sulphate Tetra hydrate	40
4.6. Spectroscopy of Manganese Sulphate Monohydrate	41
4.7. Spectroscopy of Copper Sulphate Pentahydrate	41
4.8. Conversion rate of both Catalytic Converter	42

List of Abbreviation

ICE	Internal Combustion Engines
SI	Spark Ignition Engines
CI	Compression Ignition Engines
EGR	Exhaust Gas Recirculation
HC	Hydrocarbons
NO	Nitric Oxide
CO	Carbon Monoxide
CMM	Coordinate Measuring Machine
Mn	Manganese
Cu	Copper
Ce	Cerium
FTIR	Fourier Transform Infrared Spectroscopy
U_{in}	Velocity at inlet
T_i	Inlet Temperature of exhaust gases.

List of Published Papers

1. Roman Kalvin, Juntakan Taweekun, Kittinan Maliwan and Hafiz Muhammad Ali (2021). “Fabrication of Catalytic Converter with Different Materials and Comparison with Existing Materials in Addition to Analysis of Turbine Installed at the Exhaust of 4 Stroke SI Engine”. *Sustainability*.2021;13(18):10470. <https://doi.org/10.3390/su131810470>. IF 3.25
2. Roman Kalvin, Juntakan Taweekun, Muhammad Waqas Mustafa, Saba Arif and Abdullah Javed (2021).“Investigation of Chip Formation and its Grain Structure using Vegetable Oil Based Lubricants”. *Journal of Advanced Research in Fluid Mechanics and Thermal Sciences*, 84(2), 92–97.
3. Roman Kalvin, Juntakan Taweekun, Muhammad Waqas Mustafa, Faisal Ishfaq and Saba Arif. “Design and Fabrication of Under Water Remotely Operated Vehicle”. *Journal of Advanced Research in Fluid Mechanics and Thermal Sciences*, 82(1), 133–144 -2021.
4. Roman Kalvin, Juntakan Taweekun, Kittinan Maliwan“ Investigation of Dissimilar V-Joint of Steel Alloys with Copper and Brass using Tig Welding” *International Journal of Mechanical and Production Engineering*, ISSN(p): 2320-2092, ISSN(e): 2321-2071 Volume- 8, Issue-8, Aug.-2020

CHAPTER 01

1.1. Introduction

An internal combustion engine (ICE) is a heat engine in which the burning of a fuel mix with air in a combustion chamber. In an internal combustion engine, due to the expansion of hot gases at high temperature and high pressure produced in the chamber, force is directly applied on pistons. This force further moves the component which transforms the heat or chemical energy into mechanical energy. In an IC Engine, exhaust gas recirculation (EGR) is a Nitrogen Oxide emissions reduction technique used in gasoline and diesel engines. EGR works by recirculating a portion of an engine's exhaust gas back to cylinders. Internal combustion engines are further differentiated in two ways:

- Spark-ignition (SI) Engine: Spark plug is used to initiate the combustion.
- Compression-ignition (CI) engine: Air is compressed in the cylinder, heating it, so that the heated air ignites fuel that is injected in.

1.2. Classification of Internal Combustion Engine (ICE)

1.2.1. Reciprocating Engine

A reciprocating engine is a type of engine that uses reciprocating pistons to convert pressure into a rotating motion. In reciprocating engine, the combustion of fuel takes place inside the cylinder and such engines are called as Internal Combustion Engine. These are mostly used in motor vehicles such as diesel, petrol or gas engines.

1.2.2. Rotary Engine

A rotary engine is usually designed in radial configuration with an odd number of cylinders per row. It is designed in a way in which the crankshaft remains stationary during the work with the entire crankcase and its attached cylinders rotating around it as a unit.

1.3. Problem Statement

Two-thirds of the energy from combustion in a vehicle is lost as waste heat, of which 40% is in the form of hot exhaust gases which is also the reason for environmental pollution. Energy Split in Gasoline Internal Combustion Engine is shown in figure 1.1.

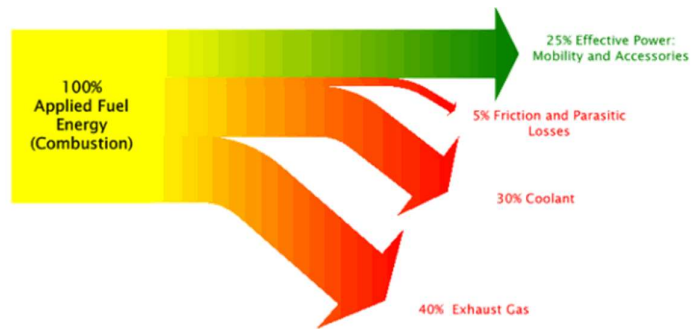


Figure 1.1: Energy Split in Gasoline Internal Combustion Engine (www.ecomodder.com)

1.4. Aims and Objectives

- Selection of an engine
- Selection of turbine
- To take coordinates of turbine using coordinate measuring machine.
- Stress-strain analysis of turbine
- Mathematical calculation of power generation from turbine
- To fabricate cost effective catalytic converter
- To compare efficiency and cost of old and upgraded catalytic converter,

1.5. Scope of Research

The main focus of this research is modification of internal combustion engine for producing power from exhaust gases. Energy is extracted by placing turbine in exhaust gas passage. Two-third of the energy from combustion in a vehicle is lost as waste heat, of which 40% is in the form of exhaust gases. Exhaust from an engine is used to generate electricity and can be stored in battery after rectification for later consumption in various utilities. First of all the complete exhaust system is studied to understand various parameters affecting the design of turbine. SOLIDWORKS were used for 3D CAD modeling and flow analysis of test bench of engine and turbine. In addition to that ANSYS was used for stress-strain analysis. In addition new catalysts material are studied in order to fabricate cost effective catalytic converter.

1.6. Significance of Study

Power Generation from Exhaust Gases of an IC Engine is a process of production of energy using the gases coming out of the engine outlet. Engine converts chemical energy into mechanical energy and waste is extracted in the form of exhaust gases from the engine which further moves towards the tail pipe of an engine. These gases move at high temperature and pressure towards the outlet. The turbine is placed in the pathway of these exhaust gases which is designed in a way that these exhaust gases tends to rotate the blades of turbine. So, depending upon the airflow coming out of the

exhaust, turbine will start rotating with a specific amount of speed. The turbine is connected to the dynamo with a shaft and dynamo produces power with it. A dynamo is a device which converts kinetic energy into electrical energy. Further this generated power is stored in the battery for further utilization.

1.7. Motivation

With the growing development in scientific field and public awareness on environmental and energy issues, it has urge people to search more around themselves for betterment and many developments are being made on high scale specially developing an efficient internal combustion engine. The level of energy consumption depends upon development and with the growing rate of population; energy demand is increasing with the time. So, to overcome those needs, many reforms are being made in the field of technology and power sectors. A heat engine is a system that performs the conversion of heat or thermal energy to mechanical work, for example the diesel engine, and the gasoline engine in an automobile. The efficiency of an IC Engine is calculated nearly equal to 35-40% in highly modified engines mostly used in sports cars. The energy in the form of heat is rejected from the exhaust. This energy can be further useful for producing power and can lead to help in the ever energy demands and economic issues. Moreover to reduce emission produced from the exhaust of an engine, cost effective catalytic convertor may be used.

1.8. Equipment Components

- Turbine
- Petrol engine
- Rechargeable DC battery
- Dynamometer
- Generator
- Engine foundation

Thesis Outline

The solution to these research questions was obtained through a procedure, which is described in following chapters;

- *Chapter 2* is all about the overview of literature and from there research gap is identified.
- *Chapter 3* describes the implementation of engine on test bench. Firstly test bench is designed and fabricated after that engine along with accessories mounted on the test bench. Moreover it also includes information about all the selection of turbine, its coordinate's extraction by using coordinate measuring machine (CMM), stress-strain analysis of turbine.

- *Chapter 4* consists of mathematical calculation of power generated from turbine. Moreover it comprises on designing a catalytic converter with new materials which are cost effective, their preparation, testing by using flue gas analyzer. Moreover infrared spectroscopy of new catalysts to check their material characterization.

- *Chapter 5* is the chapter with the conclusions and future recommendations.

CHAPTER 02

2.1. Literature Review

Antonio Garcia et al. [1] examined the emissions and performance of the series hybrid vehicle which is powered by the partially gasoline premixed with the internal combustion of engine in 2019. This work explored the execution of two vehicles adjusted to an arrangement crossover power train idea furnished with the four chamber motor working on gas ignition mode. The multi-target Pareto streamlining process was completed to decide the quantity of internal combustion engine working terms and the conditions and particular estimations of motor speed and the brake mean effective pressure to limit both the fuel utilization and NO_x outflows. From the examination, it was discovered that the quantity of internal combustion engine working focuses expected to charge batteries subject to the vehicle. The investigation of the immediate fuel utilization follows permitted to confirm the capability of hybridization in the urban rush hour gridlock terms. In such terms, regenerative braking and the low control demand results in the higher vitality investment funds. In expansion, the distinction of demonstrating that vehicle speed assumes a central job on cross breed execution. At last, the last driving cycle test results empowered the immediate examination versus the qualities got with diesel business vehicles. By and large, both the PPC half breed power-trains had the capacity to achieve comparable fuel utilization esteems amidst the range to these gotten by diesel business vehicles of percentage (22%- 7%). In these sense, it was normal that the fuel utilization advantages can be improved later on by enhancing the PPC burning maps. With respect to motor out emanations, while ash and the CO had the capacity to satisfy their standardizing limits for practically all terms. This outcomes demonstrate the possibility to limit the after treatment necessity versus a traditional diesel vehicle, turned out to be an option to the customary power-trains empowering the decrease of the tailpipe outflows esteems without pushing the execution and CO₂ esteems as shown in Figure 2.1.

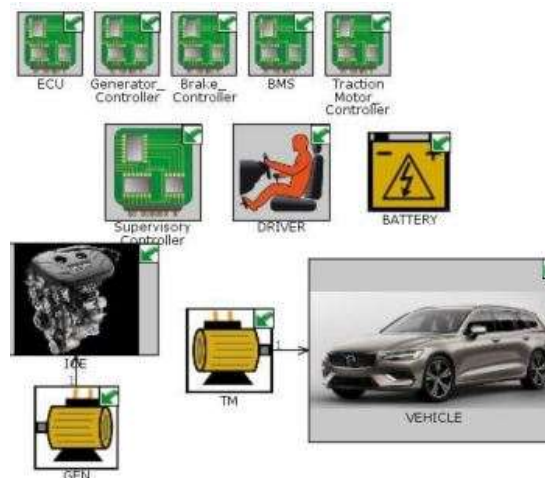


Figure 2.1: Vehicle Model Developed for Volvo V-60 (Garcia et al.,2019)

Jianbing Gao et al. [2] analyzed the flow of energy in the engine of a heavy vehicle which is turbocharged in 2019. Brake warm performance or efficiency of diesel motor was over 33 percent at lion's share of motor task conditions and terms, with the most esteem which had been more than the 38 percent. So the coolant vitality extended from the 30kW– 190kW, and the base rate was over 26% of the absolute fuel synthetic vitality, likewise, the most extreme esteem was ~66%. The possibilities of coolant vitality reusing were promising, in spite of the fact that the vitality grade level was low, if phenomenal warm administration strategies were utilized. Fumes vitality devoured by the turbine was in the scope of 1.6%– 10.4%, which changed the fumes vitality dispersions; in the interim, the progressions were significant when the motor burdens were littler than half. The propensity of the form lines of vitality conveyances were comparative for blower and intercooler, coming about because of the way that higher vitality utilization by blower would prompted higher warmth misfortune by intercooler. The reused fumes vitality in the end flowing into the motor barrels was in the scope of 1%– 3% because of much warmth misfortune in the intercooler.

In 2019, the analysis of waste engine based oil in the process of CRDI diesel engine is done by Ramanathan et al [3]. The commonly thermo chemical change forms utilized for vitality recuperation is burning, pyrolysis, gasification. Cremation causes dangerous and ozone harming substance emanations that represent an immediate peril to wellbeing of human and adds to the environmental change, mostly because of undesirable agents occurs in the waste and gases produced from the gasification or burning process (for example, polychlorinated dibenzodioxins (PCBs) and fly fiery debris) shown in figure 2.2.

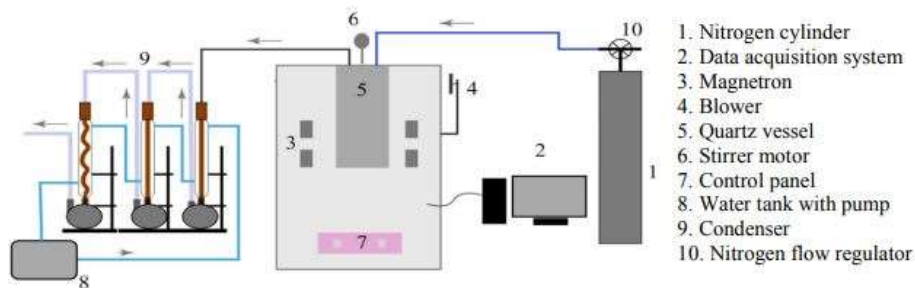


Figure 2.2: Pyrolysis Setup (Ramanathan et al., 2019)

Pyrolysis is known thermo chemical change process which has created to change over the waste material into diesel-like fuel and other progressively profitable substance stocks. Higher living arrangement timings and moderate level of warming rate leads to increment the burn yield normal amounts of side-effects, while habitation times and higher warming rates advance the arrangement of fluid or vaporous items. In this manner, the pyrolysis forms depend on two extraordinary ideas: 'quick' pyrolysis and 'moderate' pyrolysis. Instruments are being utilized for the quick warming process by the microwave and electrical changing. In this type of instrument

and the microwave frames and requires a particular method for warming where it can be seen that waves of electromagnetic process occurs.

2.2. Heat Energy Analyzation

Safarudin Gazali Herawan et al. [4] predicted the heat energy from exhaust gases of internal combustion engine by using the artificial neural network in 2018. As the waste warmth from fumes gases produce a lot of warmth vitality, which has for the most part been executed for joined power and warming uses. The paper portrays the warmth vitality from a normally suctioned inner burning motor in a vehicle. From exhaust fumes, which the heat vitality could be created, is introduced and recommended that heat vitality could altogether upgrade the effectiveness execution by recuperating the vitality. This idea is thermodynamically doable and relying upon the heap connected to the motor. In view of the outcomes, this was discovered that waste warmth vitality was 23 kW. Henceforth, to gather these fumes squander heat vitality was a commendable exertion and fake neural system forecast show is created to give sensibly great concurrence with deliberate data. The squander heat vitality could have reached to 23 kW, along these lines it was worth to recoup this waste warmth vitality from exhaust fumes framework. Henceforth, to collect this fumes squander heat vitality is a commendable exertion. Squander heat recuperation can be collected utilizing natural rankine cycle, thermoelectric, retention refrigeration, or something bad might happen.

Kate Thompson and Anna cooper [5] in December 2018, worked on the diesel engine for removing the pollutants such as NO_x or the other soot particles by using the utilization of catalytic with the help of oxidation. NO₂ has the capability to oxidize the amount of carbon that has been misused in the explosives, fireworks for a considerable length of time and, all the more as of late, in constantly recovering sediment channels fitted on hard core diesel vehicles. It additionally identifies potential for oxidizing ash at lower fumes temperature, Paradoxically, N₂O is known to be put away via carbon, yet isn't prestigious as an oxidizing agent for residue at the scope of 400– 950 °C of temperature. Outcomes demonstrate that, in spite of the high liking among residue and N₂O, an impetus is used and requires for the main response in between the basic carbon and N₂O to happen underneath 400 °C of temperature. A silver definition, it is observed that for the sediment burning, before head appears to be viable and it can be seen for sediment oxidation process by using the C+N₂O response. It can be seen that oxidation of the ash explicitly happens amid the in-situ development of N₂O by the silver impetus, amid non-specific decrease of NO_x by response with NH₃, recommending surface N₂O is responsive oxidizing agent.

In 2018 Dipak S.Patil et al. [6] created control from thermo electric generator and semi transmitter utilizing audit investigation. In present investigation, it can be seen that there is a criteria for study of the heat exchangers and thermoelectric materials with the structures in the interior. Power can be generated by using thermoelectric generator and the semiconductors. For the Reasonable usage of TEG, most highly Intense doped semiconductors shows high heat obstruction and very

minimum amount of electric opposition properties. It is very difficult for any thermoelectric generator for the assumption of waste heat exchanger. Essential heat is given by the heat exchangers to the thermoelectric based generators and also their ability and transformation proficiency rely upon the material of heat exchanger, its shape, and kind of the heat exchanger. By using different types of supplements, there can be an up gradation in the heat exchange rate and consistency of the heat exchanger. Blade structure, the main setup of heat exchanger and many other working conditions can also upgrade the heat exchange rate. Exhaust of the engine moves into the heat exchanger in the result of which there is a drop in the weight. So, it is very useful to check and assess weight drop dimension of the diverse structures as shown in figure 2.3.

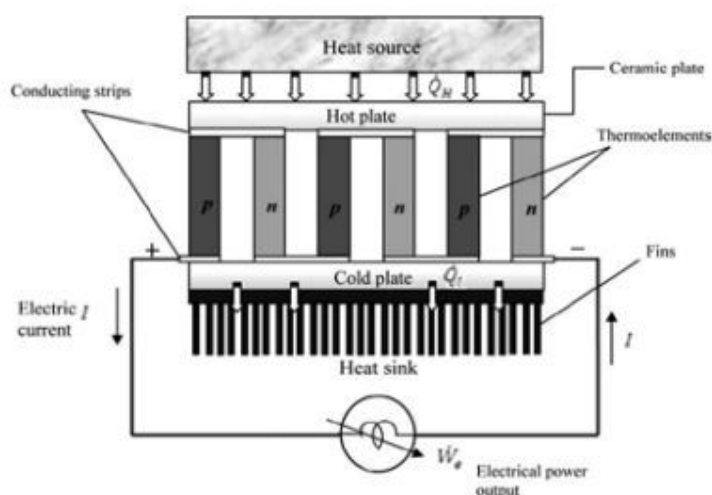


Figure 2.3: Schematic Diagram of thermoelectric power generator (Basel et al. 2009)

2.3. Review of Turbocharger

Working of air-brayton cycle and low-pressure turbine and also the working of turbo compounding as heat recovery method had done by M.Yang et al. [7] in 2018. This paper exhibits an evenhanded examination of waste heat recovery strategy on an internal ignition engine utilizing turbine of low pressure and also the air-brayton cycle. 6.8 L, seven barrels turbocharged diesel engine is utilized for contextual analysis. Recovery strategies related to the system were recreated on AVL system in which the test information is verified by using the engine model and heat exchanger. It is discovered that the every one of the three strategies can't work adequately without decreasing the turbine size to intensify the blower power. It can be finished by utilizing turbocharger region over sweep proportion financially accessible, thereupon guaranteeing the least conceivable motor equipment changing. In this case, the engine is guaranteed to convey benchmark brake control. It can be seen in the paper that lower pressure turbine can recover the most waste heat. In current paper, three fumes squander heat recuperation techniques that are appropriate for versatile motor application, low-weight turbine and Brayton cycle system are examined. So as to give an examination premise, the engine arrangements for every one of the three recovery techniques are kept indistinguishable. The examination starts by approving

the gauge regular suctioned engine model or the turbo charger execution for model info, and HEX model.

Andrew Royale [8] investigated the combustion of engine and thermal energy recovery systems in 2017. In this paper work, the alteration is done for diesel engine which is stationary for delivering the power by utilizing the turbine. These days in vehicle field numerous new advancing ideas has been created. We are utilizing basic power from vehicle exhaust which creates the power and could be put away in the battery for later utilization. In the paper, showing an idea of producing the power and the stationary single chamber diesel motor by use of turbines. So, putted a turbine in the way of exhaust gases through silencer. So, the turbine which is associated with the dynamo is used for creating power. As the exhaust gases hit the turbine, it starts rotating as the result of which dynamo would also continue to revolve. Actually, dynamo is a device which is used to create electrical energy. The produced power is transferred away to battery. This tends to be put away in battery for the rectification because it cannot be put directly into the battery. This electricity produced is then used in different accessories like indicators, head lights etc.

Stefano Trabucchi et al. [9] had worked on the model, design and controlling of the waste heat recovery unit in 2017. This research displays plausibility contemplate on a waste warmth recuperation framework for rock solid truck motors dependent on natural rankine cycle innovation. The components of oddity of this work are given as: The proposed plant arrangement and practicality think about that envelops the entire primer structure work process of the framework, in particular, from thermodynamic cycle streamlining and the segments starter measuring, to dynamic displaying and structure of the PI-based control framework. The considered rankine cycle turbo-generator utilizes hexamethyl disiloxane as the working liquid and accomplishes the most extreme appraised mechanical intensity of roughly 5 kilo-watt for the structure direct, relating to the truck voyage speed and the diesel motor power yields 85 kilometer per hour and 100 kilo-watt individually. Concerning dynamic execution, the higher reaction time delay of rankine cycle unit contrasted with the diesel motor makes the selection of a propelled control framework important. Specifically, the reenactment of the PI-based control framework demonstrates that this will end up difficult to keep the warm disintegration of the working liquid when the motor works ceaselessly for the higher power levels. So, this contextual investigation shows the significance for car oriented rankine cycle utilizations of playing out the examination of the dynamic execution and the control structure as of now in the early plan stage.

The greater part of the investigations revealed by S. Lion et al. [10] in the recovery of the heat source by using exhaust gas so as to maintain the Inexhaustible and Sustainable Energy Reviews in 2017 by using engine fuel utilization using ORC. Building up a waste warmth recovery framework, operational system should be examined all together to pick the correct framework configuration. By this reason, examination of common obligation cycle or genuine operation based information is vital in the underlying phase of each venture. Among all waste warmth recuperation innovations, ORC are by all accounts one of the most encouraging, permitting a conceivable mileage up to conceivably 10%. Despite the fact that ORC innovation is outstanding since decades, and as of now effectively connected in stationary power age and modern procedures squanders heat recuperation, vehicle applications are still

in an innovative work stage and a potential for further advancement can be perceived. The most widely recognized design is the parallel boilers arrangement.

2.4. CFD Analysis of Turbo-charged Turbine

Naveen B et al. [11] experimented the CFD analysis of turbocharged turbine in 2015. This paper shows that scaling back is a pattern in engine advancement that permits better proficiency and over discharges dependent on the expansion of intensity yield in diminished removal engines. A flammable gas engine for maker gas activity was embraced. The Producer gas fuelled Engines are the up and coming Technology and all the more agreeable to the earth contrasted with diesel and petroleum Engines. There are a few issues identified with power de-rating from the engine identified with the fuel properties. The primary driver for the power de-rating is expected to the moderately lower warming estimation of stoichiometric blend of maker gas and air. This misfortune in influence can be recouped to a much vast extent by Turbo-charging. Coordinating of the right turbocharger to an engine is of incredible significance and is essential for fruitful activity of a Turbocharged motor. It is vital to have a Turbine Map for coordinating the Turbocharger with an engine. The qualities of the Turbocharger's Turbine from the first producers were not accessible. CFD analysis for radial turbine has done for various mass stream as for the distinctive rotational rates. From the above Graph it has been affirmed that the turbine is coordinating with the engine, over the recreation were conveyed for just for impeller, the further work must be completed with amassing the packaging with same conditions.

Different innovations have been created for waste heat recuperation by H. Aghaali [12] in 2015, for example, turbo compounds, the first one is Rankine cycle and second is Thermo-electric generator that lessens utilization of fuel and CO₂ emanations. A thorough survey of turbo intensifying of ICEs was done with spotlight on its fuel-sparing potential to find imperative factors pertinent to the theme, set up the setting of the point, comprehend the structure of the subject and give experiences in to that to scholastic research and mechanical R&D. Formation of waste energy through the exhaust of IC engine is around 33% of the energy of the fuel, and on present day substantial, light-obligation Diesel, and light-obligation SI engines. AWHR framework, as turbo exacerbating, can hypothetically recovery up to a limit of 66% of this waste energy. In any case, accomplishing this most extreme isn't useful because of a few constraints, particularly the lower efficiency of turbine and additional gases reverse-weight on the engine that prompts maximum siphoning misfortune along the searching stage of the exhaust. By using Turbo compounding technique, consumption of an engine can be decreased with the help of low volume and low weight requirements. Turbo compounding give extra power to the engine to accomplish impeded start time, high ability of the driving of EGR, and improved reaction at homeless people, also. Turbo compounding considers more opportunity in structure and advancement of internal combustion motor. All of this is because of the way that for enhancing the framework, there can be a change in few parameters, for example, measure, extension proportion, effectiveness and speed of intensity the turbo, ventilation system geometry, the ratio of air and fuel proportionality, blower weight proportion, motor pressure proportion, admission and fumes valves timings,

beginning of burning planning, EGR frameworks, and fumes. In the improvement of turbo-compound motors and the choice of arrangements, more consideration ought to be given to the effectiveness of the turbine or made siphoning take a shot at the motor as shown in figure 2.4.

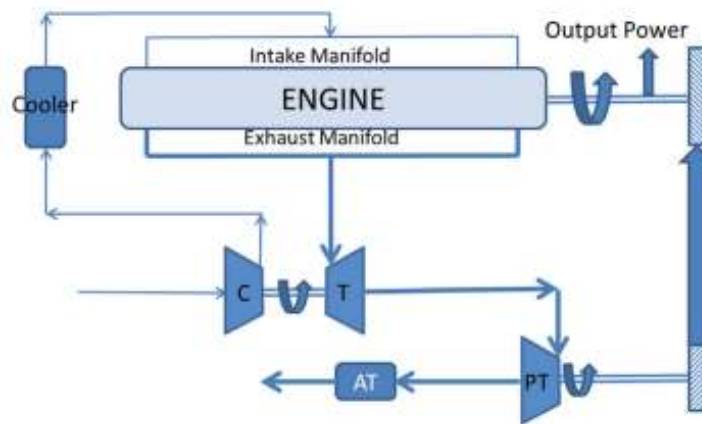


Figure 2.4: Schematic Diagram of Turbo-compounding (Aghaali et al., 2015)

In 2015, Modification in the diesel engine is finished by the Kranthi Kumar et al. [13] for creating power with the assistance of turbine. From the investigation, it has been distinguished there can be many possibilities of the energy recovery by the help heat of the waste, its recovery and its advancement. Waste heat recovery consists of reuse of the waste heat from the internal burning of combustion engine and then use it for heating purpose and can be used as any mechanical or electrical work. Examination additionally distinguished possibilities of innovations one the time when joined to different gadgets for augment potential vitality effectiveness of the engine. It can be used for producing power in the vehicle unit exhaust system. By the help of examination, there is the settlement in the diesel engine for providing the power with the help of the turbine. In the Automobile field, there are many ideas now a days for the betterment of the system. Now we can use power generated from the exhaust which can be stored in there battery and can be used whenever required.

Chou et al. [14] investigated the possibilities of using micro turbine as energy saving or scavenging device in 2014. The paper examines the likelihood of utilizing the turbine (Micro Turbine) as a vitality rummaging gadget to produce storing power using the vitality of waste gases coming from a car's exhaust. A pivotal stream miniaturized scale turbine is planned with the end goal that might be the fitted in pipe of the exhaust for a vehicle. The experimented model is the 12 cutting edge of turbine having width 4 centimeter sharp edge channel, edge of 00 with an edge outlet point of 30°. The front and back plate is additionally demonstrated to give a help to shaft of turbine. Computations have done to demonstrate the sharp edge profile and after that the CAD display is created on programming Solid Works. The recreations give bits of knowledge into the back weight following up on the get together just as the disturbance attributes of the stream. The CFD examination of a vitality searching the turbine (Micro Turbine) has completed utilizing the standard of (k-ε) turbulence

show. The outcomes got are attractive as far as the prompted back weight with a weight drop of 0.1atm just subsequently opening the likelihood of introducing the fumes pipe of a car for reinforcement control age.

Rongchao Zhao et al. [15] worked to gain waste in the form heat from exhaust and to minimize the consumption of fuel in an internal combustion of engine in 2014 Turbo-compounding is the promising innovation to recuperate squander heat from fumes and decrease fuel utilization for interior burning motor. So, plan of the power turbine assumes a key job in turbo-compound motor execution. So, the paper introduces a lot of parametric investigations of intensity turbine performed by using turbo-compound diesel motor by methods for turbine through-stream demonstrates created by the creators. This reenactment show was checked and approved utilizing motor execution test information and accomplished sensible precision. The paper originally broke down the impact of three key geometrical parameters (sharp edge stature, cutting edge span and spout leave edge) on turbine extension proportion and motor fuel utilizations. From that point forward, the effects of different parameters for power appropriation, mass of fluid stream rate, fumes temperature had dissected. So the results demonstrated that the parameters affected the motor brake specific fuel consumption and power. For high motor rates, an ideal estimation of geometric parameters is existed to acquire the most minimal brake specific fuel consumption. For low motor speeds the motor brake specific fuel consumption continued expanding or diminishing persistently as the geometric parameters are changed. The research additionally discovered the motor specific brake fuel consumption had the most touchy to spout leave sharp edge, which ought to be considered cautiously amid the structure procedure. This paper gives a valuable strategy to coordinating and structuring of a power turbine for turbo-compound motor.

M. Hatami et al. [16] took the short audit of technologies for heat recovery waste in 2014. The short audit of heat gaining innovations in (motors) engines and the exchangers (heat exchangers) had been displayed as well as a survey of heat waste recuperation innovations from the diesel motors, heat exchangers utilized in fumes of engines. Along these lines, the survey of innovations that expansion the heat move in heat exchangers were appeared and had been utilized by these in exhaust of engine was assessed and a total audit of different heat energy exchangers which beforehand were used for the expanding the exhaust squander recovery of heat is exhibited. Additionally, the future view focuses the next heat exchangers structures has been proposed to build the recovery of heat from exhaust of diesel motors. It appears that in a large portion of these advancements for which heat exchangers had a critical job to exchange heat for recovery process so an appropriate plan for exchangers ought to be connected as per this reality that heat exchange increments when weight drop is in as far as possible. Some exploratory and numerical investigates about different exchangers of heat plans existing in writing which every one of them had been inspected here. This tends to be reasoned that utilizing fins was more pertinent and suitable than froths and permeable materials because of lower weight and eventually exchange rate is high. Additionally, it appears that different techniques for expanding the heat exchange, for example, vortex generators, nana-fluids, utilizing the PCM as warmth stockpiling source.

Saiful Bari and Sheikh Rubaiyat [17] worked together for generating more power as compared to previously diesel motor engine models from exhaust gas of

diesel motor engine in 2014. The heat energy from waste gases of diesel motor engines could be the essential heating source which will give the extra power by utilizing the other rankine cycle. Water is to be the number one working liquid for all kind of utilizations as far as effectiveness of the RC framework, accessibility and natural amicability. In any case, for little engines and furthermore the part load tasks, the fume gas temperature isn't sufficiently adequate to increase the temperature of steam to the superheated zone, which is after then the development in turbine and should be in superheated zone. Smelling salts were observed to be the other working liquid for these kinds of uses which can keep running at low fumes temperature. PC recreation was completed with the improved heat exchanger which gauges extra energy with the help of water and alkali as the working liquids. Programming was utilized for recreation. It had been discovered that the total burden 24 and 11 percent extra energy was accomplished with utilizing water and smelling salts as working liquids individually. Be that as it may, for 25 percent part load, smelling salts with 11.2 percent extra power work superior to water which had the capacity to create just 2.6 percent extra power. Most extreme recuperated extra powers product 9.9 kilo-watts at 30 bars and 5 kilo-watts at 50 bar as for working weight for the water and smelling salts separately. In this manner, an extra 2 percent and 11 percent energy can be accomplished by utilizing water, smelling salts used as a working liquid for the parallel stream course of action thinking about 70% proficiency of the turbine.

Yong Wang et al. [18] in 2014 proposed and studied two novel turbo charging approaches that are steam turbo charging and steam-assist turbo charging. Steam turbo charging consist of more power than the two turbo charging methods. In the research, there are 2 types of methods of approaches, the first one is steam turbo charging and second is steam-helped turbo charging. What's more, both of them depend on the standard of interior burning (IC) engine recovery system. So as we know that there are two types of turbo approaching ideas, a near report between fumes turbo charging, steam turbo charging and steam-helped turbo charging was put into the traveller fuel motor, impacts of different weight approaches of upgrading on IC motor exhibitions just as turbo charging framework energy stream were examined. The results demonstrate that, steam turbo charging can accomplish the objective admission weight on whole engine efficiency, whereas turbo related to steam charging can improve IC motor admission weight at the minimum and low working conditions. vitality sparing possibilities starts by higher to low pressure the sequence of turbo charging, steam-helped turbo charging or fumes turbo charging; with the expanding of IC motor speed, the fumes gas vitality recuperation productivity of turbo steam charging framework diminishes and its most extreme esteem is 6.5%, while the fumes gas vitality recuperation effectiveness of steam helped turbo charging and fumes turbo charging first increments and after that diminishes.

Y. Yang [19] in 2014 proposed the studies the turbo methods and their approaches by using IC engine system. In this research paper, there are two sorts of weight approaches, the first one is steam turbo-charging and the second is steam-helped turbo-charging. Furthermore, both these two depends on the standards of the interior ignition engine waste heat vitality recuperation. So as to exhibit the benefits of the both sorts of new turbo-charging ideas, a near report among fumes of the turbo-charging technique, steam turbo-charging system and steam based turbo-charging system was directed on a traveler vehicle fuel motor, and impacts of different

approaches on IC engine exhibitions just as turbo-charging frame network vitality stream were broke down. The outcomes revealed that the technique of steam turbo-charging can accomplish the objective admission weight in the whole IC motor speed extend, whereas, steam-helped turbo-charging improves the IC engine admission weight at the low-speed working conditions. By expanding of motor efficiency, the fumes vitality recuperation productivity of the turbo charging framework diminishes and its most extreme esteem is 6.5.

2.5. Recovery of Energy from Exhaust

Tanya Wang et al. [20] worked for enhancing efficiency of an IC engine and to reduce carbon-dioxide emissions from exhaust in 2013. In this paper, The exhaust recovery of energy had been generally sought after for enhancing the complete productivity and lessening the carbon dioxide outflows of inside burning motors, the enhancement for motor proficiency has been researched with test work and mathematical reenactment dependent on the ranking cycle of steam(exhaust recovery of energy framework). Test was led on the light-obligation fuel engine associated with the multi-curl helical exchanger of heat. Joining those trials and displaying results it exhibits that the stream rate of liquid working plays an imperative and complex job for controlling outlet of steam weight and over-heat degrees. For accomplishing required over-heat and weight of steam, the stream rate should be cautiously managed. The stream rate had additionally noteworthy effect on the heat exchanger proficiency. To accomplishing good exchange heat proficiency, the stream rate ought to be kept up as high above as could be allowed. From reproduction, it was discovered the framework dependent on light-obligation test motor could build the motor fuel change productivity up to fourteen percent, however the general vehicle working conditions , simply somewhere in the range of 3 percent and 8 percent.

In June 2013, Banglin Deng et.al [21] combined thermodynamic cycle based on methanol dissociation for IC engine exhaust heat recovery system. In the research, a methodology of recovery of waste was given to maintain IC (inner burning) motor eco-friendliness and furthermore to accomplish the objective for utilization of the methanol dissociation as fuel in IC engine. In base cycle, the current substance initially experiences separation and extension forms, and is coordinated to IC engine in the form of fuel. Outer base with the IC motor principle cycle are joined together, by combining it makes a thermo approach. At that point, the idea was connected to the turbo-charged engine, and the comparing recreation model was working for the outer base with the motor primary system. The vitality sparing capability of consolidated cycle was assessed by parametric checking. Contrasted with the vapor of methane engine, engine in-chamber proficiency have an expansion of rate focuses with all burden circumstances, whereas the outside base can build the eco-friendliness up to 3.52 rate focuses at the weight by 29bar. Most extreme development to the IC motor worldwide eco-friendliness achieves 6.8 rate focuses.

Emission of CO and HC can be controlled in the muffler exhaust system of vehicle by the heap of fly ash because it can be used as the catalytic convertor. It was proposed by W.M Yang [22] in 2013. The ideal air pressure to diminish HC also, CO discharges was 0.1 MPa. Expanding speed of the engine diminished the discharges of CO and HC. After extending length of exhaust system, the discharges of HC and CO

diminished. The least HC and CO content was seen at speed of 1900 rpm, length of 9 cm and pneumatic stress of 0.1 MPa, which are 1250 and 8500 rpm, individually. The use of three-way exhaust systems is created in light of the respectable metal impetus. Impetuses are prepared to do productively changing over the toxins of HC to CO₂ and H₂O, CO to CO₂ and NO_x to nitrogen. To diminish measure of honorable metal impetuses, supports, for example, alumina and silica or clay cradle have been utilized. This method accomplishes very higher transformation about 80%; in any case, the strategy is very costly in manufacture and less reasonable to be connected in nations having and providing fuel with Pb.

R.Saidur et al. [23] focused their study for developing waste heat recovering technologies in 2012. There is a short review of recovering more energy from waste heat recovering technologies using the heat exchangers as a common way. The exchangers of heat used in the engine exhaust are introduced as like the common way. It also reviews the technologies which increases the heat transfer rate resulting in the overall efficiency of exhaust heat recovery system. New designs are presented and the future viewpoints are reviewed for the new designs of heat exchangers which will increase the exhaust heat recovery of an automobile engine motor. Technologies i.e. (Turbo-charging, ORC, TEG and other technologies etc.) the exchangers played vital role in transferring the heat in the recovery procedure.

A.Kusztelan et al. [24] focused their work and research on turbochargers in 2011. Turbochargers are broadly utilized all through the car business as they can improve the yield of an inner ignition (IC) engine without the need to build its barrel limit. The use of such a mechanical gadget empowers car producers to receive littler dislodging engines, usually known as "motor cutting back". Verifiably, turbochargers were regularly used to expand the capability of an officially ground-breaking IC engine, for example those utilized in Motorsport. The accentuation today is to give a doable designing answer for assembling financial matters and "greener" street vehicles. It is a result of these reasons that turbochargers are presently winding up significantly more mainstream in industry applications. The writing audit consider exhibited in this paper gives a general blueprint concerning how engine test methods are utilized for the test investigation of turbo-charger as shown in figure 2.5.



Figure 2.5: Typical Diagram of turbocharger (Kusztelan et al., 2011)

In 2011, R.Saidur [25] proposed the idea to save the energy from electric motor as well as their usage in the best way. From the survey, it has been recognized that vitality review is a successful apparatus that gathers information vital for evaluating engine vitality use. This audit likewise demonstrated as quantitative bases in extraordinary kinds of misfortunes that occur in electric engines. It is noticed that most astounding sum of misfortune (for example 58%) occurs at the rotor parts of an engine. It was discovered that about 75% of engines are worked beneath 60% load. Now and again it was discovered that engines are worked at 40% burden. It was accounted for by numerous specialists that engines are productive on the off chance that they are worked above 75% of their heap. Along these lines, there are gigantic potential to spare vitality and stay away from backhanded outflow by legitimate estimating/determination of engines. VSDs are a choice in such circumstances to coordinate the required loads subsequently funds vitality. In any case, it ought to be noticed that VSDs are conservative just for huge engines. In light of the talks it has been discovered that engines are not utilized at full burden and as a rule they are larger than usual that empower wastage of vitality. A standout amongst the best answer for beat this issue is to utilize PC instruments, for example, Motor Master+, Euro DEEM, Can MOST, etc. It massy additionally be noticed that vitality can be spared utilizing high-productive engines of standard-productive engines. Numerous analysts discovered utilization of effective engines financially suitable dependent on the estimation of compensation period. Along these lines, vitality productivity guidelines (for example administrative, willful, motivator based) now and again assume an essential job in decreasing vitality utilization and natural contaminations. Be that as it may, appropriate test technique must be created to set up such guidelines. As the worldwide market is getting borderless, a fit test method will be progressively helpful.

It was discovered that mechanical part devours significant offer of absolute vitality utilization of a nation by R.Saidur [26] in 2011. In this way, it is a potential segment that can be focused for decreasing vitality utilization, utilizing elective wellsprings of vitality to moderate natural contamination. Oil based powers and coal observed to be prevailing energizes in this segment as innovation is developed. These powers are moderately less expensive contrasted with option or inexhaustible powers. In any case, these energizes are in charge of ecological contamination. Consequently, natural amicable, spotless, safe and monetarily feasible fills must be scanned for. It might be noticed that numerous nations are setting arrangements and needs for elective wellsprings of vitality to energize their utilization. Ventures are utilizing diverse wellsprings of elective energies to some degree. These are not to a great extent utilized on account of numerous difficulties should be looked with the utilization of elective powers. Cost, vitality transportation, inventory network, significant ability, innovation development also, fitting approach are the significant provokes that need to be tended to so as to utilize elective wellsprings of vitality. Discoveries condensed in this paper are relied upon to help in choosing an elective fuel for modern activity. The criteria appeared in this paper may fill in as a rule in choosing an elective fuel for an industry. It might likewise be proposed that innovative work exercises are expected to conquer the difficulties revealed in this paper.

Saidur et al. [27] in 2010, saves the waste energy and generated power from the help of thermo electric generators and semiconductors. The temperature appropriation of the fume using exchanger is exceptionally critical for a thermo coupled generator. These type of exchangers give essential warmth to generators, and all to their ability or transformation proficiency rely upon the material of the heat exchanger and shape of this exchanger, and also the kind of exchanger. In any case, these energizes are in charge of ecological contamination. Consequently, natural amicable, spotless, safe and monetarily feasible fills must be scanned for. It might be noticed that numerous nations are setting arrangements and needs for elective wellsprings of vitality to energize their utilization. Ventures are utilizing diverse wellsprings of elective energies to some degree. These are not to a great extent utilized on account of numerous difficulties should be looked with the utilization of elective powers. Exhaust of the engine streams in the exchanger and exchanges the energy in the form of the heat, which will undoubtedly result in weight drop. That is how it is important to check and assess weight decrement dimension of diverse pattern by large scope of working patterns.

In 2010, Pengpengjia et.al [28] combined with point by point synergist response system, the process of transforming the gases was recreated in the fixed type bed reactor utilizing permeable model to research changing qualities under various beginning conditions. Impact of gas hourly speed, feeding segment, expansion of steam and methane temperature changing rate, yielding of hydrogen and the other parameters related to the trademark are dissected. Reproduction demonstrates that by entering the improving gas in response zone, oxygen is expended very quickly and changing of the stream assumes an overwhelming job in the last part. The fumes changing procedure essentially includes oxidation response, steam improving response and moving response of the water gas. The changing in methane and creation of hydrogen decline with the ascent of GHSV. As per proportion of the methane, a more molar can be accomplished or completed of the hydrogen at outlet portion of hydrogen and can be accomplished inferable from greater extent of fractional changing response of methane, and change rate of methane diminishes.

Necla Kara Togun and Sedat Baysec [29] worked together to develop an artificially controlled neural network which help in prediction of torque and brake specific fuel consumption in 2009. This examination exhibits a fake neural system model to anticipate torque and the brake explicit fuel utilization of the gas motor. An express network based plan is created to foresee the torque and the brake explicit fuel utilization of the gas motor as far as sparkle advance, the throttle point and motor speed. The proposed network show depends on exploratory outcomes. Test thinks about were finished to get preparing and testing information. Of every one of the 81 informational collections, the preparation and the test sets comprised of arbitrarily chosen the 63 and for the 18 sets, separately. The under consideration network demonstrate dependent on the back-spread learning calculation for motor created. The execution and a precision of proposed network demonstrate are discovered tasteful. This investigation shows that chosen network is proficient for anticipating the motor torque and the brake explicit fuel utilization. Also, the proposed network demonstration is exhibited in unequivocal structure as a numerical capacity.

Zhang Yang Jun et al. [30] designed a new model of turbocharger to increase the efficiency of engine in 2009. Turbo-charging innovation is today considered as a

promising route for interior burning motor vitality sparing and carbon-dioxide decrease. Turbocharger configuration is a noteworthy test for turbocharged motor execution improvement. The turbocharger fashioner must draw upon the data of motor task conditions, and a fitting connection between the motor necessities and configuration highlights must be deliberately created to produce the most reasonable plan suggestion. The target of this examination is to build up a turbocharger configuration approach for better turbocharger coordinating to an interior ignition motor. The advancement of the methodology depends on the idea of turbocharger structure and cooperation connects between motor cycle necessities and plan parameter esteems. A turbocharger through stream demonstrated is then used to create the structure choices. This coordinated technique has been connected with progress to a gas motor turbocharger get together.

2.6. Way to Reduce Toxic Gases and Catalytic Converter

P. Leduc et al. [31] worked together with the purpose of downsizing of a gasoline engine in 2003. So as to meet responsibilities regarding vehicle carbon-dioxide outflow decrease for the entire armada of autos for the year 2008, motor innovative work is today investigating a few fields. From carbon-dioxide perspective, gas motors experience the ill effects of an impediment in contrast with Diesel motors. Decrease of size of gas motor (scaling back) has all the earmarks of being the promising method to enhance the motor effectiveness and is liable to broad research. Viewing the long haul, the point ought to be to lessen considerably the motor removal volume. Estimation results from a vehicle reproduction represent that even a so broad scaling back won't be sufficient to convey the whole gas armada to mentioned carbon dioxide levels. This would simply be adequate to achieve the focused in 2008 for the middle-class vehicle controlled by the scaled back 0.8 l motor rather than a present 1.6l gas motor. Decrease of carbon dioxide emanation is all things considered as 18% warmer in motor conditions.

A Catalytic Converter is a device which converts the harmful pollutants such as CO, Nitrogen oxides and unburnt hydrocarbons into less harmful pollutants by catalytic activity through the process of redox reactions. The pollutants are converted to CO₂, N₂, O₂ and H₂O respectively which are less harmful to humans as well as to the environment. Typical Diagram of Catalytic Converter is shown in figure 2.6.

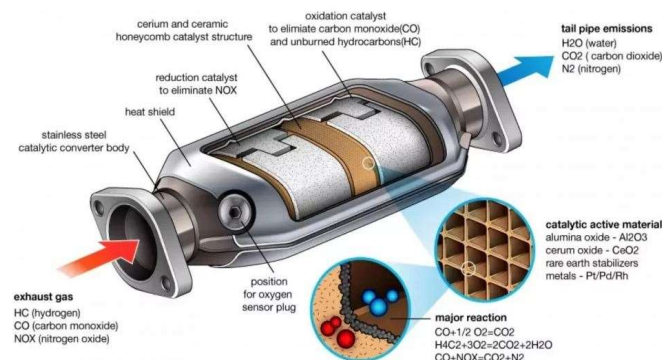


Figure 2.6: Typical Diagram of Catalytic Converter (www.catsays.blogspot.com)

Guo et al. studied copper oxide along with cerium oxide and combined the doping of manganese oxide and the final catalysts was $\text{CuO}_x\text{-MnO}_x\text{-CeO}_2$ which gave about more than 99% conversion of CO [32]. Qi and Li considered oxidization of NO to NO_2 by using the catalyst which was mixture of manganese and cerium oxides and catalysts gave conversion at about 350°C with percentage of about 50 to 70% [33]. Zhao et al. prepared CuO/Ce-Mn-O catalyst for the conversion of CO to CO_2 [34]. The catalyst gave almost complete conversion of CO at 160°C . Alphonse used $\text{Co}_x\text{Mn}_{3-x}\text{O}_4$ oxides as a catalyst for the oxidation of CO and propane at mild temperature. Co-Mn oxide spinel catalyst gave conversion of CO from 20 to 300°C [35]. Vasilyeva et al. prepared catalyst with Mn oxides, Si oxides and Ti oxides for the conversion or oxidation of CO [36]. This catalyst gave 50 % conversion at 150°C and 100 % conversion at about 210°C . (Srivastava et al., 2012) used carbon supported palladium catalyst for removal of carbon mono oxide and 5% Pd was coated on CeO_2 and ZrO_2 which have a CO to CO_2 conversion of 100% at 108°C and 140°C [37]. Pakharukova et al. used catalysts copper cerium oxide with monoclinic zirconia for checking oxidation of CO with excess of hydrogen and the catalyst gave 100% conversion at 130°C [38]. Wojciechowska et al. used catalyst for oxidation of CO by using copper and manganese or cobalt oxides supported on MgF_2 and Al_2O_3 [39]. This catalyst gave very less percentage of CO conversion that is 51% at 300°C for 15 minutes. Marbán and Fuertes used copper oxide and cerium oxide for oxidation of CO. This catalyst gave 90% conversion at about 165°C [40]. Hoflund et al. used Gold with MnO catalyst for low temperature oxidation of CO. This catalyst gave about 90 to 100 % conversion at about 225°C in 17000 minutes [41].

2.7. Research Gap

Two-third of the energy from combustion in a vehicle is lost as waste heat, of which 40% is in the form of exhaust gases. Most of the research has been conducted on turbocharged and supercharged engines but none of them utilized waste heat for later consumption of various electric utilities of four stroke petrol engine. Energy is extracted by placing turbine in exhaust gas passage and analysis of turbine by using CFD techniques. Moreover, from the literature review it has been observed that the cerium, manganese and copper nano particles have great conversion rate for CO, NO_x and HC. So, they are the best option for synthesis of catalytic converter. Selected sulphates of these metals are Cerium Sulphate Tetra hydrate ($\text{CeO}_8\text{S}_2.4\text{H}_2\text{O}$), Manganese Sulphate Mono hydrate ($\text{MnSO}_4.\text{H}_2\text{O}$) and Copper Sulphate Penta hydrate ($\text{CuSO}_4.5\text{H}_2\text{O}$) which fulfills all required factors explained above for the selection of best catalysts to achieve the maximum conversion of pollutants.

CHAPTER 03

3.1. Research Methodology

3.1.1. Fabrication of Test Bench

Test bench was fabricated in order to mount engine and its accessories in it, moreover static structural consideration were kept to avoid structural failure due to load and vibrations.

3.1.2. Turbine Selection

Best suited turbocharger turbine was selected in order to place in it the exhaust passage of engine to produce power generation.

3.1.3. 3D Modeling of Turbine

Turbine and its coordinates were extracted by using CMM as it was aforesaid that turbine was selected. Coordinate extracted from CMM enabled to develop 2D drawing sheet through which 3D CAD modeling using SOLIDWORKS. 3D generated model was then used for further requirements.

3.1.4. CFD Analysis of Turbine

Once the STEP file was imported on ANSYS, mesh independent study, stress-strain analysis and flow analysis were studied in detail.

3.1.5. Install Catalytic Converter with Engine

A Catalytic Converter is a device which converts the harmful pollutants such as CO, Nitrogen oxides and unburnt hydrocarbons into less harmful pollutants by catalytic activity through the process of redox reactions. Catalytic converter with new catalysts was installed after turbine in order to reduce emissions from engine.

3.1.6. Calculation of Emission Produce from Engine

In order to calculate the exhaust emissions, flue analyzer were used to calculate the amount of CO, NO and HC.

Flow chart of research methodology is shown in figure 3.1.

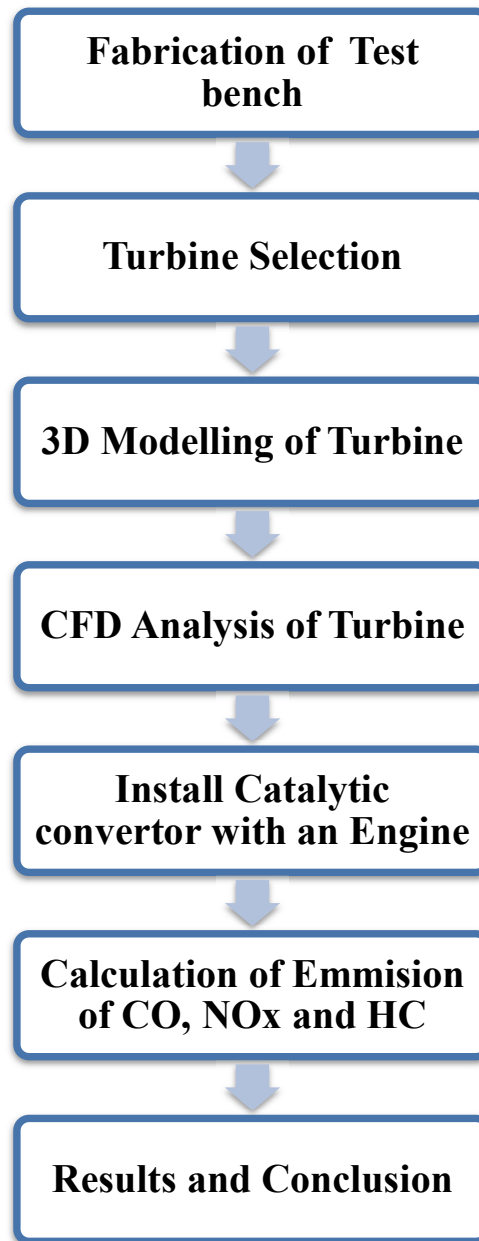


Figure 3.1: Flow Chart of Research Methodology

3.2. Engine Specification and Fabrication of Test Bench

This research has been carried out on 200cc single cylinder petrol engine and Specification of 200cc single cylinder petrol engine is shown in Table 3.1:

Table 3.1: Engine Specification

Cooling Type	Water Cooled Engine
Engine name	G200-A
Engine Type	1-cylinder, 4-stroke, water-cooled
Displacement	197cc
Net weight(kg)	33
Max.Power (KW/min)	10.3/7500
Max.Torque (N.m/min)	14.2/6000
Compression ratio	10.5:1
Bore and Stroke (mm x mm)	63.5x 62.2
Ignition method	CDI

3.3. Solid Works Model of Test Frame:

The solid work model of the test frame is design for the engine is shown as in figure 3.2.

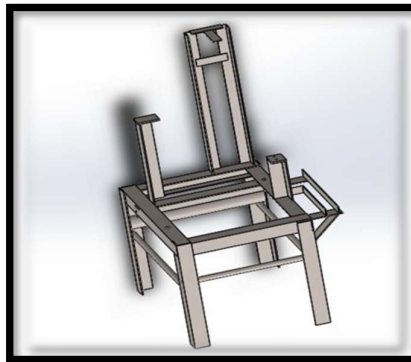


Figure 3.2: 3D view of test frame

3.4. Dimension of the Test Frame

Dimensions can be defined as the length, width, height, or depth of something. Dimension of physical quantity is more fundamental than scalar units. The dimensions are shown in figure 3.3.

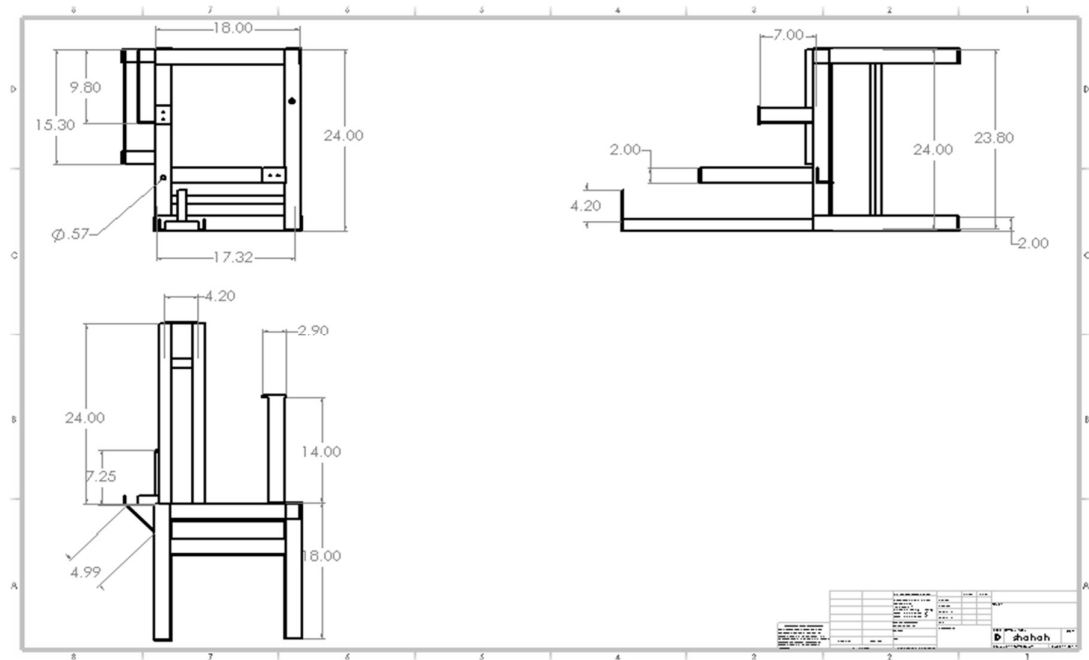
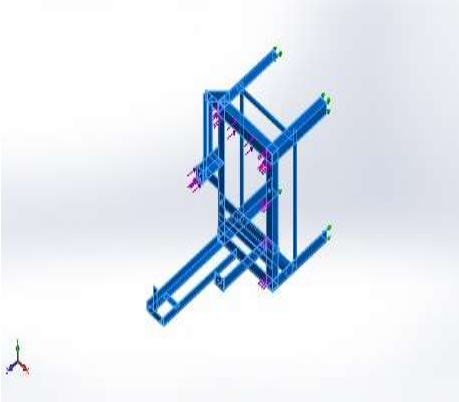


Figure 3.3: Dimensions of test frame

3.5. Material Properties

Material properties of test frame which shows the value of yield and tensile strength are shown in table 2. Solidworks simultaneously makes it easy to determine whether a structure satisfies its design criteria for a particular set of loading conditions.

Table 3.2: Material Properties

Model Reference	Properties
	<p>Name: AISI 1010 Steel, hot rolled bar</p> <p>Model type: Linear Elastic Isotropic</p> <p>Default failure criterion: Max von Mises Stress</p> <p>Yield strength: 1.8e+08 N/m²</p> <p>Tensile strength: 3.25e+08 N/m²</p> <p>Elastic modulus: 2e+11 N/m²</p> <p>Poisson's ratio: 0.29</p> <p>Mass density: 7,870 kg/m³</p> <p>Shear modulus: 8e+10 N/m²</p>

3.6. Stress Analysis of frame

Determination of the stresses in the component part of a structure when subjected to load. Stress is defined as ratio of force over area. Figure 3.4 shows stress analysis of frame on Solid Works.

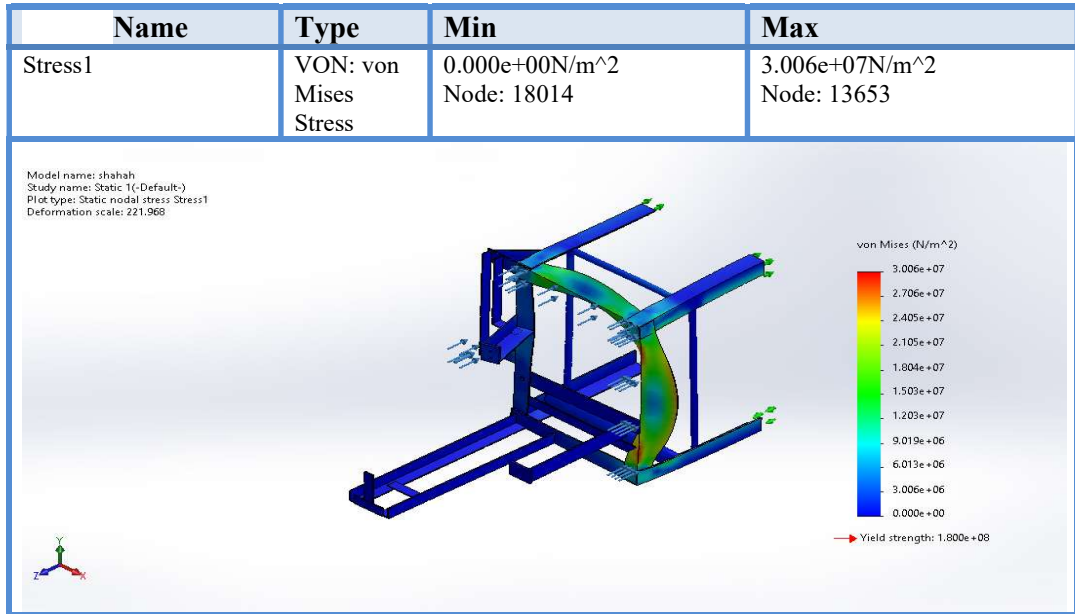


Figure 3.4: Stress Analysis of Frame

3.7. Displacement Analysis

In case of displacement method work by satisfying equation of equilibrium Unknown displacement is written in the term of load by using load displacement relation, and then these equations are solved for the displacements as shown in figure 3.5.

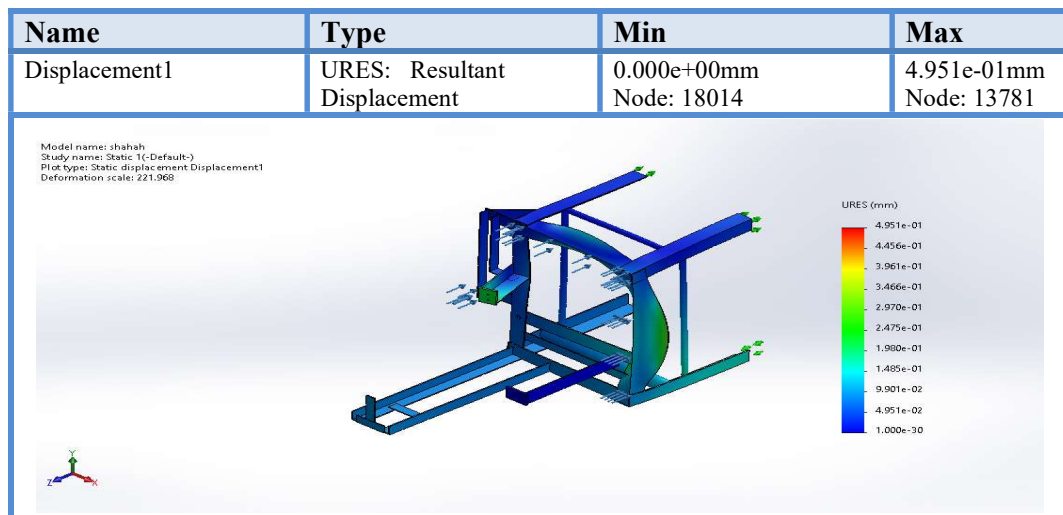


Figure 3.5: Displacement Analysis of frame

3.8. Strain Analysis

Strain analysis (or stress-strain analysis) is to change effect of material under various loadings conditions. This can be done by both physical and optical testing methodology in working environment. Figure 3.6 shows the strain Analysis on test frame.

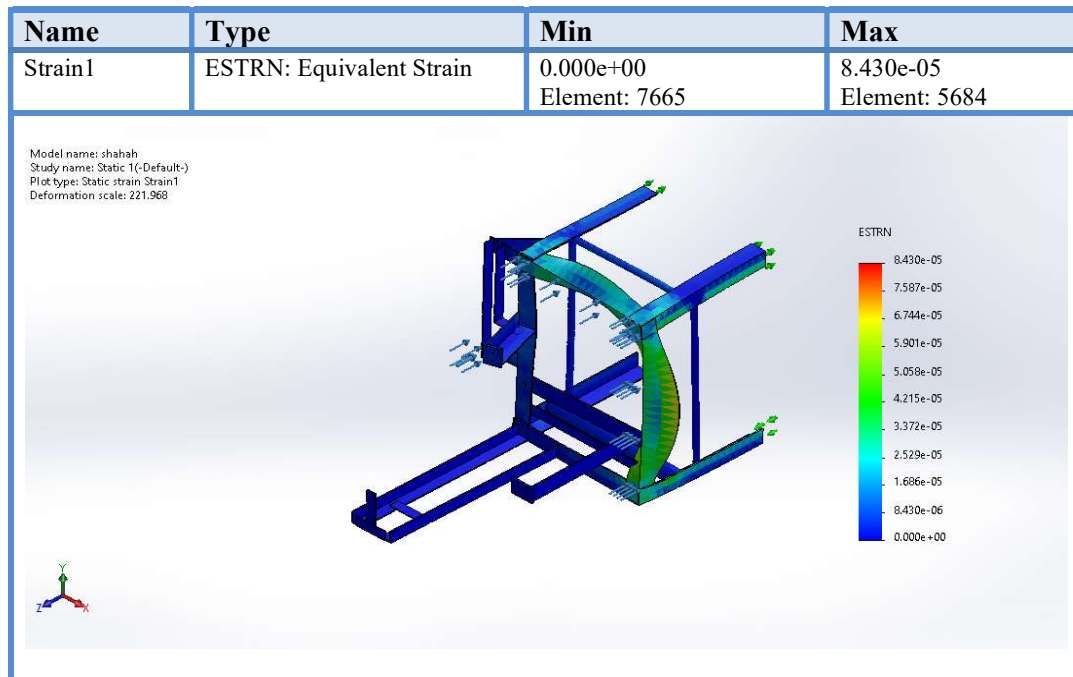


Figure 3.6: Strain Analysis on test frame

From all these analysis it is concluded that:

- The maximum Yield Strength = $1.8e+08 \text{ N/m}^2$
- The maximum Tensile strength = $3.25e+08 \text{ N/m}^2$
- The Elastic Modulus = $2e+11 \text{ N/m}^2$
- The Shear Modulus = $8e+10 \text{ N/m}^2$
- The main thing is factor of safety of any material
- The factor of safety of structure is 5.98
- The factor of safety of the required loading is 3.75

3.9. Fabrication of Engine Test Bench:

After complete analysis, the frame of an engine has been fabricated as shown in figure 3.7. Then engine is mounted on the frame as depicted in figure 3.8.



Figure 3.7: Engine Frame



Figure 3.8: Engine Mounted on Frame

All the accessories like radiator, engine battery, ignition coil, air duct have been attached with the engine and complete test bench is shown in figure 3.9.

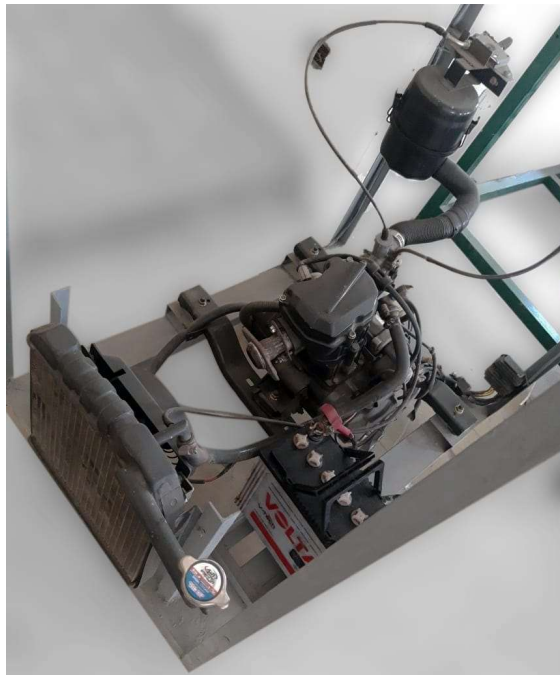


Figure 3.9: Engine Test Bench with all accessories

3.10. Coordinate Extraction, Modeling of Turbine

The aim of the research to install the turbine in the exhaust passage is to extract the power from the exhaust gases which would later utilize to run the electrical accessories of the engine. Turbine and its coordinates were extracted by using CMM as shown in figure 3.10 and figure 3.11.



Figure 3.10: Turbine

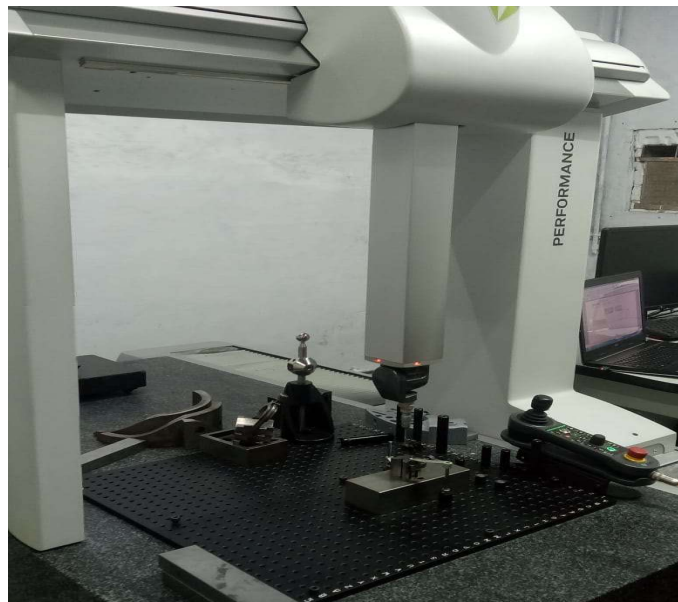


Figure 3.11: Coordinates Extraction of Turbine by using CMM

With the help of CMM the following Dimension were obtained as shown in figure 3.12.

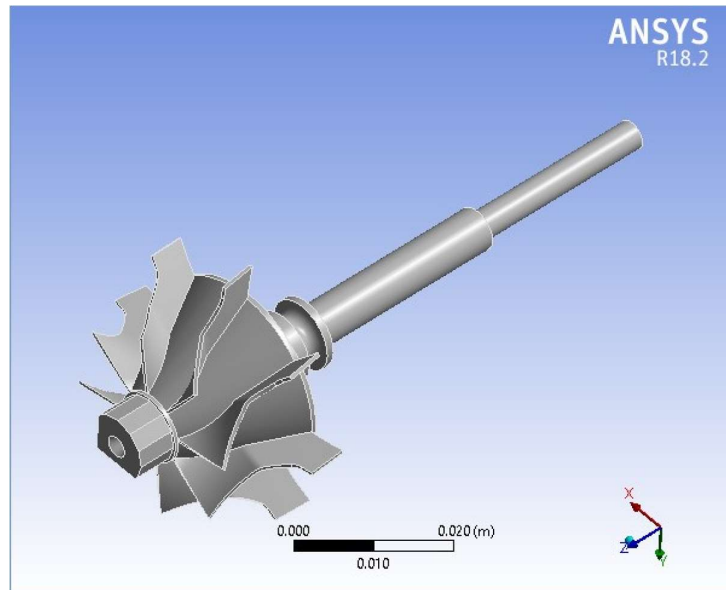


Figure 3.14: Import Turbine on ANSYS

3.11 Mesh Independent Study:

Mesh will be considered as independent when the pressure difference between two consecutive terms was found to be less than 1%. Various cases were solved having number of mesh elements. 1402154, 2010124, 25213658, 30111249, 35008547 and 40149871. The pressure difference was recorded case 5 and case 6 having number of elements 35008547 and 40149871, pressure difference were found to be approximately 0.5%. So in order to reduce the memory and computation time case 5 was considered with 35008547 elements for current study. The graph of independent mesh study was shown in figure 3.15.

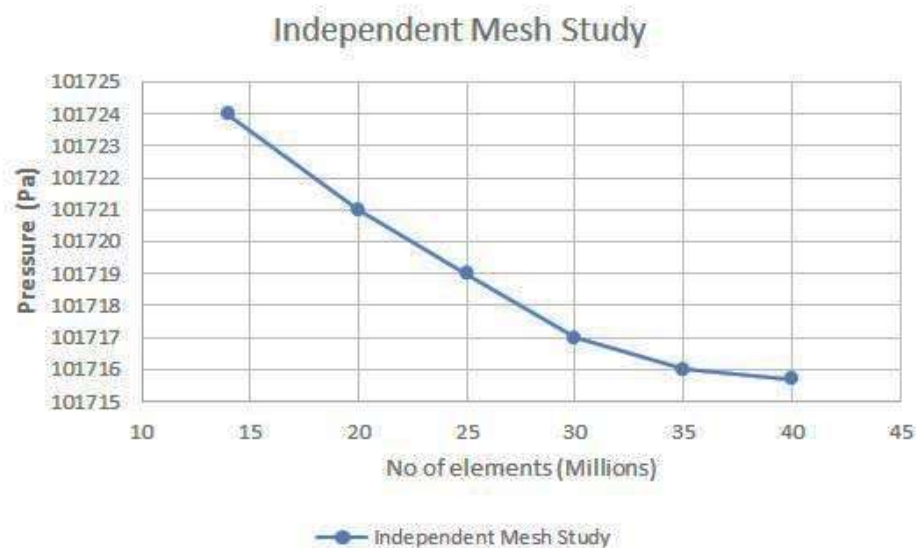


Figure 3.15: Mesh Independent Study

Meshing of turbine and shaft were shown in figure 3.16 and 3.17.

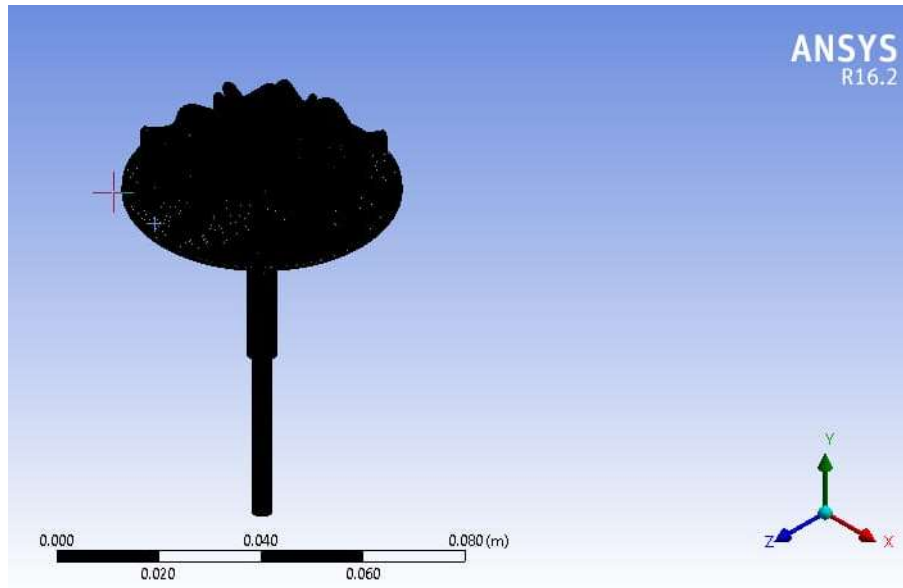


Figure 3.16: Meshing of Turbine and Shaft

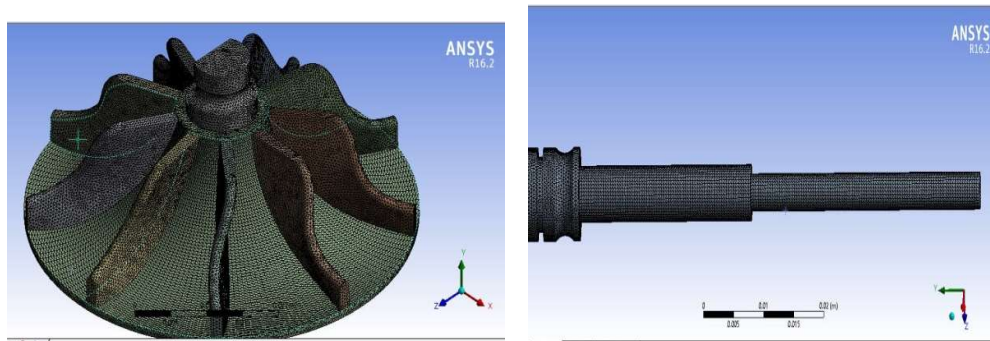


Figure 3.17: Views of Turbine and Shaft

3.11.1. System Specification and Software

ANSYS FLUENT Version 16.2 and SOLIDWORKS 2020
 Corei7 10th Generation @ 2.9 GHz, 2.9 GHz, turbo-boost 4.5GHz, RAM 32 GB
 DDR/4.

3.11.2. Boundary Conditions

Uniform velocity was considered at the inlet of turbine

At $y=h$, $u=0$, $v= -U_{in}$, $w=0$

Surface of turbine was considered as adiabatic

$$\text{At } x=0, \frac{\partial t}{\partial x} = 0$$

Exhaust gases inlet temperature was considered as constant

$$\text{At } y=h, T=T_i$$

3.12. Strain Analysis of Turbine

Results of strain analysis of turbine was done at 5500 engine speed (rpm), are shown in Figure 3.18. Static structural analysis was carried out and equivalent elastic strain distribution on various section of turbine was shown below with minimum value at the turbine shaft i.e 6.5×10^{-9} m/m and maximum value was observed where the exhaust flow at inlet of turbine casing thereby exert a force on the turbine blade which producing maximum elastic strain at the edge of the turbine blade right in front of turbine casing inlet. The maximum value of equivalent elastic strain observed is 1.42×10^{-6} m/m.

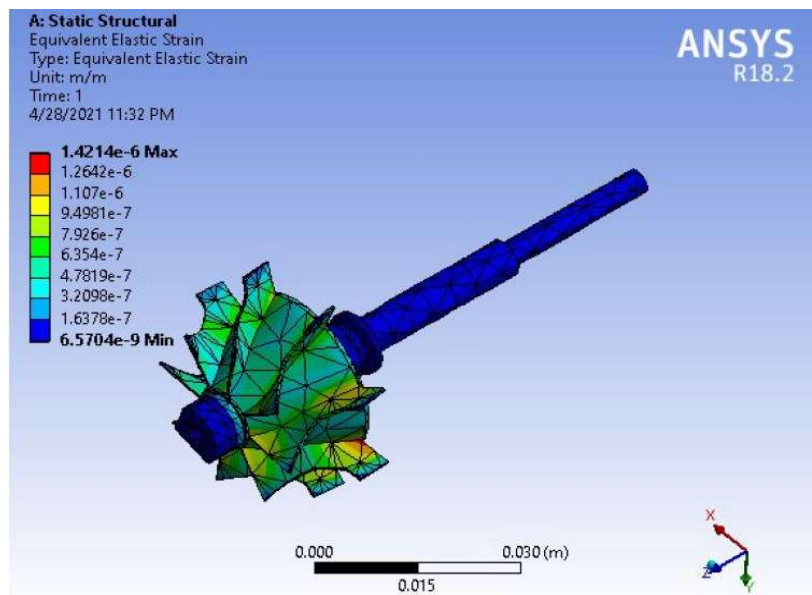


Figure 3.18: Strain Analysis of Turbine

3.13. Stress Analysis of Turbine

Results of stress analysis of turbine was done at 5500 engine speed (rpm), are shown in Figure 3.19. Static structural analysis was carried out and equivalent elastic stress distribution on various section of turbine was shown below with minimum value at the turbine shaft i.e 932.35Pa and maximum value was observed at the edge of the turbine blade right in front of turbine casing inlet is 2.46×10^5 Pa which is in range and majority section observed von-mises stress value is 55588Pa.

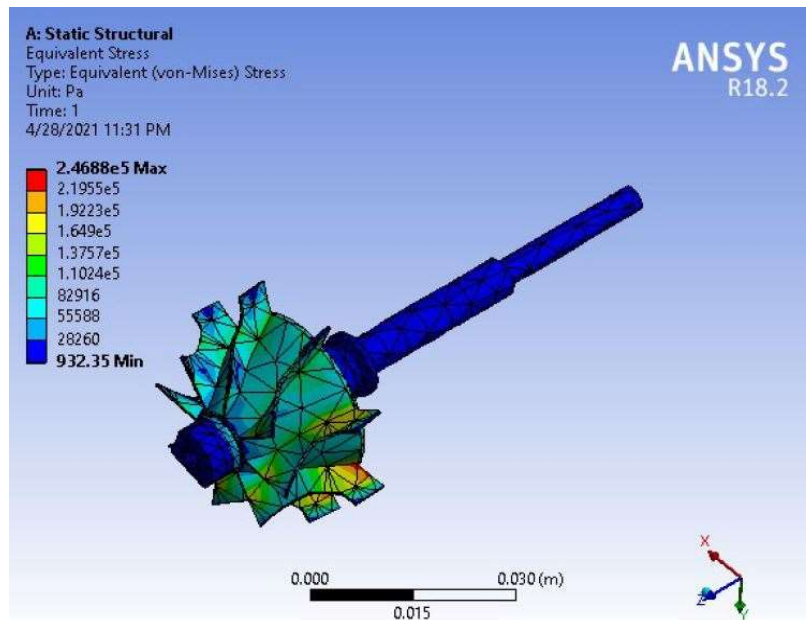


Figure 3.19: Stress Analysis of Turbine

3.14. Pressure and Velocity Contours of Turbine

These analysis are done to check the in and out flow of exhaust flue gases on turbine. From figure 3.20 and figure 3.21, it is clearly seen that there is no backflow of exhaust gases, hence there is no excess load produced on engine. Inlet and outlet value of pressure is 136846.86Pa and 101718.72Pa. Inlet value of velocity is 7.6m/s and outlet value is in range of 3.04m/s-6.08m/s.

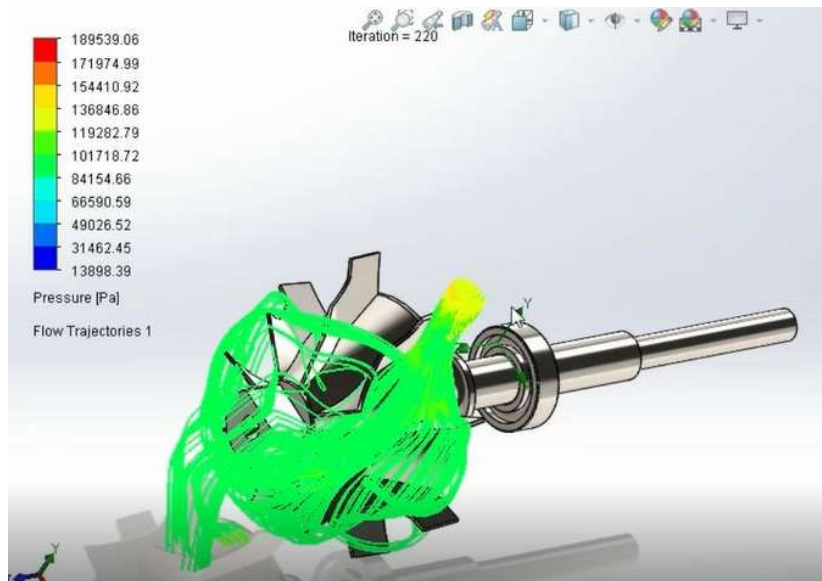


Figure 3.20: Pressure Contours of Turbine

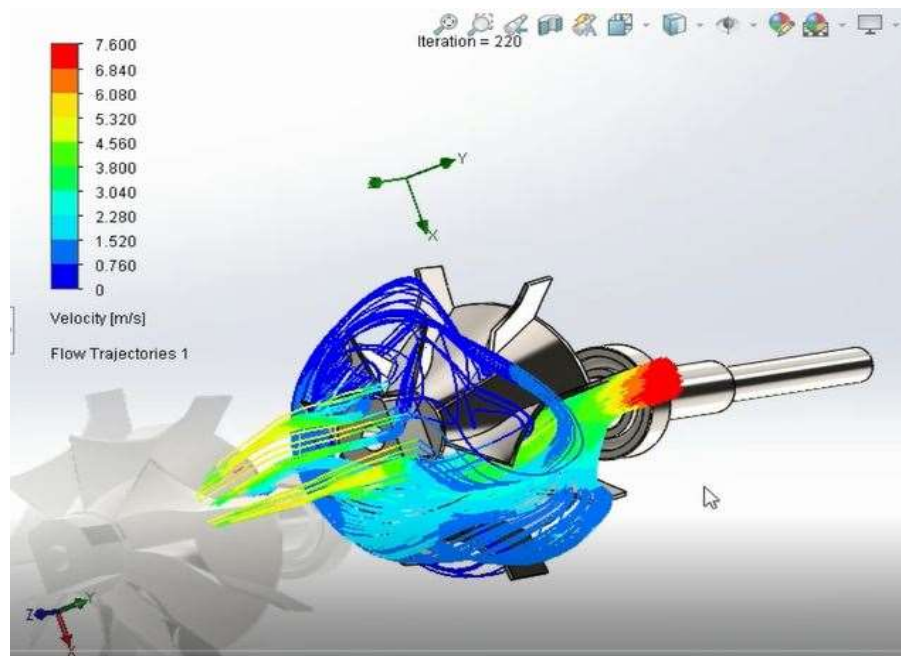


Figure 3.21: Velocity Contours of Turbine

CHAPTER 04

4.1. Results and Discussion

Power Generation from Exhaust Gases of an IC Engine is a process of production of energy using the gases coming out of the engine outlet. Engine converts chemical energy into mechanical energy and waste is extracted in the form of exhaust gases from the engine which further moves towards the tail pipe of an engine. These gases move at high temperature and pressure towards the outlet. The turbine is placed in the pathway of these exhaust gases which is designed in a way that these exhaust gases tends to rotate the blades of turbine. Following measurement were taken by help of tachometer as shown in Table 4.1.

Table 4.1: Turbine Speed

Sr. No	Engine Speed (RPM)	Turbine Speed (RPM)
1	1000	110
2	3500	318
3	5500	451

4.2. Power Generated from Turbine:

Power generated by turbine can be calculated by suing following formula:

$$P = \frac{2\pi NT}{60}$$

Where, $T = F \times R$

$F =$ Applied force

$R =$ Radius of the shaft of turbine

At $F = 4.905 \text{ N}$

$T = F \times R$

$T = 4.905 \text{ N} \times 0.05\text{m}$

$T = 0.245 \text{ Nm}$

When $N=110$

$$P = \frac{2\pi NT}{60}$$

$$P = \frac{2*3.14*110*0.245}{60}$$

$$P = 2.82 \text{ Watts.}$$

When N= 318

$$P = \frac{2\pi NT}{60}$$

$$P = \frac{2*3.14*318*0.245}{60}$$

$$P = 8.15 \text{ Watts.}$$

When N= 451

$$P = \frac{2\pi NT}{60}$$

$$P = \frac{2*3.14*451*0.245}{60}$$

$$P = 11.56 \text{ Watts.}$$

All these results are mentioned in the table 4.2 and graph between turbine speed and power generated from turbine is depicted in figure 4.1.

Table 4.2: Power generated from Turbine

Sr. No	Engine Speed (RPM)	Turbine Speed (RPM)	Mass (kg)	Force (N)	Torque (Nm)	Power (Watts)
1	1000	110	0.5 Kg	4.905	0.2452	2.82
2	3500	318				8.15
3	5500	451				11.56

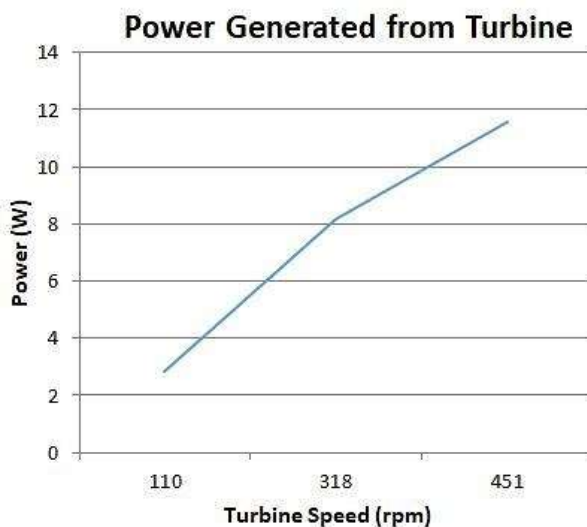


Figure 4.1: Power generated from Turbine

From the above line graph it is clearly seen that when turbine speed is increased, the more power is generated which can be utilized in various engine utilities.

4.3. Catalytic Converter

A Catalytic Converter is a device which converts the harmful pollutants such as CO, Nitrogen oxides and unburnt hydrocarbons into less harmful pollutants by catalytic activity through the process of redox reactions. The pollutants are converted to CO₂, N₂, O₂ and H₂O respectively which are less harmful to humans as well as to the environment.

4.4. Preparation of Sample Catalysts

Firstly for the preparation of saturated solution of each salt, for the purpose of co-precipitation of catalysts, distilled water was selected as a solvent because all three base salts are easily soluble in water at room temperature. For preparation of sample catalysts the correct molar ratio for each base metal was selected for the best combination as shown in Table 4.3.

Table 4.3: Molar ratio for base metal

Cu	Ce	Mn
1(2.49g)	1(4.04g)	1(1.69g)
1(2.49g)	2(8.08g)	1(1.69g)
1(2.49g)	1(4.04g)	2(3.38g)
2(4.98g)	1(4.04g)	1(1.69g)

For first sample catalyst having all the base metal in 1:1:1 combination, the correct molar ratio for each base metal was selected. For measurement of each metal salt, Electronic Balance having precision up to three decimals was used according to the required weights as shown in above table 4.3. For four test samples the required combination of metals are weighed in grams in electronic balance apparatus which is shown in figure 4.2.



Figure 4.2: Metals weight on Electronic Balance

For $(\text{CeO}_8\text{S}_2.4\text{H}_2\text{O})$ having molecular weight of 404.304 g/mol and yellow in color, 0.001 molar solution was prepared in a 10ml of distilled water by dissolving 4.04 g of salt with constant stirring of 5-10 minutes. After it the solution was placed on magnetic stirrer for 30 minutes for complete dissolution of Cerium Sulphate in water and saturated solution was obtained. In the same manner the Manganese Sulphate Mono hydrate ($\text{MnSO}_4.\text{H}_2\text{O}$) having pale white color and Copper Sulphate Penta Hydrate ($\text{CuSO}_4.5\text{H}_2\text{O}$) which has blue physical appearance, having molecular weight of 169.02 g/mol and 249.677 g/mol respectively were dissolved in 10ml of distilled water to prepare 0.001 molar solution of each base metal salt with constant stirring on magnetic stirrer for about 30 minutes each. Molar solution of each base metal in distilled water is shown in Figure 4.3.



Figure 4.3: Metal salts solution

All the above sample solutions of metal salts were poured down in a beaker with constant stirring and a chemical reaction occurred between base salts metals. The resultant solution was dark brown in color which indicated that the reaction has been completed. The resultant solution contains the precipitates of catalyst. Like the preparation of sample 1, all the four samples were prepared by dissolving the base metals in water in different ratios after weighing through electronic balance and

stirring through magnetic stirrer according to the table provided above so that the best combination of base metals could be selected for the preparation of final catalyst which gives best results for conversion of pollutants to less harmful pollutants. According to table 6.1, four samples were prepared having different molar ratios as shown below.

Cu: Ce: Mn = 1:1:1

Cu: Ce: Mn = 1:1:2

Cu: Ce: Mn = 1:2:1

Cu: Ce: Mn = 2:1:1

These all four samples obtained were kept at room temperature for 4-6 days in open air and a vibration less place because otherwise the base metals catalyst particles could again dissolve back to solution and lengthen the process. The process of crystallization of saturated solutions is referred as co-precipitation method. After 2 days crystals were started initiating in the solutions and started settling down at bottom of beaker. The process of crystallization was completed in 6 days where matured crystals were developed in solution which can be seen easily by naked eye. To completely filter the catalysts, Vacuum Suction Assembly Apparatus was used. The dark brown color of catalyst was obtained which was kept at room temperature to completely dry the catalyst. Four sample catalysts were obtained in dried form which will act as a conversion agent for pollutants.

4.5. Preparation of Test Samples

The next step was the application of the catalysts on the ceramic plates having uniform thickness and pores so that the exhaust gases can easily flow out and react on its way out to atmosphere. Ceramic plates also have great thermal resistance as exhaust gasses have very high temperature. The catalysts were dissolved in Acetone which is excellent solvent and evaporates easily and give great adhesion to the catalyst on ceramic plate. These catalysts were applied on the ceramic plate. By the same way different catalysts were dissolved in Acetone and were applied on different ceramic plates. Four test samples were obtained and dried at room temperature.

4.6. Testing and Analyzing

The all four plates were installed in a box wrapped in aluminum foil so that exhaust gasses could not escape from the box without coming in contact with the catalysts. The testing was done on the engine exhaust. The boxes were cut according to the dimensions of silencer and were fitted on it with plate facing the front face of exhaust. The Flue Gas Analyzer placed in the exhaust to take the sample of gasses coming out from the catalyst to give results. All the four samples with different molar ratios were tested one by one through the Flue Gas Analyzer (E-Instruments Model: E-4400-S, E-

4400-C) to check the conversion of pollutants by each catalyst. Each catalyst gave different rate of conversion of pollutants as shown in Table 4.4.

Table 4.4: Results without catalytic converter and with different ratio of materials

Test #	Molar Ratios			Pollutants (ppm)		
	Cu	Ce	Mn	CO	NO	HC
1	Without Catalytic Converter			36400	95	37400
2	1	1	1	27400	45	25400
3	2	1	1	28100	61	27700
4	1	2	1	31300	84	29000
5	1	1	2	31100	73	28600

The graph below (Figure 4.4) shows the comparison between different catalysts.

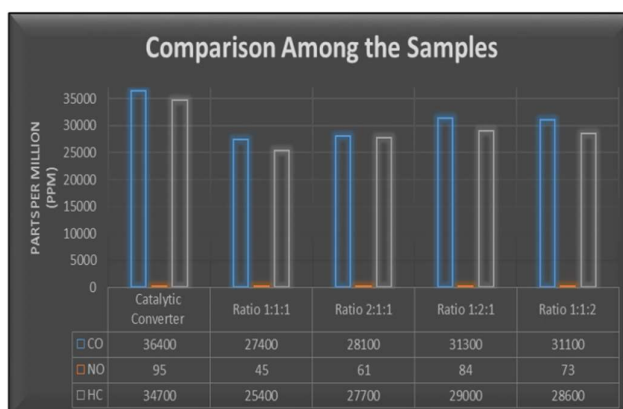


Figure 4.4: Comparison of conversion of all pollutants by each catalyst

On the basis of above discussion and verified results it was decided to choose the base metals in ratio of Cu (1): Ce (1): Mn (1) due to more conversion rate of pollutants as compared to other molar ratios of Cu, Ce and Mn.

4.7. Preparation of New Catalytic Converter

The final catalyst was prepared according to the above given ratios of base metals. The method used for the preparation of the catalyst was same as before when the sample was prepared. The ratios used for preparation of catalyst are shown in table 4.5

Table 4.5: Ratio used in preparation of catalytic converter

Cu	Ce	Mn
5(12.45g)	5(20.2g)	5(8.45g)

After weighing on Electronic Balance, the solution of each was made by dissolving them into a 30ml of distilled water with constant stirring on Magnetic Stirrer. The resultant black solution was obtained after mixing all the solutions. Solution was left for about 5-6 days to obtain mature catalyst. The resultant catalyst was obtained by evaporating the water by use of Rotary Evaporating Apparatus for 3-4 hours which was further crushed into fine powder. After dissolving it in acetone, catalysts were applied on monolithic honeycomb structure of catalytic converter because it counters the phenomenon of back pressure and due to its greater cell density for conversion to less harmful gasses.

4.8. Infrared Spectroscopy of Synthesized Materials

Spectroscopy is a useful method to provide structural clues to the overall molecular structure of the unknown chemical composition, in order to identify them. The large number of wavelengths emitted by this technique, makes it possible to investigate their structures. In figure 4.5, 4.6 and 4.7 it was clearly seen that transmittance value was above 95% which showed that new catalysts materials absorbed less amount of radiation. In figure 4.5, large broad band at 3415 cm^{-1} is ascribed to the O-H stretching vibration in OH⁻ groups of absorb water molecules. The intense band at 500 cm^{-1} corresponds to the Ce-O stretching vibration. A band near 1625 cm^{-1} represents the carbonate like group on the surface of catalyst. Overall FTIR spectra confirm the formation of desired catalyst.

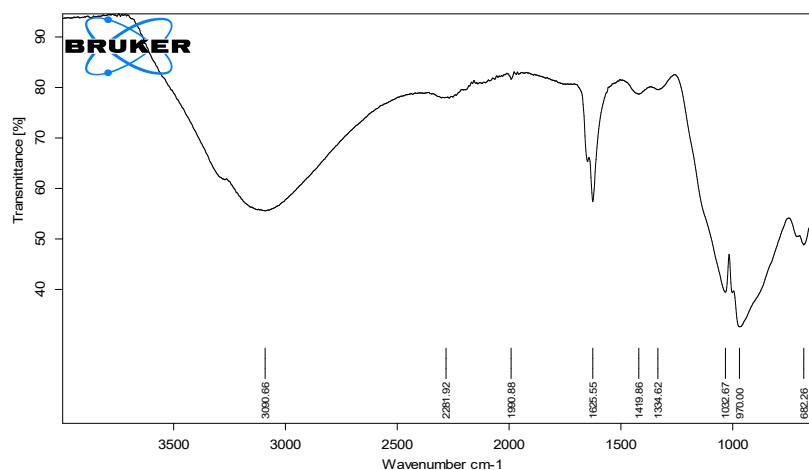


Figure 4.5: Spectroscopy of Cerium Sulphate Tetra hydrate ($\text{CeO}_8\text{S}_2\cdot 4\text{H}_2\text{O}$)

In Figure 4.6 FTIR spectra of $\text{MnSO}_4\cdot\text{H}_2\text{O}$. The bands at around 3200 and 1499 cm^{-1} correspond to the O-H vibrating mode of traces of absorbed water. The bands at about 761.9 , 623.6 and 604.3 cm^{-1} that are below 750 cm^{-1} can be attributed to the Mn-O vibrations. Overall FTIR spectra confirm the formation of desired catalyst.

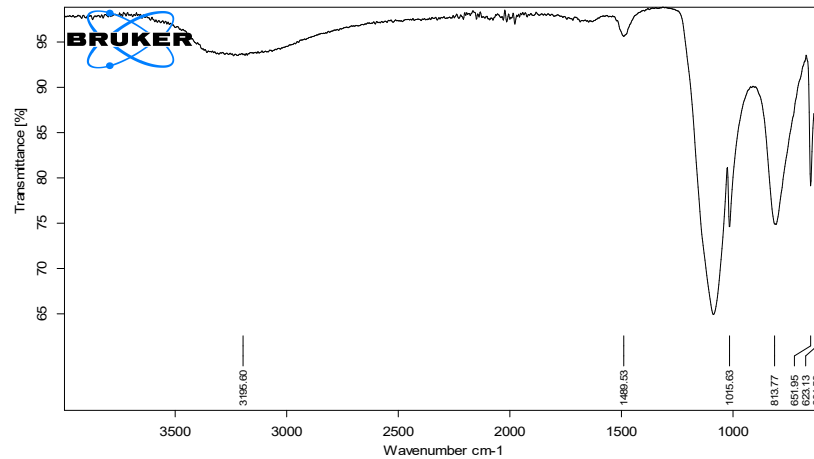


Figure 4.6: Spectroscopy of Manganese Sulphate Mono hydrate ($\text{MnSO}_4 \cdot \text{H}_2\text{O}$)

In Figure 4.7, $\text{CuSO}_4 \cdot 5\text{H}_2\text{O}$ spectrum have the characteristic peaks at the band values of 3114, 1667, 1063 and 860 cm^{-1} . In these spectra, the peaks over 3000 cm^{-1} may explain with the crystal water in structure. The peaks at lower band values can be explained with the vibrations between O and non-metal atoms. Overall FTIR spectra confirm the formation of desired catalyst.

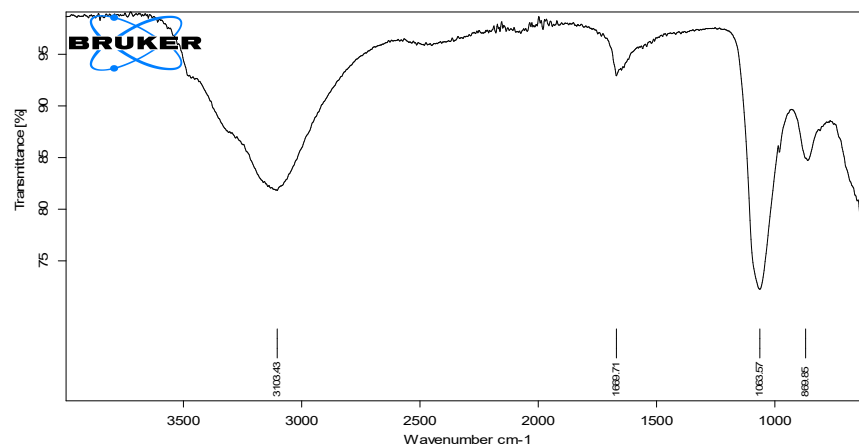


Figure 4.7: Spectroscopy of Copper Sulphate Penta hydrate ($\text{CuSO}_4 \cdot 5\text{H}_2\text{O}$)

4.9. Final Testing and Comparison with Old Installed Catalytic Converter

The original company provided Catalytic Converter that contains the catalyst combination of noble metals like Platinum, Rhodium, and Palladium. Noble metals are very expensive because of limited production which increases their cost. The old catalytic converter was first tested by using flue gas analyzer. The results obtained are shown in Table 4.6.

Table 4.6: Old Catalytic Converter results

Old Catalytic Converter	CO(ppm)	NO(ppm)	HC(ppm)
	17400	213	2900

After removing the old catalytic converter, the upgraded catalytic converter was installed on Engine Test Bench. It was then tested by the flue gas analyzer by placing its probe in exhaust duct. The results obtained are shown in table 4.7.

Table 4.7: Upgraded Catalytic Converter results

Upgraded Catalytic Converter	CO (ppm)	NO (ppm)	HC (ppm)
	7000	203	3800

4.10. Conversion Comparison of Exhaust gases produced by both Catalytic Converter

A graph was plotted to have a clear idea about the conversion efficiency of old and upgraded catalytic converter as depicted in figure 4.8.

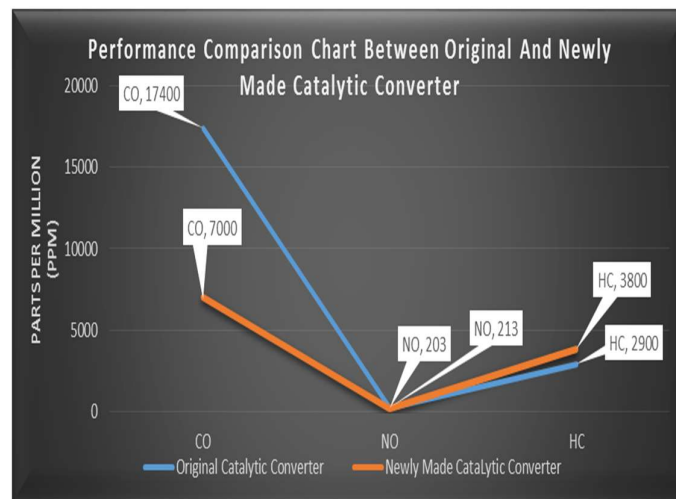
**Figure 4.8: Conversion rate of both Catalytic Converter**

Figure 4.8 shows that there has been a great increase in the conversion rate of CO but slight increase in NO, but there is decrease in conversion rate of HC as compared to the Original Catalytic Converter. The efficiency of conversion of newly manufactured catalytic converter is:

For CO

$$\% \text{ Increase} = \frac{17400 - 7000}{17400} \times 100 = 59.77\%$$

For NO

$$\% \text{ Increase} = \frac{213 - 203}{213} \times 100 = 4.69\%$$

For HC

$$\% \text{ Decrease} = \frac{3800 - 2900}{3800} \times 100 = 23.68\%$$

Upgraded catalytic converter 59.77% and 4.69% efficient in reducing CO and NO respectively. In old manufactured catalytic converter, the precious noble metals like Platinum, Rhodium and Palladium were used which also have limited production. Base metals salts of Cu, Ce and Mn were used as catalysts in newly manufactured catalytic converter which are easily available as well as cost effective.

CHAPTER 05

5.1. Conclusions

It is concluded that when turbine speed is increased, the more power is generated which can be utilized in various engine utilities in addition pressure reduction from inlet to outlet indicates transfer of momentum from the exhaust gases to the turbine. Further focusing on the velocity contour and pressure contour it is clearly indicated that there is no backflow of exhaust gases in an engine. Moreover, it is concluded that the base metal have greater conversion efficiency of CO into CO₂ & NO_x into N₂ as compared to noble metals but in case of HC, original catalytic converter gives good results. But on the basis of prior discussion, it is proved that the base metals have greater efficiency according to its performance and it is economical as well. So, the noble metals which are Platinum, Palladium and Rhodium could be replaced by the base metals Cerium, Manganese and Copper. During the experimentation work it was observed that base metals catalyst have low thermal stability at higher temperature and it adversely alters the performance of the catalysts.

5.2. Future Recommendations

- Fabrication of turbine with different material.
- Making the turbine enclosure more compact.
- To change turbine blade geometry and turbine housing.
- To change inlet/outlet diameter (converge/expand).
- Compare results of petrol engine with diesel engine of same specification.
- The results were obtained by performing tests on different molar ratios (1:1:1, 2:1:1, 1:2:1 and 1:1:2) for the preparation of catalyst. Future study can be done with variation of molar ratios of base metals.
- For current study base metals Cerium, Manganese and Copper were used. In future various base metals can be used as catalysts.
- During the experimentation work it was observed that base metals catalyst have low thermal stability at higher temperature and it adversely altered the performance of the catalyst greatly. Future study can be done to do research on increasing the thermal stability.

REFERENCES

- [1] García, A., Monsalve-Serrano, J., Sari, R., Dimitrakopoulos, N., Tunér, M., & Tunestål, P. (2019). Performance and emissions of a series hybrid vehicle powered by a gasoline partially premixed combustion engine. *Applied Thermal Engineering*, 150, 564-575.
- [2] Gao, J., Chen, H., Tian, G., Ma, C., & Zhu, F. (2019). An analysis of energy flow in a turbocharged diesel engine of a heavy truck and potentials of improving fuel economy and reducing exhaust emissions. *Energy Conversion and Management*, 184, 456-465.
- [3] Ramanathan, A., & Santhoshkumar, A. (2019). Feasibility Analysis of Pyrolysis Waste Engine Oil in CRDI Diesel Engine. *Energy Procedia*, 158, 755-760.
- [4] Herawan, S. G., Talib, K., & Putra, A. (2018). Prediction of heat energy from the naturally aspirated internal combustion engine exhaust gas using artificial neural network. *Procedia Computer Science*, 135, 267-274.
- [5] Davies, C., Thompson, K., Cooper, A., Golunski, S., Taylor, S. H., Macias, M. B., & Tsolakis, A. (2018). Simultaneous removal of NO_x and soot particulate from diesel exhaust by in-situ catalytic generation and utilisation of N₂O. *Applied Catalysis B: Environmental*, 239, 10-15
- [6] Patil, D., & Arakerimath, R. R. (2013). A review of thermoelectric generator for waste heat recovery from engine exhaust. *International Journal of Research In Aeronautical And Mechanical Engineering* 1, 1-9.
- [7] Teo, A. E., Chiong, M. S., Yang, M., Romagnoli, A., Martinez-Botas, R. F., & Rajoo, S. (2019). Performance evaluation of low-pressure turbine, turbo-compounding and air-Brayton cycle as engine waste heat recovery method. *Energy*, 166, 895-907.
- [8] Royale, A., Simic, M., & Lappas, P. (2017). Engine heat sink thermal energy recovery system. *Procedia computer science*, 112, 2406-2415.
- [9] Trabucchi, S., De Servi, C., Casella, F., & Colonna, P. (2017). Design, Modelling, and Control of a Waste Heat Recovery Unit for Heavy-Duty Truck Engines. *Energy Procedia*, 129, 802-809.

- [10] Lion, S., Michos, C. N., Vlaskos, I., Rouaud, C., & Taccani, R. (2017). A review of waste heat recovery and Organic Rankine Cycles (ORC) in on-off highway vehicle Heavy Duty Diesel Engine applications. *Renewable and Sustainable Energy Reviews*, 79, 691-708.
- [11] B.Naveen ,Galindo, J., Fajardo, P., Navarro, R., & García-Cuevas, L. M. (2013). Characterization of a radial turbocharger turbine in pulsating flow by means of CFD and its application to engine modeling. *Applied Energy*, 103, 116-127.
- [12] Aghaali, H., & Ångström, H. E. (2015). A review of turbo compounding as a waste heat recovery system for internal combustion engines. *Renewable and sustainable energy reviews*, 49, 813-824.
- [13] Guduru, K. K., & Ipak, Y. K. (2015). Power Generation by Exhaust Gases on Diesel Engine. *International Journal of Research and Computational Technology*, 7(5), 6-13.
- [14] Chou, S. K., Yang, W. M., Chua, K. J., Li, J., & Zhang, K. L. (2011). Development of micro power generators—a review. *Applied Energy*, 88(1), 1-16.
- [15] Zhao, R., Zhuge, W., Zhang, Y., Yin, Y., Chen, Z., & Li, Z. (2014). Parametric study of power turbine for diesel engine waste heat recovery. *Applied Thermal Engineering*, 67(1-2), 308-319.
- [16] Hatami, M., Ganji, D. D., & Gorji-Bandpy, M. (2014). A review of different heat exchangers designs for increasing the diesel exhaust waste heat recovery. *Renewable and sustainable energy reviews*, 37, 168-181.
- [17] Bari, S., & Rubaiyat, S. (2014). Additional power generation from the exhaust gas of a diesel engine using ammonia as the working fluid (No. 2014-01-0677). SAE Technical Paper.
- [18] Fu, J., Liu, J., Wang, Y., Deng, B., Yang, Y., Feng, R., & Yang, J. (2014). A comparative study on various turbocharging approaches based on IC engine exhaust gas energy recovery. *Applied energy*, 113, 248-257.
- [19] Fu, J., Liu, J., Deng, B., Feng, R., Yang, J., Zhou, F., & Zhao, X. (2014). An approach for exhaust gas energy recovery of internal combustion engine: Steam-assisted turbocharging. *Energy conversion and management*, 85, 234-244.

- [20] Wang, T., Zhang, Y., Zhang, J., Shu, G., & Peng, Z. (2013). Analysis of recoverable exhaust energy from a light-duty gasoline engine. *Applied Thermal Engineering*, 53(2), 414-419.
- [21] Fu, J., Liu, J., Xu, Z., Ren, C., & Deng, B. (2013). A combined thermodynamic cycle based on methanol dissociation for IC (internal combustion) engine exhaust heat recovery. *Energy*, 55, 778-786
- [22] Vallinayagam, R., Vedharaj, S., Yang, W. M., Saravanan, C. G., Lee, P. S., Chua, K. J. E., & Chou, S. K. (2013). Emission reduction from a diesel engine fueled by pine oil biofuel using SCR and catalytic converter. *Atmospheric environment*, 80, 190-197
- [23] Saidur, R., Rezaei, M., Muzammil, W. K., Hassan, M. H., Paria, S., & Hasanuzzaman, M. (2012). Technologies to recover exhaust heat from internal combustion engines. *Renewable and sustainable energy reviews*, 16(8), 5649-5659.
- [24] Kuzstelan, A., Yao, Y. F., Marchant, D. R., & Wang, Y. (2011). A review of novel turbocharger concepts for enhancements in energy efficiency. *Int. J. of Thermal & Environmental Engineering*, 2(2), 75-82.
- [25] Saidur, R. (2010). A review on electrical motors energy use and energy savings. *Renewable and sustainable energy reviews*, 14(3), 877-898.
- [26] Madloul, N. A., Saidur, R., Hossain, M. S., & Rahim, N. A. (2011). A critical review on energy use and savings in the cement industries. *Renewable and Sustainable Energy Reviews*, 15(4), 2042-2060.
- [27] Saidur, R., Patil, D. S., Arakerimath, R. R., & Walke, P. V. (2010). Thermoelectric materials and heat exchangers for power generation—A review. *Renewable and Sustainable Energy Reviews*, 95, 1-22.
- [28] Zhang, Z., Jia, P., Feng, S., Liang, J., Long, Y., & Li, G. (2018). Numerical simulation of exhaust reforming characteristics in catalytic fixed-bed reactors for a natural gas engine. *Chemical Engineering Science*, 191, 200-207
- [29] Togun, N. K., & Baysec, S. (2010). Prediction of torque and specific fuel consumption of a gasoline engine by using artificial neural networks. *Applied Energy*, 87(1), 349-355.

- [30] Zhang, Y., Chen, T., Zhuge, W., Zhang, S., & Xu, J. (2010). An integrated turbocharger design approach to improve engine performance. *Science in China Series E: Technological Sciences*, 53(1), 69-74.
- [31] Leduc, P., Dubar, B., Ranini, A., & Monnier, G. (2003). Downsizing of gasoline engine: an efficient way to reduce CO₂ emissions. *Oil & gas science and technology*, 58(1), 115-127.
- [32] Guo et al., "Catalytic performance of manganese doped CuO–CeO₂ catalysts for selective oxidation of CO in hydrogen-rich gas," *Fuel*, pp. 56-64, 2016.
- [33] Qi and Li, "NO oxidation to NO₂ over manganese-cerium mixed oxides," *Catalysis Today*, pp. 205-213, 2015
- [34] Zhao et al., "Effect of the loading content of CuO on the activity and structure of CuO/Ce-Mn-O catalysts for CO oxidation," *J. Rare Earths*, vol. 604, 2015.
- [35] Alphonse, "Co–Mn-oxide spinel catalysts for CO and propane oxidation at mild temperature," *Applied Catalysis B: Environmental*, pp. 715-725, 2016
- [36] Vasilyeva, M. S., & Rudnev, V. S. Composition, surface structure and catalytic properties of manganese-and cobalt-containing oxide layers on titanium. In *Advanced Materials Research* (Vol. 875, pp. 351-355). Trans Tech Publications Ltd. 2014
- [37] Srivastava et al., "Catalytic removal of carbon monoxide over carbon supported palladium catalyst," *Journal of hazardous materials*, vol. 241, pp. 463-471, 2012.
- [38] Pakharukova et al., "Copper–cerium oxide catalysts supported on monoclinic zirconia: Structural features and catalytic behavior in preferential oxidation of carbon monoxide in hydrogen excess," *Applied Catalysis A: General*, pp. 159-164, 2009.
- [39] Wojciechowska et al., "CO oxidation catalysts based on copper and manganese or cobalt oxides supported on MgF₂ and Al₂O₃," *Catalysis Today*, pp. 338-341, 2007.
- [40] Marban and Fuertes, "Highly active and selective CuO_x/CeO₂ catalyst prepared by a single-step citrate method for preferential oxidation of carbon monoxide," *Applied Catalysis B: Environmental*, pp. 43-53, 2005

- [41] Hoflund et al., "Effect of CO₂ on the performance of Au/MnO_x and Pt/SnO_x low-temperature CO oxidation catalysts," *Langmuir*, pp. 3431-3434, 1995.
- [42] Basel I. Ismail, Wael H. Ahmed, "Thermoelectric Power Generation Using Waste-Heat Energy as an Alternative Green Technology," *Recent Patents on Electrical Engineering*, 2009, 2, pp. 27-39

APPENDICES



Article

Fabrication of Catalytic Converter with Different Materials and Comparison with Existing Materials in Addition to Analysis of Turbine Installed at the Exhaust of 4 Stroke SI Engine

Roman Kalvin ^{1,2}, Juntakan Taweekun ^{3,*}, Kittinan Maliwan ³ and Hafiz Muhammad Ali ^{4,5,*}

¹ Energy Technology Program, Faculty of Engineering, Prince of Songkla University Hatyai, Songkhla 90110, Thailand; romankalvin12@gmail.com

² Department of Mechanical Engineering, University of Wah, Wah Cantt 47040, Pakistan

³ Department of Mechanical and Mechatronics Engineering, Faculty of Engineering, Prince of Songkla University Hatyai, Songkhla 90110, Thailand; mkittina@gmail.com

⁴ Mechanical Engineering Department, King Fahd University of Petroleum and Minerals (KFUPM), Dhahran 31261, Saudi Arabia

⁵ Interdisciplinary Research Center for Renewable Energy and Power Systems (IRC-REPS), King Fahd University of Petroleum and Minerals, Dhahran 31261, Saudi Arabia

* Correspondence: juntakan.t@psu.ac.th (J.T.); hafiz.ali@kfupm.edu.sa (H.M.A.)



Citation: Kalvin, R.; Taweekun, J.; Maliwan, K.; Ali, H.M. Fabrication of Catalytic Converter with Different Materials and Comparison with Existing Materials in Addition to Analysis of Turbine Installed at the Exhaust of 4 Stroke SI Engine. *Sustainability* **2021**, *13*, 470. <https://doi.org/10.3390/su131810470>

Academic Editor: Changhyun Roh

Received: 30 August 2021

Accepted: 17 September 2021

Published: 21 September 2021

Publisher's Note: MDPI stays neutral with regard to jurisdictional claims in published maps and institutional affiliations.



Copyright: © 2021 by the authors. Licensee MDPI, Basel, Switzerland. This article is an open access article distributed under the terms and conditions of the Creative Commons Attribution (CC BY) license (<https://creativecommons.org/licenses/by/4.0/>).

Abstract: Harmful pollutants (CO, NO, and unburnt hydrocarbons) coming out from the exhaust manifold of an engine must be converted into harmless gases by using catalytic converter. This field has seen vast research for increasing the conversion efficiency of pollutants by using different cheap metals. Nowadays, catalysts used in catalytic converter are noble metals, and they are also critical in the sense that they are not abundant on Earth. Platinum, palladium and rhodium are very expensive; hence, low-cost cars are not installed with catalytic converter, especially in third world countries. This research has been carried out to assess the catalytic activity of catalysts made from the salt/metal precursors, cerium sulphate tetra hydrate, manganese sulphate mono hydrate and copper sulphate penta hydrate that are not expensive and also less affected by the poison. Test sample catalysts were prepared through a coprecipitation method having different molar concentrations, and then tested for the conversion efficiency by applying the catalysts on ceramic plates by using flue gas analyzer. On the basis of the results, final catalysts were prepared and applied on a monolithic ceramic plate and then tested with regard to the resulting conversion rate of pollutants as compared to already installed catalytic converter. Moreover, turbine was installed in the exhaust passage to generate the power that would be utilized to run the electrical accessories of the engine. SOLIDWORKS were used for 3D CAD modeling and the flow analysis of turbine with radial inlet-axial outlet. In addition, ANSYS was used for stress-strain analysis.

Keywords: catalytic converter; noble metals; base metals; gas analyzer; pollutants; solidworks; ansys

1. Introduction

A catalytic converter is a device that converts harmful pollutants, such as CO, nitrogen oxides, and unburnt hydrocarbons into less harmful pollutants by catalytic activity through the process of redox reactions. The pollutants are converted to CO₂, N₂, O₂, and H₂O, respectively, which are less harmful to humans as well as to the environment. These pollutants are responsible for ozone depletion and global warming. They have hazardous effects on human health that cause problems related to the respiratory system, as well as general health problems. Nitrogen oxide is responsible for smog formation and acid rain. In this study, the materials that were already used in catalytic converter were replaced by base earth metals that are not as expensive. Test sample catalysts were prepared, and the experimentation was performed.

After rigorous study of the literature, it was concluded that most of the research work was done on the selection of appropriate base metal catalysts for the redox reaction occurring inside the catalytic converter, in place of noble earth metals, because they are not only expensive but also have limited production. Guo et al. studied copper oxide along with cerium oxide and combined the doping of manganese oxide. The final catalyst was $\text{CuO}_x\text{-MnO}_x\text{-CeO}_2$, which gave more than a 99% conversion of CO "Guo16" [1].

Qi and Li considered the oxidization of NO to NO_2 by using a catalyst that was a mixture of manganese and cerium oxides. The catalyst obtained conversion at about 350 °C with a percentage of ranging from 50 to 70% [2]. Zhao et al. prepared CuO/Ce-Mn-O catalyst for the conversion of CO to CO_2 "Zha15" [3]. The catalyst gave an almost complete conversion of CO at 160 °C. Alphonse used $\text{Co}_x\text{Mn}_3-x\text{O}_4$ oxides as a catalyst for the oxidation of CO and propane at mild temperatures. Co-Mn oxide spinel catalyst gave conversion of CO from 20 to 300 °C [4]. Vasilyeva et al. prepared catalyst with Mn oxides, Si oxides, and Ti oxides for the conversion or oxidation of CO "Vas14" [5]. This catalyst gave 50% conversion at 150 °C, and 100% conversion at about 210 °C. (Srivastava et al., 2012) used carbon-supported palladium catalyst for the removal of carbon monoxide: 5% Pd was coated on CeO_2 and ZrO_2 that have a CO to CO_2 conversion of 100% at 108 °C and 140 °C [6]. Pakharukova et al. used the catalyst copper cerium oxide with monoclinic zirconia for assessing the oxidation of CO with excess of hydrogen and the catalyst obtained 100% conversion at 130 °C "Pak09" [7]. Wojciechowska et al. used catalyst for the oxidation of CO by using copper and manganese, or cobalt oxides, supported on MgF_2 and Al_2O_3 [8]. This catalyst gave a much smaller percentage of CO conversion of 51% at 300 °C for 15 min. Marbán and Fuertes used copper oxide and cerium oxide for the oxidation of CO. This catalyst obtained 90% conversion at about 165 °C "Mar05" [9]. Hoflund et al. used gold with a MnO catalyst for the low-temperature oxidation of CO. This catalyst obtained about 90 to 100% conversion at about 225 °C in 17,000 min. [10].

Energy is extracted by placing the turbine in an exhaust gas passage. Two-thirds of the energy from combustion in a vehicle is lost as waste heat, of which 40% is in the form of exhaust gases. Exhaust from an engine is used to generate electricity and can be stored in the battery after rectification for later consumption in various utilities. Hence stress and strain analysis have been carried out on the turbine. Podesvin et al. provided a 3D CFD template for the friction failures of the turbocharger bearing [11]. Alessandro et al. performed an experiment on the turbocharger efficiency, under nonadiabatic circumstances, to evaluate the thermal transfer effect. Quantify thermal fluxes through the use of the turbocharger evaluated their impact on engine reliability decay [12]. Deligant et al. discussed the impact of axial force, oil inlet pressure, the delivery of rubbing force and oil mass stream among the push bearing and journal bearings, and the reckoning models for estimating the friction losses of the journal and thrust bearings [13]. Mueller et al. carried out the optimization of radial turbine by using a two-level optimization algorithm created by the von Karman Institute for Fluid Dynamics [14]. Ravindra et al. provided a guideline on the methods utilized in turbocharging to upsurge the engine productivity and decrease the exhaust gas secretion levels. Turbocharging is good with regard to economic considerations and engine efficiency [15]. Emara et al. developed flow simulation modeling and performance prediction for the centrifugal compressor of a substantial diesel engine. Its results indicate that the developed mathematical computation model can give better predictions of performance for a centrifugal compressor stage in a turbocharger system [16]. Salh et al. computationally analyzed the blade angle of the turbine rotor. He found that the blade angle impacts the air-compressed wheel's stream area [17].

2. Selection of Catalyst Materials

After extensive research and study of the literature review, it has been observed that the important factors that must be considered for the selection of materials are: cost-effectiveness; the easy precipitation from its saturated solution; and having thermal durability and resistance to poison Sulphur, phosphorus, and lead. The best catalysts should have

good active sites for the adsorption and desorption of the molecules of the pollutants. From the literature review, it is observed that the cerium, manganese, and copper nano particles have a great conversion rate for CO, NO_x and HC. Thus, they are the best option for the synthesis of catalytic converter. Selected sulphates of these metals are cerium sulphate tetra hydrate (CeO₈S₂·4H₂O), manganese sulphate mono hydrate (MnSO₄·H₂O), and copper sulphate penta hydrate (CuSO₄·5H₂O), which fulfill all the required factors explained above for the selection of the best catalysts for achieving the maximum conversion of pollutants.

3. Preparation of Sample Catalysts

Firstly, for the preparation of the saturated solution of each salt for the purpose of the coprecipitation of the catalysts, distilled water was selected as a solvent because all three base salts are easily soluble in water at room temperature. For the preparation of sample catalysts, the correct molar ratio for each base metal was selected for the best combination, as shown in Table 1.

Table 1. Molar ratio for base metal.

Cu	Ce	Mn
1 (2.49 g)	1 (4.04 g)	1 (1.69 g)
1 (2.49 g)	2 (8.08 g)	1 (1.69 g)
1 (2.49 g)	1 (4.04 g)	2 (3.38 g)
2 (4.98 g)	1 (4.04 g)	1 (1.69 g)

For the first sample catalyst, having all the base metal in a 1:1:1 combination, the correct molar ratio for each base metal was selected. For the measurement of each metal salt, an electronic balance having precision up to three decimals was used according to the required weights, as shown in Table 1. For four test samples, the required combination of metals are weighed in grams in the electronic balance apparatus shown in Figure 1.



Figure 1. Metals weight on electronic balance.

For (CeO₈S₂·4H₂O), having a molecular weight of 404.304 g/mol, and yellow in color, 0.001 molar solution was prepared in 10 mL of distilled water by dissolving 4.04 g of salt with constant stirring for 5–10 min. After the solution was placed on the magnetic stirrer for 30 min, the complete dissolution of cerium sulphate in water and saturated solution was obtained. In the same manner, the manganese sulphate mono hydrate (MnSO₄·H₂O), having a pale white color, and copper sulphate penta hydrate (CuSO₄·5H₂O), which has a blue physical appearance and having a molecular weight of 169.02 g/mol and 249.677 g/mol, respectively, were dissolved in 10 mL of distilled water to prepare 0.001 molar solution of each base metal salt with constant stirring on a magnetic stirrer for about 30 min each. Molar solution of each base metal in distilled water is shown in Figure 2.



Figure 2. Metal salts solution.

All the above sample solutions of metal salts were poured in a beaker with constant stirring until a chemical reaction occurred between base salts metals. The resultant solution was dark brown in color, which indicated that the reaction had been completed. The resultant solution contained the precipitates of the catalyst. Like the preparation of Sample 1, all four samples were prepared by dissolving the base metals in water in different ratios after weighing on an electronic balance, and stirring through a magnetic stirrer according to the table provided above, so that the best combination of base metals could be selected for the preparation of the final catalyst that gives the best results for the conversion of pollutants into less harmful pollutants. According to Table 1, four samples were prepared, having different molar ratios, as shown below.

Cu: Ce: Mn = 1:1:1

Cu: Ce: Mn = 1:1:2

Cu: Ce: Mn = 1:2:1

Cu: Ce: Mn = 2:1:1

All four samples obtained were kept at room temperature for 4–6 days in open air and in a vibrationless place; otherwise, the base metal catalyst particles could again dissolve back into solution and, thus, lengthen the process. The process of the crystallization of the saturated solutions is referred to as the coprecipitation method. After 2 days, crystals began initiating in the solutions and started settling down at the bottom of the beaker. The process of crystallization was completed in 6 days, where matured crystals were developed in a solution, which can be easily seen by the naked eye. To completely filter the catalysts, a vacuum suction assembly apparatus was used. The dark brown color of the catalyst was obtained and it was kept at room temperature to completely dry the catalyst. Four sample catalysts were obtained in dried form which acted as a conversion agent for the pollutants.

4. Preparation of Test Samples

The next step was the application of the catalysts on the ceramic plates, having uniform thickness and pores, so that the exhaust gases can easily flow out and react on their way out to the atmosphere. Ceramic plates also have great thermal resistance, as exhaust gasses have very high temperatures. The catalysts were dissolved in acetone, which is an excellent solvent, evaporates easily, and obtains good adhesion to the catalyst on the ceramic plate. These catalysts were applied on the ceramic plate. In the same way, different catalysts were dissolved in acetone and were applied on different ceramic plates. Four test samples were obtained and dried at room temperature.

5. Testing and Analyzing

All four plates were installed in a box wrapped in aluminum foil so that the exhaust gasses could not escape from the box without coming into contact with the catalysts. The testing was done on the engine exhaust. The boxes were cut according to the dimensions of the silencer and were fitted on it with the plate facing the front face of the exhaust. The

flue gas analyzer was placed in the exhaust to take a sample of the gasses coming out from the catalyst to give results. All four samples, with different molar ratios, were tested one by one through the flue gas analyzer (E-Instruments Model: E-4400-S, E-4400-C) to check the conversion of pollutants by each catalyst. Each catalyst gave different rates for the conversion of pollutants, as shown in Table 2.

Table 2. Results without catalytic converter and with different ratios of materials.

Test No.	Mole Ratios			Pollutants (ppm)		
	Cu	Ce	Mn	CO	NO	HC
1	Without Catalytic Converter			36,400	95	37,400
2	1	1	1	27,400	45	25,400
3	2	1	1	28,100	61	27,700
4	1	2	1	31,300	84	29,000
5	1	1	2	31,100	73	28,600

The graph below (Figure 3) shows the comparison between different catalysts.

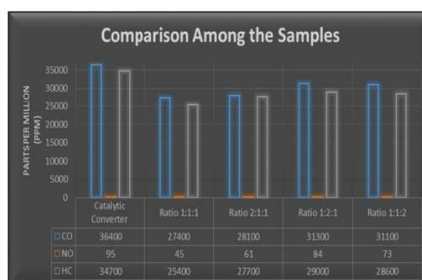


Figure 3. Comparison of conversion of all pollutants by catalysts.

On the basis of the above discussion and verified results, it was decided to choose the base metals in the ratios of Cu (1): Ce (1): Mn (1) because of the higher conversion rate of pollutants as compared to the other molar ratios of Cu, Ce and Mn.

6. Preparation of New Catalytic Converter

The final catalyst was prepared according to the above given ratios of the base metals. The method used for the preparation of the catalyst was the same as when the sample was prepared before. The ratios used for the preparation of the catalyst are shown in Table 3.

Table 3. Ratio used in preparation of catalytic converter.

Cu	Ce	Mn
5 (12.45 g)	5 (20.2 g)	5 (8.45 g)

After being weighed on the electronic balance, the solution of each was made by dissolving them into 30 mL of distilled water with constant stirring on a magnetic stirrer. The resultant black solution was obtained after mixing all the solutions. The solution was left for about 5–6 days in order to obtain the mature catalyst. The resultant catalyst was obtained by evaporating the water by use of a rotary evaporating apparatus for 3–4 h, which was then further crushed into a fine powder. After being dissolved in acetone, the catalysts were applied on a monolithic honeycomb structure of catalytic converter because

it counters the phenomenon of back pressure due to its greater cell density for conversion to less harmful gasses.

7. Infrared Spectroscopy of Synthesized Materials

Spectroscopy is a useful method for providing structural clues as to the overall molecular structure of the unknown chemical composition in order to identify it. The large number of wavelengths emitted by this technique makes it possible to investigate their structures. In Figures 4–6, it is clearly observed that the transmittance value was above 95%, which showed that the new catalyst materials absorbed a smaller amount of radiation. In Figure 4, large broad band at 3415 cm^{-1} is ascribed to the O-H stretching vibration in the OH- groups of absorbent water molecules. The intense band at 500 cm^{-1} corresponds to the Ce-O stretching vibration. A band near 1625 cm^{-1} represents the carbonate-like group on the surface of the catalyst. Overall, FTIR spectra confirm the formation of the desired catalyst.

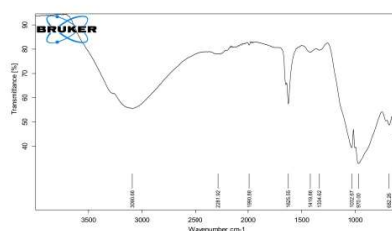


Figure 4. Spectroscopy of cerium sulphate tetra hydrate ($\text{CeO}_8\text{S}_2\cdot 4\text{H}_2\text{O}$).

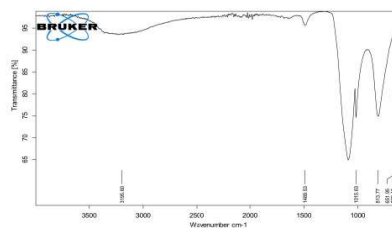


Figure 5. Spectroscopy of manganese sulphate mono hydrate ($\text{MnSO}_4\cdot\text{H}_2\text{O}$).

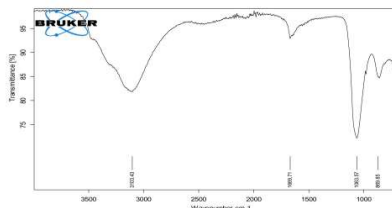


Figure 6. Spectroscopy of copper sulphate penta hydrate ($\text{CuSO}_4\cdot 5\text{H}_2\text{O}$).

In Figure 5 that presents the FTIR spectra of $\text{MnSO}_4\cdot\text{H}_2\text{O}$, the bands at around 3200 and 1499 cm^{-1} correspond to the O-H vibrating modes of the traces of absorbed water.

The bands at 761.9, 623.6, and 604.3 cm^{-1} that are below 750 cm^{-1} can be attributed to the Mn–O vibrations. Overall, the FTIR spectra confirm the formation of the desired catalyst.

In Figure 6, a $\text{CuSO}_4 \cdot 5\text{H}_2\text{O}$ spectrum has the characteristic peaks at the band values of 3114, 1667, 1063, and 860 cm^{-1} . In these spectra, the peaks over 3000 cm^{-1} may be explained by the crystal water in the structure. The peaks at lower band values can be explained as the vibrations between O and nonmetal atoms. Overall, FTIR spectra confirm the formation of the desired catalyst.

8. Final Testing and Comparison with Old Installed Catalytic Converter

The original company provided catalytic converter that contains the catalyst combination of noble metals, such as platinum, rhodium, and palladium. Noble metals are very expensive because of their limited production, which increases their cost. The old catalytic converter was first tested by using flue gas analyzer. The results obtained are shown in Table 4.

Table 4. Old catalytic converter results.

Old Catalytic Converter	CO (ppm)	NO (ppm)	HC (ppm)
	17,400	213	2900

After removing the old catalytic converter, the upgraded catalytic converter was installed on an engine test bench. It was then tested by the flue gas analyzer by placing its probe in the exhaust duct. The results obtained are shown in Table 5.

Table 5. Upgraded catalytic converter results.

Upgraded Catalytic Converter	CO (ppm)	NO (ppm)	HC (ppm)
	7000	203	3800

8.1. Conversion Comparison of Exhaust Gases Produced by Both Catalytic Convertors

A graph was plotted to have a clear idea as to the conversion efficiency of the old and upgraded catalytic converter, as depicted in Figure 7.

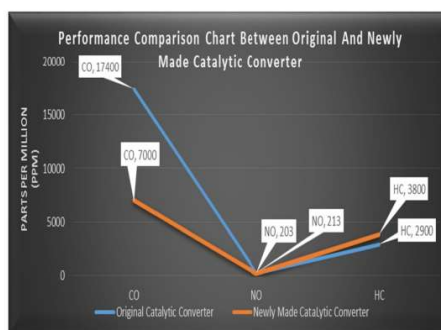


Figure 7. Conversion rate of both catalytic converters.

Figure 7 shows that there has been a strong increase in the conversion rate of CO, but a slight increase in NO. There is decrease in the conversion rate of HC as compared to the original catalytic converter. The efficiency of the conversion of newly manufactured catalytic converter is:

For CO

$$\% \text{ Increase} = \frac{17400 - 7000}{17400} \times 100 = 59.77\% \quad (1)$$

For NO

$$\% \text{ Increase} = \frac{213 - 203}{213} \times 100 = 4.69\% \quad (2)$$

For HC

$$\% \text{ Decrease} = \frac{3800 - 2900}{3800} \times 100 = 23.68\% \quad (3)$$

Upgraded catalytic converter, 59.77% and 4.69% efficient in reducing CO and NO, respectively.

8.2. Cost Comparison

In the old manufactured catalytic converter, the precious noble metals, such as platinum, rhodium, and palladium were used, which also have limited production. Base metals salts of Cu, Ce, and Mn were used as catalysts in the newly manufactured catalytic converter, which are easily available as well as cost-effective.

9. 3D Modeling, Stress-Strain, and Flow Analysis of Turbine

The aim of the study was to install the turbine in the exhaust passage to extract power from the exhaust gases, which would later be utilized to run the electrical accessories of the engine. For this purpose, a typical turbine was modeled over SOLIDWORKS. The 2D drawing of the turbine with various views is shown in Figure 8a, and a machined turbine is shown in Figure 8b.

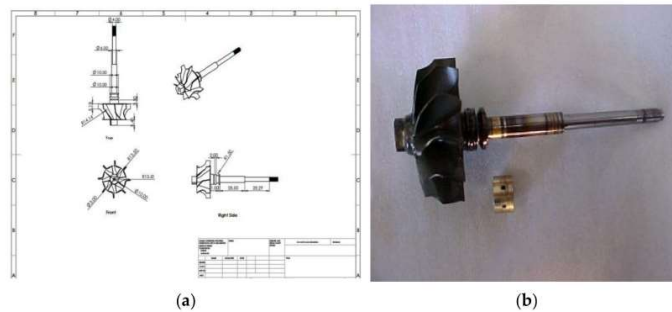


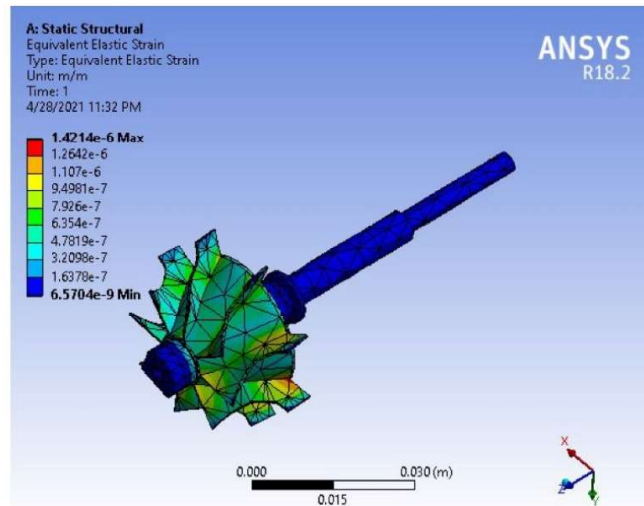
Figure 8. (a) 2D and Isometric view of Turbine; (b) Machined Turbine.

The power generated from the exhaust gases of an internal combustion engine is a process of the production of energy. The engine converts chemical energy into mechanical energy, and waste is extracted in the form of exhaust gases from the engine, which further moves towards the tail pipe of an engine. These gases move at high temperatures and pressures towards the outlet. The turbine is placed in the pathway of these exhaust gases which is designed in a way so that these exhaust gases tend to rotate the blades of the turbine, following the measurements that were taken by the help of a tachometer, as shown in Table 6.

Table 6. Turbine speed.

Sr. No	Engine Speed (RPM)	Turbine Speed (RPM)
1	1000	110
2	3500	318
3	5500	451

The strain analysis of the turbine was done at a 5500 engine speed (rpm), and is shown in Figure 9. The static structural analysis on ANSYS was carried out and equivalent elastic strain distributions on various section of the turbine is shown below with the minimum value at the turbine shaft, i.e., 6.5×10^{-9} m/m, and the maximum value was observed where the exhaust flow at the inlet of the turbine casing exerts a force on the turbine blade, which produces the maximum elastic strain at the edge of the turbine blade, right in front of the turbine casing inlet. The maximum value of the equivalent elastic strain observed was 1.42×10^{-6} m/m.

**Figure 9.** Strain analysis of the turbine.

Stress analysis of the turbine was done at 5500 engine speed (rpm) and is shown in Figure 10. The static structural analysis on ANSYS was carried out, and the equivalent elastic stress distribution on various sections of the turbine is shown below, with the minimum value at the turbine shaft, i.e., 932.35 Pa, and the maximum value observed at the edge of the turbine blade, right in front of the turbine casing inlet is 2.46×10^5 Pa, which is in the range and majority section. The observed Von Mises stress value is 55,588 Pa.

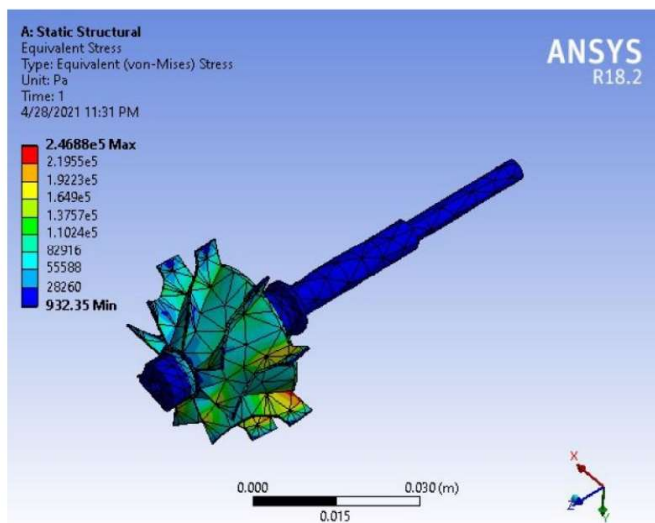


Figure 10. Stress analysis of the turbine.

In Figure 11a,b it is clearly observed that there is no backflow of the exhaust gases. Hence, there is no excess load produced on the engine. The inlet and outlet values of pressure are 136,846.86 Pa and 101,718.72 Pa. The inlet value of the velocity is 7.6 m/s, and the outlet value is in the range of 3.04 m/s–6.08 m/s.

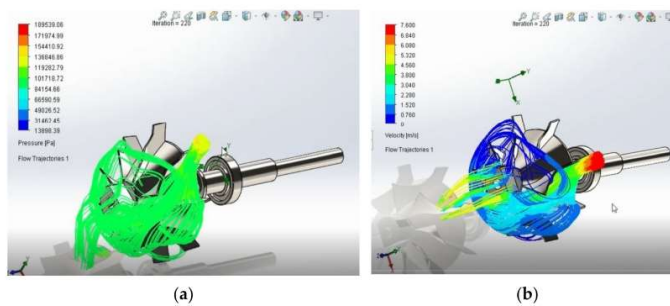


Figure 11. (a) Pressure contours turbine; (b) velocity contours turbine.

10. Conclusions

From the above discussion and experimentation, it is concluded that base metals have greater conversion efficiency of CO into CO₂, and NO_x into N₂, as compared to noble metals. However, in the case of HC, original catalytic converter gives good results. On the basis of the prior discussion, it is proven that base metals have greater efficiency according to their performance, and that they are economical as well. Thus, the noble metals, which are platinum, palladium, and rhodium, could be replaced by the base metals

cerium, manganese, and copper. During the experimentation work, it was observed that base metals catalysts have low thermal stability at higher temperatures and this adversely alters the performance of the catalysts.

Moreover, the pressure reduction from the inlet to the outlet indicates the transfer of momentum from the exhaust gases to the turbine. Further focus on the velocity contour and pressure contour clearly indicates that there is no backflow of the exhaust gases in an engine.

Author Contributions: Conceptualization, R.K. and J.T.; methodology, R.K.; software, R.K.; validation, R.K.; formal analysis, R.K.; investigation, R.K. and J.T.; resources, R.K.; data curation, R.K.; writing—original draft preparation, R.K.; writing—review and editing, R.K.; visualization, J.T. and K.M.; supervision, J.T. and H.M.A.; project administration, J.T. and H.M.A.; funding acquisition, R.K. and J.T. All authors have read and agreed to the published version of the manuscript.

Funding: This research received no external funding.

Institutional Review Board Statement: Not applicable.

Informed Consent Statement: Not applicable.

Data Availability Statement: Not applicable.

Acknowledgments: This work was supported by the Interdisciplinary Graduate School of Energy Systems, Prince of Songkla University. Special thanks to University of Wah, M. Ahsaan Yousaf, M. Wajahat Rasool and Maryam Arshad for the fabrication of engine bench, catalytic converter and facilitation.

Conflicts of Interest: The authors declare no conflict of interest.

References

- Guo, X.; Li, J.; Zhou, R. Catalytic performance of manganese doped CuO–CeO₂ catalysts for selective oxidation of CO in hydrogen-rich gas. *Fuel* **2016**, *163*, 56–64. [[CrossRef](#)]
- Qi, G.; Li, W. NO oxidation to NO₂ over manganese-cerium mixed oxides. *Catal. Today* **2015**, *258*, 205–213. [[CrossRef](#)]
- Zhao, F.; Gong, M.; Zhang, G.; Li, J. Effect of the loading content of CuO on the activity and structure of CuO/Ce–Mn–O catalysts for CO oxidation. *J. Rare Earths* **2015**, *33*, 604–610. [[CrossRef](#)]
- Alphonse, P. Alphonse Co–Mn-oxide spinel catalysts for CO and propane oxidation at mild temperature. *Appl. Catal. B Environ.* **2016**, *180*, 715–725.
- Vasilyeva, M.S.; Rudnev, V.S. Composition, surface structure and catalytic properties of manganese-and cobalt-containing oxide layers on titanium. *Adv. Mater. Res.* **2014**, *875*, 351–355. [[CrossRef](#)]
- Srivastava, A.K.; Saxena, A.; Shah, D.; Mahato, T.H.; Singh, B.; Shrivastava, A.R.; Gutch, P.K.; Shinde, C.P. Catalytic removal of carbon monoxide over carbon supported palladium catalyst. *J. Hazard. Mater.* **2012**, *241*, 463–471. [[CrossRef](#)] [[PubMed](#)]
- Pakharukova, V.P.; Moroz, E.M.; Kriventsov, V.V.; Zyuzin, D.A.; Kosmambetova, G.R.; Strizhak, P.E. Copper–cerium oxide catalysts supported on monoclinic zirconia: Structural features and catalytic behavior in preferential oxidation of carbon monoxide in hydrogen excess. *Appl. Catal. A Gen.* **2009**, *365*, 159–164. [[CrossRef](#)]
- Wojciechowska, M.; Przystajko, W.; Zieliński, M. CO oxidation catalysts based on copper and manganese or cobalt oxides supported on MgF₂ and Al₂O₃. *Catal. Today* **2007**, *119*, 338–341. [[CrossRef](#)]
- Marbán, G.; Fuertes, A.B. Marban and Fuertes Highly active and selective CuO_x/CeO₂ catalyst prepared by a single-step citrate method for preferential oxidation of carbon monoxide. *Appl. Catal. B Environ.* **2005**, *57*, 43–53. [[CrossRef](#)]
- Hoflund, G.B.; Gardner, S.D.; Schryer, D.R.; Upchurch, B.T.; Kielin, E.J. Effect of CO₂ on the performance of Au/MnO_x and Pt/SnO_x low-temperature CO oxidation catalysts. *Langmuir* **1995**, *11*, 3431–3434. [[CrossRef](#)]
- Deligant, M.; Podevin, P.; Descombes, G. CFD model for turbocharger journal bearing performances. *Appl. Eng.* **2011**, *31*, 811–819. [[CrossRef](#)]
- Romagnoli, A.; Martinez-Botas, R. Heat transfer analysis in a turbocharger turbine: An experimental and computational evaluation. *Appl. Therm. Eng.* **2012**, *38*, 58–77. [[CrossRef](#)]
- Deligant, M.; Podevin, P.; Descombes, G. Experimental identification of turbocharger mechanical friction losses. *Energy* **2012**, *39*, 388–394. [[CrossRef](#)]
- Mueller, L.; Alsalihi, Z.; Verstraete, T. Multidisciplinary optimization of a turbocharger radial turbine. *J. Turbomach.* **2013**, *135*, 021022. [[CrossRef](#)]
- Sanap, R.S.; Gite, R.E.; Patel, K.M.; Patel, D.H. Design and Development of Turbo-Charger for Two Stroke Engine. *Int. Adv. Res. J. Sci. Eng. Technol.* **2016**, *3*, 144–149.

16. Soliman, I.M.; Emara, A.A.; Razeq, A.M.E.; Moneib, H.A. Modeling and CFD Analysis of Air Flow through Automotive Turbocharger Compressor: Analytical Approach and Validation. In Proceedings of the International Conference on Aerospace Sciences and Aviation Technology, Cairo, Egypt, 11–13 April 2017; Volume 17, pp. 1–15.
17. Sawadi, A.S.; Shkhair, M.M.; Tilefih, R.J. Optimize and Analysis Compressor Wheel of Turbo Charger. *J. Mech. Eng. Res. Dev.* **2018**, *41*, 59–64. [[CrossRef](#)]



Journal of Advanced Research in Fluid Mechanics and Thermal Sciences

Journal homepage: www.akademiabaru.com/arfmts.html
ISSN: 2289-7879



Investigation of Chip Formation and its Grain Structure using Vegetable Oil Based Lubricants

Roman Kalvin^{1,3}, Juntakan Taweekun^{2,*}, Muhammad Waqas Mustafa³, Saba Arif¹, Abdullah Javed³

¹ Energy Technology Program, Faculty of Engineering, Prince of Songkla University Hat Yai, Thailand

² Department of Mechanical Engineering, Faculty of Engineering, Prince of Songkla University Hat Yai, 90112 Songkhla, Thailand

³ Department of Mechanical Engineering, Wah Engineering College, Wah Cantt. Pakistan

ARTICLE INFO	ABSTRACT
<p>Article history: Received 29 March 2021 Received in revised form 1 June 2021 Accepted 9 June 2021 Available online 17 July 2021</p> <p>Keywords: Vegetable oils; drilling; chip structure; mild steel</p>	<p>This research aims to compare the chips formed by using different vegetable oil based lubricants such as coconut oil, cooking oil, hair oil etc. For this purpose, drilling was affordable and easy process which was used. The process was applied on AISI 1080 Mild Steel and chips and their grain structure were examined through Material Testing Microscope model TESCAN (MIRA 3 XMU Type) to check surface morphology. As a result of chip analysis through Material Testing Microscope; coconut oil gave better chip length with better grain structure. The lubricants or material can be changed to see the difference or resemblance of chip structure formed as a result.</p>

1. Introduction

The lubrication technique in the machining processes was an important factor considered by analysts. The ease and efficiency of cutting process were under observation during machining processes. Drilling was one of the most important machining processes which was and is used for producing holes and cavities in the work materials. In drilling, various types of lubricants were used to avoid friction between the contacting materials which were generally mineral oils based. The material removed from the work during a machining process was in the form of chips which can be recycled and reused if the grain structure is better and continuous.

Braga *et al.*, worked on drilling of alloys of silicon-aluminum by using a diamond coated drill and minimum quantity lubrication technique [1]. There was not any advantage of using drill with diamond coat as compared to uncoated K10 drill.

Belluco and Chiffre [2] evaluated six cutting oils efficiency, using conventional HSS-Co tools, to drill AISI 316L stainless steel by measuring tool life, cutting forces, tool wear and chip formation. All vegetable oils had better results than the reference mineral oil. Nam *et al.*, experimentally characterized the micro-drilling process by using MQL [3]. It was observed that the magnitudes of

* Corresponding author.

E-mail address: jantakan.t@psu.ac.th

<https://doi.org/10.37934/arfmts.84.2.9297>

thrust forces and drilling torques were significantly reduced by using the nano-fluid minimum quantity lubrication using nano-diamond particles.

Ozcelik *et al.*, worked on four cutting fluids performance, two distinct vegetable oils extracted from sunflower oil and two commercial type cutting fluids (mineral and semi-synthetic), on roughness of surface while drilling stainless steel AISI304 with HSS tool [4]. Vegetable oils performed better as compared to mineral-based or semi-synthetic cutting oils. Fairuz *et al.*, investigated the application of vegetable oils as a lubricant in drilling process to perceive the chip formation, tool wear and to predict whether coconut oil could give superior chip if used as lubricant in drilling process [5]. Rubio *et al.*, worked on friction force between work material and tool used for making hole and concluded that sandwich type material was more appropriate for friction drilling process [6]. By proper cutting speed, reduced point angle and low feed rate; delamination can be decreased.

Davim *et al.*, worked on the high speed drill having 118, 82 and 100 drill point angles and observed that temperature of drilling specimen increases with the increase in feed rate and the speed [7]. Davim and Reis worked on the penetrating effect parameters and condition of machining on surface roughness with time [8]. Harshness of surface was diminished from 7032 to 2032 μm with cutting rate increment and feed lessening. Machining time was expanded from 7.4 to 31.5 seconds. Domingo *et al.*, worked on required strength in drilling dry of PEEK GF30 a material of thermo plastic and forth. Composite penetrate was the more played influent factor [9].

Singh *et al.*, worked on HSS exhibition, K20 carbide and HSS covered tin apparatuses in dry drilling of AISI 304 [10]. HSS covered tin penetrate demonstrate the most astounding execution with longer device life. Stein and David worked on burr formation in drilling process and proposed that the inclusion of burr formation data in planning process [11]. It was concluded that by increasing feed sensitivity, speed and drill; wear can cause the increase in size and shape of burrs. Feng Ke *et al.*, worked on chip removing motion and forces in two models to predict spiral and string chips formation. After analysis it was found that smoothness in chip formation and average chip length could be predicted qualitatively [12].

Lawal *et al.*, worked on lubrication techniques by analyzing factors like work material, tool material and machining conditions [13]. After analysis, vegetable oils as lubricants were observed and preferred because of its extinguishing characteristics. Kim *et al.*, analyzed chip formation using milling 360 brass with flute end mill [14]. It was observed that appreciable cutting could be if feed per tooth done is not so small. Davim *et al.*, worked on the use of fluid during machining processes and predicted that flood coolant lubrication could replace MQL technique if parameters were chosen carefully [15].

Basavrajappa *et al.*, worked on drills of carbide and work pieces of A122191155i cp and A12219/155 Si cp [16]. Senthil Kumar *et al.*, worked on the machining parameters like cutting speed and feed rate [17]. Khalil *et al.*, studied the machining characteristics (surface roughness, temperature and dimensional accuracy) of two dissimilar composite blends named LLDPE/PALMAC 95 -16 Palm Oil-Based Wax and LLDPE/PALMAC 98-18 Palm Oil-Based Wax [18].

After studied the literature it was observed that cutting speed and feed rate could be optimized using generic algorithm and obtained the results accordingly.

2. Selection of Work Material and Lubricants

A piece of AISI 1018 MILD STEEL with the dimensions of 92 X 12 X 12 mm (as shown in Figure 1), was used in the process because of its good physical and chemical properties. It contains 0.14-0.20% of carbon and 98.81-99.26% iron and traces of some other elements like manganese,

phosphorus and sulphur. An uncoated drill bit of High Speed Steel (HSS) was used which was 12 mm in diameter as shown in Figure 2. The Process was done on upright drilling machine. The lubricants used in this process were vegetable oils which were used in routine life and preferred because of ease of availability. The four type of oils were used which includes hair oil, cooking oil, olive oil and coconut oil.



Fig. 1. AISI 1018 mild steel



Fig. 2. HSS drill bit

3. Experimental Procedure

Drilling operation was performed on the MS material, using upright drill machine. The drilling was done at a constant speed to avoid the human errors in the process. The lubricants were applied constantly during the process to avoid the chances of low lubrication at any moment. Total four holes were drilled at an average depth of 23 mm each as shown in Figure 3. In each drill, different lubricant was used. The chips formed in each drill was collected from their respective holes and samples were gathered carefully. Each sample was named and differentiated as that of the lubricant oil being used. The chips obtained from the process were shown in Figure 4 - Figure 7.



Fig. 3. MS material after Drilling



Fig. 4. Chips using coconut oil



Fig. 5. Chips using cooking oil



Fig. 6. Chips using olive oil



Fig. 7. Chips using hair oil

4. Observations

The purpose of this operation using different lubricants was to observe the grain structure and continuity of chips formed during the process. Chips and their grain structure were then examined through Material Testing Microscope model TESCAN (MIRA 3 XMU Type) to check surface morphology as shown in Figure 8 - Figure 11.

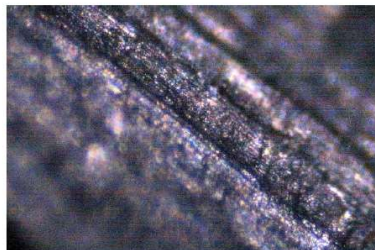


Fig. 8. Chip structure using coconut oil

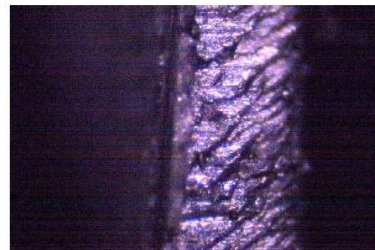


Fig. 9. Chip structure using cooking oil

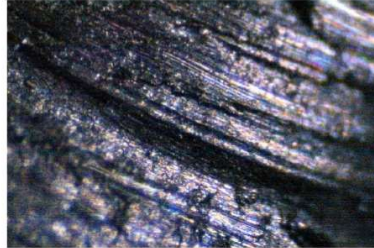


Fig. 10. Chip structure using olive oil

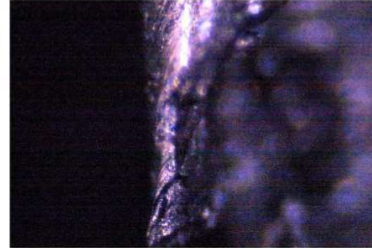


Fig. 11. Chip structure using hair oil

It was observed that the chip formed using coconut oil has a better grain structure, smooth surface and chip length than any lubrication oils and can be recycled and reused.

5. Conclusion

The use of lubricants in a machining process was necessary as it has a key role in the chip structure formation. As chips could be recycled and reused; so, the chip with continuous length and better grain structure could be used again in different processes. From this experiment, we concluded that the coconut oil could be used vastly to produce better chip structure, cost effective and non-reactive as well

In future, other organic oil based lubricants such as kerosene oil, jatropa, rapeseed oil etc. could also be used to see whether the chips structure formed as a result would be preferred or not. Also by varying RPM of machine and by varying applied vertical force in drill operation; experimentation would be done to analyze chip structure formed as a result. Other than that same technique could be applied on other materials such as copper bar, carbon steel bar, Silver bar etc. to observe whether these lubricants could give same chip structures or the chip structure varies.

References

- [1] Braga, Durval U., Anselmo E. Diniz, Gilberto WA Miranda, and Nivaldo L. Coppini. "Using a minimum quantity of lubricant (MQL) and a diamond coated tool in the drilling of aluminum-silicon alloys." *Journal of Materials Processing Technology* 122, no. 1 (2002): 127-138. [https://doi.org/10.1016/S0924-0136\(01\)01249-3](https://doi.org/10.1016/S0924-0136(01)01249-3)
- [2] Belluco, Walter, and Leonardo De Chiffre. "Performance evaluation of vegetable-based oils in drilling austenitic stainless steel." *Journal of materials processing technology* 148, no. 2 (2004): 171-176. [https://doi.org/10.1016/S0924-0136\(03\)00679-4](https://doi.org/10.1016/S0924-0136(03)00679-4)
- [3] Nam, Jung Soo, Pil-Ho Lee, and Sang Won Lee. "Experimental characterization of micro-drilling process using nanofluid minimum quantity lubrication." *International Journal of Machine Tools and Manufacture* 51, no. 7-8 (2011): 649-652. <https://doi.org/10.1016/j.ijmactools.2011.04.005>
- [4] Ozcelik, Babur, Emel Kuram, Erhan Demirbas, and Emrah Şik. "Optimization of surface roughness in drilling using vegetable-based cutting oils developed from sunflower oil." *Industrial Lubrication and Tribology* (2011). <https://doi.org/10.1108/00368791111140486>
- [5] Fairuz, M. A., M. J. Nurul Adlina, Azwan Iskandar Azmi, M. R. M. Hafiezal, and K. W. Leong. "Investigation of chip formation and tool wear in drilling process using various types of vegetable-oil based lubricants." In *Applied Mechanics and Materials*, vol. 799, pp. 247-250. Trans Tech Publications Ltd, 2015. <https://doi.org/10.4028/www.scientific.net/AMM.799-800.247>
- [6] Rubio, J. Campos, A. M. Abrao, P. E. Faria, A. Esteves Correia, and J. Paulo Davim. "Effects of high speed in the drilling of glass fibre reinforced plastic: evaluation of the delamination factor." *International Journal of Machine Tools and Manufacture* 48, no. 6 (2008): 715-720. <https://doi.org/10.1016/j.ijmactools.2007.10.015>
- [7] J.P. Davim, F. Mata, V.N. Gaitonde, S.R. Karnik. "Drilling temperature of the specimen with increase in both cutting speed and feed rate." *J Biomech Engineering* 122, no. 2 (2010): 159-165.

- [8] Strenkowski, J. S., C. C. Hsieh, and A. J. Shih. "An analytical finite element technique for predicting thrust force and torque in drilling." *International Journal of Machine Tools and Manufacture* 44, no. 12-13 (2004): 1413-1421. <https://doi.org/10.1016/j.ijmachtools.2004.01.005>
- [9] R. Domingo, M. García, M.A. Sebastián. "Vitality during the dry drilling of PEEK GF30, a thermoplastic material and polyether." *J. Eng. Ind* 96, no. 4 (2015): 1207-1215.
- [10] A.P. Singh, M. Sharma, I. Singh. "Exhibitions of HSS, K20 strong carbide, and TiN-covered HSS apparatuses in dry drilling of AISI 304." (2016).
- [11] Stein, Julie M., and David A. Dornfeld. "Burr formation in drilling miniature holes." *Cirp Annals* 46, no. 1 (1997): 63-66. [https://doi.org/10.1016/S0007-8506\(07\)60776-8](https://doi.org/10.1016/S0007-8506(07)60776-8)
- [12] Ke, Feng, Jun Ni, and D. A. Stephenson. "Continuous chip formation in drilling." *International Journal of Machine Tools and Manufacture* 45, no. 15 (2005): 1652-1658. <https://doi.org/10.1016/j.ijmachtools.2005.03.011>
- [13] Lawal, Sunday Albert, Imtiaz Ahmed Choudhury, and Yusoff Nukman. "A critical assessment of lubrication techniques in machining processes: a case for minimum quantity lubrication using vegetable oil-based lubricant." *Journal of Cleaner Production* 41 (2013): 210-221. <https://doi.org/10.1016/j.jclepro.2012.10.016>
- [14] Kim, Chang-Ju, Matthew Bono, and Jun Ni. "Experimental analysis of chip formation in micro-milling." *TECHNICAL PAPERS-SOCIETY OF MANUFACTURING ENGINEERS-ALL SERIES-* (2002).
- [15] Basavarajappa, S., G. Chandramohan, M. Prabu, K. Mukund, and M. Ashwin. "Drilling of hybrid metal matrix composites—Workpiece surface integrity." *International Journal of Machine Tools and Manufacture* 47, no. 1 (2007): 92-96. <https://doi.org/10.1016/j.ijmachtools.2006.02.008>
- [16] Davim, J. P., P. S. Sreejith, R. Gomes, and C. Peixoto. "Experimental studies on drilling of aluminium (AA1050) under dry, minimum quantity of lubricant, and flood-lubricated conditions." *Proceedings of the Institution of Mechanical Engineers, Part B: Journal of Engineering Manufacture* 220, no. 10 (2006): 1605-1611. <https://doi.org/10.1243/09544054JEM557>
- [17] SenthilKumar, M., A. Prabukarthi, and V. Krishnaraj. "Study on tool wear and chip formation during drilling carbon fiber reinforced polymer (CFRP)/titanium alloy (Ti6Al4 V) stacks." *Procedia engineering* 64 (2013): 582-592. <https://doi.org/10.1016/j.proeng.2013.09.133>
- [18] Khalil, M., H. Radwan, F. Annuar, H. Azmi, and M. Z. Zakaria. "Study of Machining Characteristics of LLPDE/Palmac Palm Oil-Based Wax Blend for Prototype Application." *Journal of Advanced Research Design* 6, no. 1 (2015): 11-20.



Journal of Advanced Research in Fluid Mechanics and Thermal Sciences

Journal homepage: www.akademiabaru.com/arfmnts.html
ISSN: 2289-7879



Design and Fabrication of Under Water Remotely Operated Vehicle

Roman Kalvin^{1,3}, Juntakan Taweekun^{2,*}, Muhammad Waqas Mustafa³, Faisla Ishfaq³, Saba Arif¹

¹ Energy Technology Program, Faculty of Engineering, Prince of Songkla University Hat Yai, Thailand

² Department of Mechanical Engineering, Faculty of Engineering, Prince of Songkla University Hat Yai, Songkhla 90112, Thailand

³ Department of Mechanical Engineering, Wah Engineering College, Wah Cantt., Pakistan

ARTICLE INFO

Article history:

Received 17 October 2020
Received in revised form 3 March 2021
Accepted 7 March 2021
Available online 20 April 2021

Keywords:

Propellers; Buoyancy; Thrust force

ABSTRACT

Underwater Remotely Operated vehicle is a tethered mobile vehicle most often used to monitor underwater oil and gas drilling inspection, telecommunications and homeland security. The main focus of this research is to design a vehicle at low cost which is safe, portable, and easy to use while increasing the maneuverability and efficiency to reach a depth of 5 meters. While conducting research a unique design is selected based on a novel fin propulsion mechanism rather than propellers. Propellers though have high speed but cannot work on low flow rates and their blades can be damaged if jelly fish or other material is struck in its shaft. Two shapes have been considered to remove above difficulties i.e. Fish and Turtle. Due to higher stability, larger area and greater hydrodynamic efficiency Sea Turtle has been selected, as it can easily overcome the forces like buoyancy, pressure and thrust force. The results extracted from this research shows that the underwater vehicles based on the biological locomotion principle can perform very well than other propeller counterparts. The research concludes with the performance of a working system that validates motion capabilities related to speed, depth and hydrodynamic efficiency which can be further improved by using sophisticated control systems, outer shell and highly integrated processors.

1. Introduction

The design and implementation of underwater robot will be discussed in this paper. Rather than the conventional based propulsion by propellers, a novel bio-inspired propulsive mechanism similar to sea turtles is actualized. The main motivation of this research is to meet the round the clock underwater surveillance, sea exploration, scientific search and diving assistance.

An underwater remotely operated vehicle (UROV) is considered best approach to achieve above objectives. One of the main trends for UROVs is "autonomy" for some specific tasks, such as position tracking, dynamic positioning (or station-keeping), auto-heading and auto depth control. The ROV system is highly maneuverable unmanned which is operated by a person using tethered cable or by sensors through remote. It is connected to the vehicle by a tether or known as an

* Corresponding author.

E-mail address: jantakan.t@psu.ac.th

<https://doi.org/10.37934/arfmnts.82.1.133144>

umbilical cable. Under water vehicles are becoming useful source for commercial uses, mine hunting and sea. The underwater vehicle raised its cost effectiveness due to greater sea diving extreme environment conditions and maneuverability.

Lygouras *et al.*, [1] developed unmanned underwater remotely operated vehicle (ROV) called THETIS, which is used for measuring the water pollution in ocean environments. It is composed of remotely operated vehicle, a cable wire for power supply optical fibers and four DC motors, pivoting exceptionally outlined propellers for controlling profundity, location on the level plane, and caption of the vehicle. The DC engine propeller framework will be eluded as the thruster. AC or DC motor is adjusted to the vehicle as thrusters-First, click on the View menu and choose Print Layout. Yamamoto and Terada [2] adapted a propulsion control system on a robotic fish. They proposed an oscillating fin propulsion system. They arranged different types of tests on fins. As mentioned in this research that there are two types of fins (rigid and flexible). They work on flexible fins because it has more advantages than rigid ones to push out any text that may try to fill in next to the graphic. First, they generate a controlling algorithm for controlling the fin oscillating system.

Pan-Mook *et al.*, [3], the Ocean Exploration System Research Division of KORDI-MOERI "Korea Ocean Research & Development Institute" improved the arrangement of a 6,000-meter profundity appraised unmanned submerged vehicle (USV) for oceanographic inquire about in Korea. The USV framework consists of two vehicles: a "HEMIRE" remote vehicle and a "HENUVY" dive initiator had collaborated with the remotely operated vehicle. In 2006, Hu *et al.*, [4] designed and developed an autonomous robotic fish which swims like a real fish mechanism. The thrust for swimming is generated by bending or moving their one half or one third body. The body of fish is made up of 3 or 4 tail joints. These 4 joints connected with each other by Linkages.it consist of four servo motor and two DC motors. The four servo motors are used to bend the tail at greater angle with minimum time. A team of six students Tan *et al.*, [5], Michigan State University developed an autonomous underwater robotic fish for mobile sensing. Firstly they made a working prototype that could be operated with remote with the help of radio controller. After prototype, they built a circuit in which a GPS system, sensor, autonomous navigation, communication are installed and these are sealed with silicone adhesive. Shao *et al.*, [6] investigated cooperation control group of micro robots which are implemented by fish like propulsive system. The purpose of this work is; first to designed a fish like robot and realized; Secondly to use these multi-unit robots for underwater transportation.

Ye *et al.*, [7] developed a remote-control centimeter-scale Robotic fish. There works is related to design a robotic fish. Though so many scientists, researchers have done more work on robotic fish, they are all worked on larger scale but only few were done on small scale autonomous robotic fish. Because when the length, width and height is decrease of its actual size than its overall size will also decrease. They use infrared sensor for operating the remote control function. Font *et al.*, [8] adapted a design and implement a propulsive Autonomous Underwater Vehicle Hydrofoil that is similar to the turtle's hydrofoil. They selected the hydrofoil NACA 0014 (National Advisory Committee for Aeronautics) because it gives a good relationship among drag and lift force. The profile selected is biomimetic ally to the sea turtle. In this there are 4 different phases' upstroke, upstroke, supination, and pronation. They use ball and socket mechanism for generating this type of hydrofoil which gives three degree of freedom and it is so compact. Aras *et al.*, [9] worked on low cost four degree of freedom remotely operated vehicle which is integrated with (IMU) and the pressure sensor. The purpose of this robot is to reduce the involvement of human activities under water because of high cost. To improve the efficiency and productivity, different industries develop a micro robot for their purpose. Martos *et al.*, [10] developed a remotely operated vehicle which is used in water for marine purposes. They just introduced a robot and also design a robot for general purposes. In this report they give about the idea of robot and also history of robot. They just made

a robot which is fully equipped from video camera, propulsion system and lights. They designed a special type of robot called tuna shaped. These designs were also tested successfully.

Liu *et al.*, [11] provided a novel mechatronics plan for a 3D swimming automated fish, specifically MT1 (Mechanical Tail) mechanical fish. It has tail shape which utilizes just a single engine to create fish like swimming movement utilizing C-twists tail shapes. This outline empowers MT1 to wind up the primary little size mechanical fish (<0.5m long) and have the capacity to plunge more than 3 meters somewhere down in water. A successful control strategy with just 5 parameters is proposed to control its 3D swimming practices. Trial comes about are displayed to demonstrate the possibility and great execution of the proposed control calculations. The Tuna fish have a more prominent capacity to fish and swim with rapid. This property of Tuna angle pulls in the specialist, researcher to enhance the execution of Robotic fish. Zhuoyi *et al.*, [12] worked on the structure design of underwater vehicle which is made up of composite material. The structure of underwater vehicle depends upon buoyancy factor and gravity of the vehicle in water. Composite materials as good strength and also have stiffness, and stable against chemical reaction. Composite materials also have the ability to absorb sound. Their work is related to reduce the weight of vehicle. For this purpose, they used carbon fiber for their requirements.

Anwar *et al.*, [13] fabricated and implemented remotely operated vehicle by using single thruster, this robot is design for surveying hollow tubes or shell has been done. It moves in 2 degree forward/backward with the help of thruster, and up/down with the help of changing density. For changing the density two water chamber on each side of hull is used. The density is changed by draining or filling this chamber, but all the main electrical components is attached to the main chamber. Chen *et al.*, [14] investigated Magnetically Actuated Miniature Robotic Fish is actualized. It works on law of electromagnetic induction. It consists of two magnets and a solenoid which is fixed with caudal. The two magnets generate their magnetic field and solenoid also generates its magnetic field when the pulse and frequency of electric current passing through the solenoid is changed or modulated. When the two magnetic fields is coupled than a force is developed which moves the fins of Miniature Robotic Fish. For controlling and power Bluetooth Low Energy (BLE) is used.

2. Mechanical Design

The project design phase was divided into four main parts: (1) Selecting a bio-inspired shape considering its stability, maneuverability and can contain many instruments within its structure, (2) Mechanism to move fin in 3 DOF motion, (3) Designing of fin, (4) Controls. Initial design inspiration took shape as shown in Figure 1.

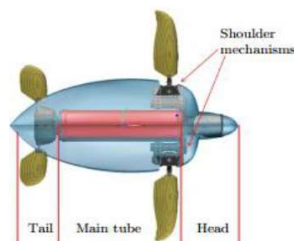


Fig. 1. Selected Shape

Initial design ideas provided were then used in creation of the CAD model for the entire system for designing overall structure, mechanism and control of UROV. For specifying the shape of the UROV research paper gives us the previous work on the different shapes of the bio-inspired vehicles. The reasons are as (i) Due to its larger area we can place many components (sensors, motors, large battery) in it, (ii) Maneuverability, (iii) Hydrodynamic efficiency.

Selection of a material for a process is based on its strength, application, availability, process and economically suitability. With reference to the product design the core objective of a material selection is to minimize the cost while meeting the performance goals. Systematic choice of the best material begins with cost and properties of candidate material. So, materials used and their properties are as follows

- Acrylic, PMMA(For front and back portions so that we can see if there is any leakage occurs)
- Unbreakable PVC(for internal components(electronics, motors...etc.) casing
- High carbon fiber/Epoxy.

Selected and implemented mechanism to achieve 3DOF (Degree of Freedom) is Combination of servo motors. This is the most flexible mechanism in which five servo motors are assembled together in such a way that this joint gives three degree of freedom system. Three out of five are high torque motors which give 3DOF at any maximum displacement. The requirement to design the flapper must meet the following conditions:

- Must move in 3DOF
- Have enough suitable strength to bear forces of water
- Have less drag coefficient and generates the maximum lift during the downward stroke

So, keeping these objectives in mind two hydrofoils are finally considered named as NACA0014 and RYAN BQM-34 FIREBEE AIR FOIL. So being on the save side NACCA 0014 is finally selected as flapper for underwater remotely operated vehicle. Mechanical components design of UROV is shown in Table 1.

Table 1
Mechanical components Design

Vehicle Parameter	Value	Unit
Body Material	PVC pipe, PMMA, fibreglass	
Length of main hull	600	Mm
Diameter of main hull	165.1	Mm
Diameter of water chamber	76.2	Mm
Total mass of vehicle	12	Kg
Density of water (at 20°)	998.2	Kg/m ³
Nominal Speed	1.0	m/s
Drag Force	1.579	N
Thrust Force	3.436	N

3. Design and Calculation

3.1 Drag Force

In liquid progression, drag constrain is the power acting against the movement of a question moving in respect to the encompassing liquid. Torpedoes and submarines make them thing in like manner that is, they have a streamline body and a focal barrel that is utilized for lodging of a wide range of instrumentation, weapons, and valuable lives. In the majority of the cases, the body utilized is round and hollow fit as a fiddle because of its quality and capacity to agree to the dynamic powers following up on it. Despite the fact that, it is very productive in the auxiliary outline than different states of geometrical measurements, yet it gives less space to the frameworks

dwelling in it. This is because of the way that every one of the frameworks set in it are normally square or rectangular. So, drag is calculated as

$$C_D = C_{D,PRESSURE} + C_{D,FRICITION}$$

C_D , $C_{D,PRESSURE}$ and $C_{D,FRICITION}$ represent coefficients of viscous drag, pressure drag and friction drag respectively.

$$C_F = \frac{0.075}{(\log R_N - 1)^2}$$

$$R_N = \rho V L / \mu$$

Drag coefficient also depends on characteristic area. It is reported that frontal area is used as a characteristic area for cylindrical shapes.

$$F_D = \frac{1}{2} \rho V^2 A C_D$$

ρ is the density of the fluid, V is the velocity, A is the frontal area (in this case) and C_D is the drag coefficient.

While moving downward towards the depth in the sea lift is also the unfavourable and opposing force acting on the body which was fine by

$$F_D = \frac{1}{2} \rho V^2 A C_L$$

3.2 Force Due to Weight

Apart from drag there is another force acting which has to be counter to move and this is force due to weight. It is calculated as

$$F = W = mg$$

3.3 Thrust Force and Torque

Thrust force is the driving force for the vehicle against any friction or drag. This force can be provided by many means. For this type of vehicle flapper-based mechanism is used

$$F_t - F_D - F_L = m\ddot{x}$$

Also, torque;

$$T = F \times r$$

3.4 Waterproofing and Sealing

Waterproofing is the most crucial part to be considered for the integrity of operations of vehicle. Motors are sealed by using grease and silicon cement/gel while cylinders are by use of PVC cement and glue. Waterproofing is the most important factor to be considered for the integrity of the operations of the vehicle. Two acrylic, transparent, disks are installed on both ends of the main hull. These disks are permanently sealed. These disks are installed for quick visual inspection of inner side of the main hull. Electrical plate is removed by opening the cap on the rear side of the main hull. Both the cap and the main hull have threads which provide mechanical seal. O-ring seal is also used with threads to complement the waterproofing of the main hull.

3.5 Calculations

3.5.1 Known parameters

For sea water

Density = $\rho = 1013 \text{ kg/m}^3$

Salinity = 20 g/kg

Dynamic viscosity = $1.043 \times 10^{-3} \text{ kg/m.s}$

Velocity of water = $v_{\text{water}} = 0.8217 \text{ m/s}$

Temperature = $20^\circ\text{C} = 293 \text{ K}$

Secondly the area of the overall body of robot without fin is calculated and is as follows

Area of the flapper = 229cm^2

Area of center body = 990cm^2

Area of the hind flappers = 114cm^2

3.5.2 Drag calculations

Firstly, for the fin

$C_{D,\text{pressure}} = 0.7$

Area = 229cm^2

$V = 1.5 \text{ m/s}$

Overall C_D formula

$$C_D = C_{D,\text{PRESSURE}} + C_{D,\text{FRICTION}}$$

Where C_D = Viscous Drag

$C_{D,\text{PRESSURE}}$ = Pressure Drag

$C_{D,\text{FRICTION}}$ = Friction Drag

Skin Friction Drag is the function of Reynold's number which is defined by

$$C_F = \frac{0.075}{(\log R_N - 1)^2}$$

where, R_N = Reynold number and is defined by

$$R_N = \rho VL / \mu$$

where,

ρ = density of fluid

V = velocity of Vehicle

L = diameter of vehicle

μ = dynamic viscosity of fluid

$$R_N = \frac{1013 \times 1.5 \times 1.5}{1.043 \times 10^{-3}} = 2185282.83$$

Viscous Drag Co-efficient is then computed to find the drag force and the expression is as follows

$$C_v = C_F \left[1 + 0.5 \left(\frac{d}{l} \right) + 3 \left(\frac{d}{l} \right)^3 \right], C_v = 0.7 [1 + 0.5(3) + 3(3)^3], C_v = 5.8$$

So, finally the Drag equation is

$$F_D = \frac{1}{2} \rho V^2 A C_D$$

where,

F_D = drag force

V = velocity of vehicle

A = area of vehicle

$$F_D = \frac{1}{2} \times 1013 \times 1.5^2 \times 0.0229 \times 0.9$$

$$F_D = 12.932 \text{ N}$$

3.5.3 Drag for the hind flapper

$$C_D = 0.9$$

$$\text{Area} = 114.5 \text{ cm}^2$$

$$F_D = \frac{1}{2} \rho V^2 A C_D$$

$$F_D = 1.3389 \text{ N}$$

3.5.4 Drag of the body

$$C_D = 1.2$$

$$\text{Area} = 990 \text{ cm}^2$$

$$F_D = \frac{1}{2} \rho V^2 A C_D$$

$$F_D = 12.932 \text{ N}$$

3.5.5 Drag of fore limb flappers

$$F_D = \frac{1}{2} \rho V^2 A C_D$$

$$C_D = C_{PD} + C_{DF}$$

As $C_{PD} = 0.45$. So, $C_D = 0.45 + 0.02$

$$C_D = 0.47$$

$$F_D = \frac{1}{2} \rho V^2 A C_D$$

$$F_D = \frac{1}{2} \times 1020 \times 0.7^2 \times 0.0229 \times 0.47$$

$$F_D = 2.68 \text{ N}$$

As, $\theta = 70^\circ$. So, $F_D \sin \theta = 2.68 \times \sin 70 = 2.527 \text{ N}$. Thus, on two flappers

$$2F_D = 2 \times 2.527 = 5.05 \text{ N}$$

So total drag is, $D = 50.056 + 2.678 + 12.932 = 20.66 \text{ N}$

3.5.6 Lift coefficient

$$F_D = \frac{1}{2} \rho V^2 A C_L$$

$$F_D = \frac{1}{2} \times 1020 \times 0.7^2 \times 0.1035 \times 0.9$$

$$F_D = 14.27 \text{ N}$$

3.5.7 Force due to weight

$$F = W = mg$$

As, $\theta = 20^\circ$. So, $F = W = mg \cos \theta = \frac{12}{2} \times 9.8 \times \cos 20 = 55.25 \text{ N}$

So, for two flappers

$$2F_w = 2 \times 55.25 = 110 \text{ N}$$

3.5.8 Thrust calculations

$$F_t - F_D = m\ddot{x}$$

$$F_t = m\ddot{x} + F_D$$

$$F_t \times t = t m \frac{dv}{dt} + F_D \times t$$

Now,

$$v_f = v_i + at$$

$$v_f = 1.5 \text{ m/s}$$

$$v_i = 0$$

$$t = 3 \text{ secs}$$

$$1.5 = 0 + a \times 3$$

$$a = 0.5 \text{ m/s}^2$$

$$F_t = 12 \times 0.5 + F_D = 6 + 20.66 = 26.66 \text{ N}$$

For single fin,

$$F_t = 26.66/2 = 13.33 \text{ N}$$

3.5.9 Torque calculations

$$T = F \times r, T = 6 \times 0.130, T = 0.78 \text{ Nm}$$

Now, torque for drag

$$T = F \times r, T = 20.66 \times 0.307, T = 6.34 \text{ N}$$

So, Stall torque at 6 volts = 11kg. fcm

So, Stall torque at 6 volts = 1.07Nm

For 5 motors: $1.07 \times 5 = 5.35 \text{ Nm}$

3.5.10 Torque for hind limbs

$$T = F \times r = 1.33 \times 0.130 = 0.1729 \text{ Nm}$$

For both hind limbs

$$T = 0.1729 \times 2 = 0.3548 \text{ Nm}$$

3.5.11 Current calculations

Fore limbs

Let, $I = 700 \text{ mA}$ (From Data sheet of servomotors)

So, for 5 servomotors $I = 700 \times 5 = 3500 \text{ mA} = 3.5 \text{ A}$

For both joints

$$I = 3.5 \times 2 = 7 A$$

For hind limbs,

$$\text{Let, } I = 700 \text{ mA (From Data sheet of servomotors)} = 700 \times 2 = 1400 \text{ mA} = 1.4 A$$

$$\text{Now total Current} = I = 7000 + 1400 = 8400 \text{ mA} = 8.4 A$$

3.5.12 Battery calculations

For 1 hour

According to calculations 8400 mAh battery is required. As our requirement is 7 hours, so for 7 hours = $7 \times 8400 = 58800 \text{ mAh}$ $A \approx 60,000 \text{ mAh}$

These are self-contained electric devices which rotate/push different portions of machine with high precision. Servos are found in numerous applications: from toys to home electronics to cars and airplanes. RC car, airplane, or helicopter, use a few servos.

As five servo motors are attached at each fin for the thrust, so the distances which the flapper covers in xyz direction are as

$$x = 1.5 \text{ cm}$$

$$y = 9 \text{ cm}$$

$$z = \pm 100^\circ$$

Assembly of UROV with flappers are shown in Figure 2.



Fig. 2. UROV Assembly with Flappers

4. Electrical System

The electrical system of UROV is divided into two parts. One part indicates the controlling elements like circuit board, camera, servo motors and sensors. Second part comprises the control given to the operator at the station. Arduino UNO was used for the controlling and communicating with the vehicle. Camera is connected by USB cable which directly comes to the base station to give output at PC. All the motors and sensors communicate signal by using a tethered wire which was 10 meters long. Tethered wire is best suitable solution for short distance operations but for deeper operations the voltage and signal drops and is vulnerable to a number of risks due to less strength.

Electrical components attached with UROV are presented in Table 2 and final assembly of UROV with all electrical components is shown in Figure 3.

Table 2
Electrical Components

Component	Parameter	Value
Electronic Speed Controller	Maximum Current	55 A for 10sec
Sensing Devices	Two sensors	Proximity sensor, Temperature sensor
Microcontroller	Arduino UNO	Digital I/O, 13 Analog Inputs
Joystick	Logitech Attack3	Programmable buttons, throttle button
Camera	USB 2.0	30 frames/second
Power bank	Li-ion battery	2x6V 4.0Ah rating



Fig. 3. Final UROV Model

5. Conclusion

This research concludes determination of the relationship between buoyancy forces, propulsion and thrust forces. The purpose is to design the project at low cost which is safe, portable and easy to use. Two shapes have been selected while making designs i.e. Fish and Turtle. Shape of turtle is selected as it has more stability and components can be placed easily due to larger area. However it has low speed then Fish. The major problem is identification about control system, coupling and maneuverability which has been discussed in detail. Also the force of buoyancy, coefficient of drag and thrust force on Fins and body are calculated. Desired depth of 5 meters and velocity of 1.0 m/s have been achieved. NACA 0014 is selected for fins and flappers as it has greater maneuverability and hydrodynamic efficiency. Drag forces acting on fins, hind flappers and body were found by using Reynolds number and drag formulas.

6. Future Recommendations

- Modifications could be made on design and shape of the fins to reduce drag and increase its speed.
- Tethered wires could be improved to reduce buoyancy effects.
- Servo motors failed on numerous occasions while testing, other methods such as ball and socket, four bar link mechanism could be used to achieve 3 degree of freedom.
- Underwater Remotely operated vehicle could also be used for study about the environment disturbances such as waves, tides, tsunami and unexpected changes in climate.
- Better communication systems could be used for UROV for wireless networking.

References

- [1] Lygouras, John N., Konstantinos A. Lalakos, and Ph G. Tsalides. "THETIS: an underwater remotely operated vehicle for water pollution measurements." *Microprocessors and Microsystems* 22, no. 5 (1998): 227-237. [https://doi.org/10.1016/S0141-9331\(98\)00083-0](https://doi.org/10.1016/S0141-9331(98)00083-0)
- [2] Yamamoto, Ikuo, and Yuuzi Terada. "Research on flexible oscillating fin propulsion system and robotic fish." *IFAC Proceedings Volumes* 34, no. 7 (2001): 119-123. [https://doi.org/10.1016/S1474-6670\(17\)35069-3](https://doi.org/10.1016/S1474-6670(17)35069-3)
- [3] Pan-Mook, Lee, Lee Chong-Moo, Jun Bong-Huan, Hyun Taek Choi, Li Ji-Hong, Ki Sea-Moon, Kihun Kim et al. "System design and development of a deep-sea unmanned underwater vehicle 'HEMIRE' for oceanographic research." In *The Sixteenth International Offshore and Polar Engineering Conference. International Society of Offshore and Polar Engineers*, 2006.
- [4] Hu, Huosheng, Jindong Liu, Ian Dukes, and George Francis. "Design of 3D swim patterns for autonomous robotic fish." In *2006 IEEE/RSJ International Conference on Intelligent Robots and Systems*, pp. 2406-2411. IEEE, 2006. <https://doi.org/10.1109/IROS.2006.281680>
- [5] Tan, Xiaobo, Drew Kim, Nathan Usher, Dan Laboy, Joel Jackson, Azra Kapetanovic, Jason Rapai, Benjamin Sabadus, and Xin Zhou. "An autonomous robotic fish for mobile sensing." In *2006 IEEE/RSJ International Conference on Intelligent Robots and Systems*, pp. 5424-5429. IEEE, 2006. <https://doi.org/10.1109/IROS.2006.282110>
- [6] Shao, J., L. Wang, and Junzhi Yu. "Development of an artificial fish-like robot and its application in cooperative transportation." *Control Engineering Practice* 16, no. 5 (2008): 569-584. <https://doi.org/10.1016/j.conengprac.2007.06.005>
- [7] Ye, Xiufen, Yudong Su, Shuxiang Guo, and Liquan Wang. "Design and realization of a remote control centimeter-scale robotic fish." In *2008 IEEE/ASME International Conference on Advanced Intelligent Mechatronics*, pp. 25-30. IEEE, 2008. <https://doi.org/10.1109/AIM.2008.4601629>
- [8] Font, Davinia, Marcel Tresanchez, Cedric Siegentahler, Tomàs Pallejà, Mercè Teixidó, Cedric Pradalier, and Jordi Palacin. "Design and implementation of a biomimetic turtle hydrofoil for an autonomous underwater vehicle." *Sensors* 11, no. 12 (2011): 11168-11187. <https://doi.org/10.3390/s111211168>
- [9] Aras, M. S. M., F. A. Azis, M. N. Othman, and S. S. Abdullah. "A low cost 4 DOF remotely operated underwater vehicle integrated with IMU and pressure sensor." In *4th International Conference on Underwater System Technology: Theory and Applications*, vol. 2012, pp. 18-23. 2012.
- [10] Martos, Gabriel, Ashley Abreu, and Sahivy Gonzalez. "Remotely Operated Underwater Vehicle." *A BS Thesis Prepared in Partial Fulfillment of the Requirement for the Degree of Bachelor of Science in Mechanical Engineering* (2013).
- [11] Liu, Jindong, Ian Dukes, and Huosheng Hu. "Novel mechatronics design for a robotic fish." In *2005 IEEE/RSJ International Conference on Intelligent Robots and Systems*, pp. 807-812. IEEE, 2005. <https://doi.org/10.1109/IROS.2005.1545283>
- [12] Zhuoyi, Yang, Shen Hailong, Su Yumin, and Liao Yulei. "Structure design of an autonomous underwater vehicle made of composite material." In *OCEANS 2014-TAIPEI*, pp. 1-4. IEEE, 2014. <https://doi.org/10.1109/OCEANS-TAIPEI.2014.6964281>
- [13] Anwar, Inzamam, M. Owais Mohsin, Saqib Iqbal, Zain Ul Abideen, Attique Ur Rehman, and Nisar Ahmed. "Design and fabrication of an underwater remotely operated vehicle (Single thruster configuration)." In *2016 13th International Bhurban Conference on Applied Sciences and Technology (IBCAST)*, pp. 547-553. IEEE, 2016. <https://doi.org/10.1109/IBCAST.2016.7429932>
- [14] Chen, Xingyu, Zhengxing Wu, Chao Zhou, and Junzhi Yu. "Design and implementation of a magnetically actuated miniature robotic fish." *IFAC-PapersOnLine* 50, no. 1 (2017): 6851-6856. <https://doi.org/10.1016/j.ifacol.2017.08.1206>



THE IIER REGISTRATION FORM

INTERNATIONAL INSTITUTE OF ENGINEERS AND RESEARCHERS
(IN ASSOCIATION WITH PET)
e-mail : info@theier.org
web: www.theier.org

Payment of a registration fee covers the cost to attend all conference activities, coffee breaks, conference reception and banquet, and all lunches during the conference. In addition, each registrant will receive a copy of the conference proceedings with ISBN. Notice that this registration fee does not cover transportation fee, accommodation fee, and after conference tour fee.

All questions and inquiries concerning registration and payment should be addressed to:
info@theier.org

Please complete this form and email a scanned copy to:
info@theier.org

Event Name	2020 IIER 875th International Conference on Recent Innovations in Engineering and Technology (ICRIET)
Venue/Place of Event	RAWALPINDI, PAKISTAN
Date of Event	28-29 May, 2020

PLEASE KINDLY FILL IN A SEPARATE REGISTRATION FORM FOR EACH CONFERENCE PARTICIPANT

Author's Full Name (Prof./Dr./Mr./Mrs)	Mr. Roman Kalvin	Highest Qualification	PhD (In Progress)
Affiliation/Designation	Prince of Songkla University, Hatyai Thailand		Nationality Pakistan
Mailing Address	H# CB-13, Gulshan Colony, Wah Cantt, Pakistan		Age 29
City, Zip, Country	Wah Cantt, 47040, Pakistan	Passport Number:	BZ4799373
Mobile (With Country code)	+923455979377	Email	Romankalvin12@gmail.com
ACCEPTED PAPER INFORMATION	Paper ID: II-RIETRAWAL-280520-18051 Title of the paper: Investigation Of Dissimilar V-Joint Of Steel Alloys With Copper And Brass Using TIG Welding		
Co-Author's Name & Designation	1. Dr. Juntakan Taweekun (Professor, PSU Thailand)	2. Dr. Kittinan Maliwan (Assistant Professor, PSU Thailand)	Guided by: Mail ID: Contact No: Affiliation:

PAYMENT INFORMATION

Total Amount (USD)	Bank Name	Remitter	Date	Ref. No
150 USD	Bank Alfalah	Roman Kalvin	11-5-2020	197568
	For online transfer (Debit card/Credit card/Online Banking)	Order ID/Traction ID: 16476-IIERCONFERENCE2015209		

Note: It is mandatory to provide a scan copy of ID Proof/Passport along with this Registration form


ADDITIONAL INFORMATION

- Will you present physically at the event _____ N _____ (Y/N).
- No. of Persons attending the event with you? (Including your Co-authors) _____ online _____.
- Will your Guide/HOD/Principal attending will attend the Event? _____ N _____ (Y/N).
- Total years of Experience (if any Academic and Industry) _____ 4 _____.



Declaration & Undertaking

1. I have not published this paper anywhere before and I am transferring the Copyright of my paper to IIER
2. I will not cause or involve in any sort of violence or disturbance within and Outside of the Conference/Event Venue or during the travel to the venue at any Country during my Visa Period.
3. IIER has all rights reserved to shift the venue, rescheduling the date of the Event.
4. I do here by declare that all the information given by me is true and if at any moment it is found to be wrong my registration for event will be cancelled by IIER and take necessary action against me.
5. I have read all the rules and regulations at http://theier.org/rules_regulations.php and agreed.
6. IIER is not responsible for any violation of Rules and Regulations by me or by my Co-authors of this paper at any country during the Event.

Signature (Author):  Date: 11-5-2020

Remarks: I present paper through online video conference via zoom app.







INVESTIGATION OF DISSIMILAR V-JOINT OF STEEL ALLOYS WITH COPPER AND BRASS USING TIG WELDING

¹ROMAN KALVIN, ²JUNTAKAN TAWEEKUN, ³KITTINAN MALIWAN

¹Energy Technology Program, Faculty of Engineering, Prince of Songkla University Hat Yai, Thailand

^{2,3}Department of Mechanical Engineering, Faculty of Engineering, Prince of Songkla University Hat Yai, Songkhla
 Thailand, 90112

E-mail: ¹Romankalvin12@gmail.com, ²jantakan.t@psu.ac.th, ³mkittina@me.psu.ac.th

Abstract - The aim of this research was to explore the new domain of dissimilar welding owing to its increasing industrial applications. Using tungsten inert gas(TIG) welding technique, the four different materials Copper c15000,Brass c260, Mild Steel and Stainless steel were bevel-joined each with a sample of Stainless Steel as a base material, under controlled welding parameters. The experiments were performed using ER70S-6 Filler rod. The tensile strength of the specimens was analyzed, and stress-strain curve was obtained using Universal Testing machine(UTS). All the specimens depicted good weld strength with SS304-Mild Steel showing better quality. The highest tensile strength obtained was 42KN for Stainless Steel(SS304)-Mild Steel specimen compared to BC260-Mild Steel(28KN) and C15000-Mild Steel(25KN) specimens. It was concluded that the SS304-Mild steel sample showed optimal mechanical strength. These results are restricted under specified welding parameters and can be further optimized by varying different welding parameters.

Keywords - Dissimilar Welding, TIG welding, V-Joint Weld, Steel Alloys, Copper Alloys, Brass Alloys, Radiography, Mechanical Testing

I. INTRODUCTION

In the present Era welding is the most common and durable option to join the materials permanently. It is applicable in almost all the industries i.e. from aerospace fabrication to the automotive generations. Because of its versatility and the strength, welding process is applied in almost all the manufacturing processes for making the products that are used in daily life. The variety in the shapes of products can be brought by using welding techniques. The most common technique of welding that is under use is tungsten inert gas (TIG) welding. Now a day a new trend Dissimilar Welding that is the welding between the metals with different grades and types is becoming so popular in industrial market to meet the raising demand and requirements. It is very complicated and challenging process because every material has different properties with respect to others. A lot of research has done on the Dissimilar welding. The new material that is under consideration for the dissimilar welding is steel and this process is all about dissimilar welding of steel. The unique quality of the Stainless Steel is that it not only makes the welding fusion with other materials but also it makes with its own alloys and that are more durable and long lasting. It shows variety of mechanical properties when welded with other materials according to the requirement and desired conditions. Steel can be easily welded with Copper, Brass, Aluminium etc and its own alloys too. When welded with Aluminium the final specimen can have tensile strength from 130 to 220 MPa, the variation depends upon the welding parameters, and its yield strength is upto 176 Mpa. Similarly the researches shows that when Steel is welded with its own alloys i.e Mild Steel its strength increases up to 160 MPa. Steel

Copper welding also yields ultimate tensile strength up to 166 MPa. There is a great strength that is achieved by having welding of Steel and Brass, its hardness is also very attractive.

II. LITERATURE REVIEW

Liming, Liu Xujing & Shunhua Liu [1] investigated the microstructure of laser welding formed between dissimilar metals i.e Mg alloy and Al alloy with Ce as interlayer and founded elimination of the formed intermetallic phases between aluminum and magnesium alloy. Peng Liu [2] studied microstructure characteristics of welded joint of Mg/Al and deduced the results that micro-hardness near fusion zone of Mg is HM 275-300, and of Al is HM 160-200, and of weld metal is HM 60-100. San-bao Lin [3] studied welding of aluminum alloy to galvanized and recorded that steel zinc coated layer can improve the wettability and spread ability of liquid aluminum filler metal on the surface of the steel when the wetting angle reach less than 20°. J.L song, S.B Lin, C.L Yang, G.C Ma & H.Liu [4] together investigated spreading behavior and microstructure characteristics of aluminium alloy to stainless steel welding and founded that tensile strength of butt joint reached 120MPa. Cracks occur from top part of brittle Fe2Al5 when its thickness exceed 10 µm. Xiaodong Qi [5] investigated Interfacial structure of magnesium alloy and mild steel welding and founded that the shear strength of the joints could reach around 176 MPa, 110% that of base material of Mg alloy whose shear strength is 160 MPa. J. L. Song [6] analyzed the intermetallic layer of aluminium alloy to stainless steel welding and founded that filler (Al,Si)13Fe4 layer presents high crack resistance with tensile strength of 155-175 MPa. R.Borrisutthekul,

P.Mitsomwang, S. Rattanachan& Y. Mutoh [7] studied feasibility of Steel/Aluminum Alloy and concluded that the load resistance of welded zone of joint as higher than that of A1100 aluminum alloy after welding. Liming Liu & Xiaodong Qi [8] investigated strengthening effect of nickel and copper interlayers between the welding of magnesium alloy and mild steel and founded that 160 MPa is the UTSS of base material AZ31B Mg alloy and UTSS of Cu-added joint which is 170 MPa is a little larger than that of Ni-added one that is 166 MPa. R. Borrisutthekula, P. Mitsomwanga, & S. Rattanachana [9] investigated effects of TIG Welding Parameters on welding between Mild Steel and 5052 Aluminum Alloy and founded that at constant heat by increasing arc length increases weld width of lap joint. ZhiZenga, that the welding was feasible, have Better Strength and high hardness. Prashant Kumar Singh, Pankaj Kumar & Rahul Kumar [15] reviewed TIG Welding for optimizing process of SS-304 and MS-1018 and concluded that welding conditions can affected the weld strength and microstructure. L.H. Shah [16] did research on welding of Aluminium 6061 and Galvanized Iron and knew that GI-Al configuration with filler ER4043 can give better mechanical properties. Van Nhat & Nguyen [17] investigated welding of Aluminum Alloys to Stainless Steel and found fracture on the area adjacent between welding seam and A6061 alloys plate which was due to highly applied current. Pooja Angolkar, J. Saikrishna, Dr. R. Venkat & P. Ravikanth Raju [18] investigated welding of SS316 and Monel400 and founded that average hardness was 234 and tensile strength of 200KN. Pushp Kumar & Baghel [19] studied Mechanical properties and microstructural of welding of aluminum alloy 5083 and 6061 and founded that welded joints shows 213MPa ultimate tensile strength and yield Strength of 176 Mpa with rupture at the surface because of excessive or insufficient heat. on welding of 5083 Aluminum Alloy to CuZn34 Brass and founded that the maximum tensile shear strength of aluminum and brass through FSW can be achieved at welding speed of 6.5 mm/min and at 1120 rpm. Caiwang Tan, Liqun Li, Yanbin Chen & Wei Guo [12] investigated welding of AZ31B Mg alloy to Zn coated Steel and found that welded joints shows 68MPa and 52.3% joint efficiency as compared to Mg base metal. A. R. Khalife, A. Dehghan & E. Hajjari [13] investigated joining of AISI 304L/Si37 steels by welding and founded that highest impact energy was 160. Xunbo Li, Yugang Miao, Gang Wu & Zijun Zhao [10] did numerical and experiment analysis of residual stresses on magnesium and steel butt joints and concluded that the residual stress on the 304L steel plate is lower than that on the AZ31B magnesium plate. Mostafa Akbari [11] did research J when welded by ER310 electrode and the lowest impact energy was 120 J when ER309L electrode was used.

J. Pasupathy & V. Ravisankar [14] did detailed Study on welding of Low Carbon Steel with AA1050 and concluded

III. EXPERIMENTAL METHODOLOGY

3.1 Materials:

Three welded samples of dissimilar metals were prepared. The basic materials used were non-ferrous metals such as Copper and Brass and ferrous metals such as mild Steel and Stainless steel plates. According to ASME SECTION IX, the dimensions and the geometry of initial raw materials are given in table1:

Raw Materials	Geometry	Length	Width	Thickness
Copper, Brass, Mild Steel and SS	Plate	240mm	31.7mm	3mm

Table1: Raw Materials and geometry of specimen

3.2 Raw Materials composition:

The raw materials are used in this research are stainless steel SS304, copper C15000, and brass C260 each with a thickness of 3mm and length of 240mm. Chemical composition of raw materials in tabulated form is:

	C	Mn	Si	P	S	Cr	Mo
Steel 304	0.07	2	0.075	0.045	0.030	19.5	-

Table2: Composition of Steel 304 in wt%

Elements	Zr	Cu	Si	P	S	Cr	Mo
Copper C15000	0.02	99.8	-	-	-	-	-

Table3: Composition of Copper c15000 in wt%

Elements	Fe	Cu	Si	Pb	S	Cr	Mo
Brass C260	0.05	71.5	-	0.07	-	-	-

Table4: Composition of Brass c260 in wt%

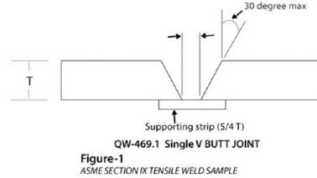
3.3 Pre-Weld treatment of Raw Materials:

As the preparation of raw material is necessary to obtain quality welded joints. So, the raw plates were made to undergo the pre-weld treatment which included cleaning of metal surfaces, removing rust or any other coatings, removing moisture and lowering yield temperature to ensure that the area to be welded is in the best condition.

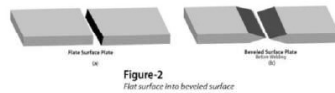
3.4 Welding Requirements:

Joint:

The V butt joint as per ASME SECTION IX is shown below:



Now as per requirements of sample the work piece is sheared in two rectangular parts each of 120mm length by successive machining later on the sharp edges of rectangular parts are removed by machining process to create bevel joint as shown in below figure2.



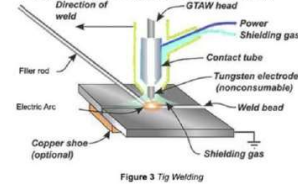
After the cutting action, three different specimens are welded in different manner (stainless steel to copper c15000) using available Argon Tig Welding machine 200amps.

3.5 Welding Parameters:

Current	Voltage	Frequency	Electrode Tip Angle	Welding Speed
125Amps	18V	50Hz	20°	3.8mm/s

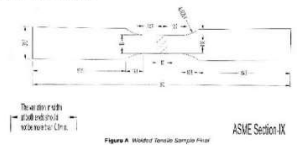
3.6 Filler Rod:

(3.2mm ER70S-6 Mild Steel Filler Rod)



3.7 Cutting Weld Samples Dimensions:

The Tensile samples to be analyzed according to ASME section IX is shown below in Figure A. The length of specimen is taken to be 240mm, and a plate thickness of 3mm.

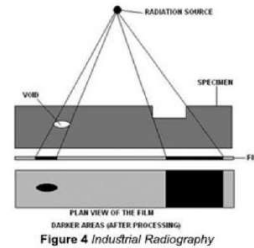


The specimen is divided into two rectangular parts equally, and the welding operation is performed at the center of the specimen. The dimensions of the specimen are taken according to standard to get an optimum result.

IV. ANALYSIS TECHNIQUES EMPLOYED

4.1 Radiography

Radio graphic welding method is one of the most usual non-destructive testing apply to observe gap within in internal shape of welds. The salient advantage of this method is its capability to conduct the weld's internal unification without damaging the welded part. In radiographic testing,X-rays created by X-ray tube or gamma-rays created by a radioactive isotope is utilized.Via jellied entity the perforation radiation proceed onto photographic film, processing the image of entity's internal formation being shove on the film. The amount of energy depends on the solidity and broadness of the entity sponge up by it. Remaining consignment of energy will root vulnerability of the radiographic film. After deployment of film, the area will become dark.



Those area will be lighter which is exposed to less energy. Hatswly, the area of the entity will emerge as dark outlines film where the thickness has been changed due to discontinuities, such as cracks orporosity. Insertion of low solidity(slag) will appear as dark while insertion of high solidity(tungsten) will appear as light area. All discontinuities are distinguished by review shape and variety in thickness of the handled film. Radiographic testing can produce a perpetual film information of weld standard that is comparatively uncomplicated to elucidate by indoctrinate manpower.

This testing technique is generally suited to having ingress to both sides of the welded joint. While this is a ponderous and costly technique of non-destructive testing, it is a constructive technique for perceiving permeability, incretion, crevice, and gaps in the inner of welds. It is necessary that indoctrinate manpower conduct radiographic elucidation since false elucidation of radiographs can be costly and constrain soberly with productivity. There are evident protection deliberation when conducting radiographic

testing. X-ray and gamma radiation is useable to the human eye and can have dangerous health and safety implications. Only suitably instructed and qualified personnel should perform this kind of testing.

4.2 Tensile Testing

Tensile testing is a test in which a specimen is exposed to a supervise tension till failure. Properties that are directly calculated through a tensile test are ultimate tensile strength, breaking strength, maximum elongation and reduction in area. Tensile testing is conducted as it tells how a specimen will behave under normal and extreme forces or stresses providing data for other engineering and quality assurance purposes. Material strength testing, using the tensile tension test technique apply an ever-increasing load on test specimen up to the point of failure. The data created from tensile testing is utilized to find mechanical properties of specimen and provides the following quantitative measurements:

- **Ultimate Tensile Strength (UTS)**, is the maximum tensile stress bear by the specimen, defined as the maximum load divided by the original cross-sectional area of the test specimen.
- **Yield strength** is the stress at which time permanent (plastic) deformation or yielding is observed to begin.
- **Ductility measurements** are typically elongation, defined as the strain at, or after, the point of fracture, and reduction of area after the fracture of the test sample.



Figure 5 Universal Testing Machine(UTS)

The test specimen is gripped between bottom and top chuck universal testing machine which is shown below in Figure 5. During the tension test, the grips are moved apart at a constant rate to tug and extend the specimen. The force on the specimen and its displacement is continuously observed. After the tensile test specimen has broken tensile strength, yield strength and ductility, are calculated by the personnel. The test specimen is place back jointly to quantify the final length, then this measurement is

compared to the starting length to get change in length.



Figure 6 Tensile Testing on UTS MACHINE

V. RESULTS AND DISCUSSION

5.1 Specimen Appearance

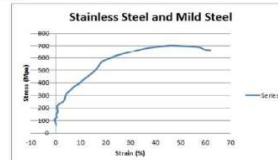
After destruction of specimen, the specimen appearance shows the stress concentrations and mentions the parts of weld where the defects are present. The figure 7 shows the appearance of broken specimen. Stainless steel and brass specimen breaks near the joint from brass side showing that the joint is stronger than the brass. Stainless and mild steel specimen breaks near the joint from stainless steel side showing that the joint is stronger than the stainless steel. The stainless steel and copper specimen breaks at the weld showing that the joint is weak.



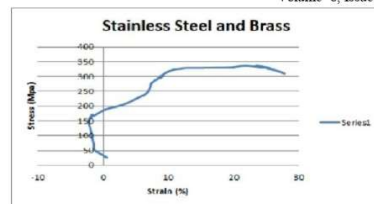
Figure 7 Broken specimen

5.2 Fracture and Mechanical Properties

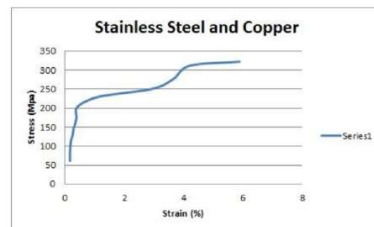
A tensile test was performed on the specimen and the results of test in the form of stress strain curve are shown in Graph 1, Graph 2 and Graph 3. The Graph 1 shows that the ultimate tensile stress (UTS) of stainless steel is 702MPa. The Graph 2 shows that the ultimate tensile stress (UTS) of brass is 338.9MPa. The Graph 3 shows that the ultimate tensile stress (UTS) of stainless steel and copper joint is 322.2MPa. The breaking of stainless steel and copper joint at 322.2MPa shows that the welding is defected.



Graph 1 Stress strain curve for stainless steel and mild steel joint



Graph 2 Stress strain curve for stainless steel and brass joint



Graph 1 Stress strain curve for stainless steel and copper joint

VI. CONCLUSION

In this paper, an attempt was made to investigate the v-joint TIG dissimilar welding of non-ferrous metals such as brass c260, copper c15000 and ferrous metals such as stainless steel, mild steel plates by using tungsten red as filler material. The tensile test performed on the specimen shows that the weld between mild steel and stainless steel (strength=42kN) is stronger than the weld between brass and stainless steel (strength=28kN) and weld between copper and stainless steel (strength=25kN) is lesser. So, it can be concluded that the dissimilar welding between mild steel and stainless steel is more strong. However, this experiment is restricted to only a few specimens and welding parameters. The joint strength can be further enhanced in the future by additional parameter optimization, including other welding variables, using an automated welding machine, as well as proper customized jig fixtures to ensure a better weld quality finish.

ACKNOWLEDGEMENT

Special thanks to Abdullah and Talha for their support.

REFERENCE

- [1] Liu, L., Liu, X., & Liu, S. (2006). Microstructure of laser-TIG hybrid welds of dissimilar Mg alloy and Al alloy with Ce as interlayer. *Scripta Materialia*, 55(4), 383-386.
- [2] Liu, P., Li, Y., Geng, H., & Wang, J. (2007). Microstructure characteristics in TIG welded joint of Mg/Al dissimilar materials. *Materials Letters*, 61(6), 1288-1291.
- [3] Lin, S. B., Song, J. L., Ma, G. C., & Yang, C. L. (2009). Dissimilar metals TIG welding-brazing of aluminum alloy to galvanized steel. *Frontiers of Materials Science in China*, 3(1), 78-83.
- [4] Song, J. L., Lin, S. B., Yang, C. L., Ma, G. C., & Liu, H. (2009). Spreading behavior and microstructure characteristics of dissimilar metals TIG welding-brazing of aluminum alloy to stainless steel. *Materials Science and Engineering: A*, 509(1-2), 31-40.
- [5] Qi, X., & Song, G. (2010). Interfacial structure of the joints between magnesium alloy and mild steel with nickel as interlayer by hybrid laser-TIG welding. *Materials & Design*, 31(1), 605-609.
- [6] Song, J. L., Lin, S. B., Yang, C. L., Fan, C. L., & Ma, G. C. (2010). Analysis of intermetallic layer in dissimilar TIG welding-brazing butt joint of aluminum alloy to stainless steel. *Science and Technology of Welding and Joining*, 15(3), 213-218.
- [7] Bornisutthekul, R., Mitsomwang, P., Rattanachan, S., & Mutoh, Y. (2010). Feasibility of using TIG welding in dissimilar metals between steel/aluminum alloy. *Energy Research Journal*, 1(2), 82-86.
- [8] Liu, L., & Qi, X. (2010). Strengthening effect of nickel and copper interlayers on hybrid laser-TIG welded joints between magnesium alloy and mild steel. *Materials & Design*, 31(8), 3960-3963.
- [9] Bornisutthekula, R., Mitsomwanga, P., & Rattanachana, S. (2010). Effects of TIG Welding Parameters on Dissimilar Metals Welding between Mild Steel and 5052 Aluminum Alloy.
- [10] Zeng, Z., Li, X., Miao, Y., Wu, G., & Zhao, Z. (2011). Numerical and experiment analysis of residual stress on magnesium alloy and steel butt joint by hybrid laser-TIG welding. *Computational Materials Science*, 50(5), 1763-1769.
- [11] Akbari, M., & Behnagh, R. A. (2012). Dissimilar friction-stir lap joining of 5083 aluminum alloy to CuZn34 brass. *Metallurgical and Materials Transactions B*, 43(5), 1177-1186.
- [12] Tan, C., Li, L., Chen, Y., & Guo, W. (2013). Laser-tungsten inert gas hybrid welding of dissimilar metals AZ31B Mg alloys to Zn coated steel. *Materials & Design*, 49, 766-773.
- [13] Khalifeh, A. R., Delghau, A., & Hajjan, E. (2013). Dissimilar joining of AISI 304L/S37 steels by TIG welding process. *Acta Metallurgica Sinica (English Letters)*, 26(6), 721-727.
- [14] Pasupathy, J., & Ravisankar, V. (2013). Detailed study on dissimilar welding of low carbon steel with AA1050 using TIG welding. *Int. J. Eng. Res. Tech.*, 2(11), 1588-1594.
- [15] Singh, P. K., Kumar, P., Singh, B., & Singh, R. K. (2015). A review on TIG welding for optimizing process parameters on dissimilar joints. *Int. J. Eng. Res. Appl.*, 5(2), 125-89.
- [16] Shah, L. H., Mohamad, U. K., Yaakob, K. I., Razali, A. R., & Ishak, M. (2016). Lap joint dissimilar welding of aluminum AA6061 and galvanized iron using TIG welding. *Journal of Mechanical Engineering and Sciences*, 10, 1817-26.
- [17] Nguyen, V. N., Nguyen, Q. M., Thao, H., Thi, D., & Huang, S. C. (2017). An Investigation of Dissimilar Welding Aluminum Alloys to Stainless Steel by the Tungsten Inert Gas (TIG) Welding Process. In *Materials Science Forum* (Vol. 904, pp. 19-23). Trans Tech Publications Ltd.
- [18] Angolkar, P., Saikrishna, J., Reddy, R. V., & Raju, P. R. (2017). Experimental Analysis of Dissimilar Weldments Ss316 And Monel400 in Gtaw Process. *International Journal of Engineering Research and Development*, 13, 39-46.
- [19] Baghel, P. K., & Nagesh, D. S. (2018). Mechanical properties and microstructural characterization of automated pulse TIG welding of dissimilar aluminum alloy.

VITAE

Name Mr. Roman Kalvin
Student ID 6110130027

Educational Attainment

Degree	Name of Institution	Year of Graduation
Bachelor of Engineering (Mechanical Engineering)	University of Wah, Wah Cantt Pakistan	2013
Master of Science (Mechanical Engineering)	University of Wah, Wah Cantt Pakistan	2017

Scholarship Awards during Enrolment

1. IGS-Energy Scholarship award for PhD studies.

List of Publication and Proceedings

1. Roman Kalvin et al. (2021). "Fabrication of Catalytic Converter with Different Materials and Comparison with Existing Materials in Addition to Analysis of Turbine Installed at the Exhaust of 4 Stroke SI Engine". *Sustainability*.2021;13(18):10470.<https://doi.org/10.3390/su131810470>. IF 3.25
2. Roman Kalvin et al. (2021). "Investigation of Chip Formation and its Grain Structure using Vegetable Oil Based Lubricants". *Journal of Advanced Research in Fluid Mechanics and Thermal Sciences*, 84(2), 92–97
3. Roman Kalvin et al. (2021). "Aerodynamics Analysis and Range Enhancement Study of 81mm Mortar Shell (French Design)". *Journal of Advanced Research in Fluid Mechanics and Thermal Sciences*, 84(1), 148–159.
4. Roman Kalvin et al. "Design and Fabrication of Under Water Remotely Operated Vehicle". *Journal of Advanced Research in Fluid Mechanics and Thermal Sciences*, 82(1), 133–144 -2021
5. Roman Kalvin et al. "Effect of Refrigeration Assisted Intercooler Turbocharging on Engine's Horse Power". *Journal of Advanced Research in Fluid Mechanics and Thermal Sciences*, 79(2), 95-111, March-2021.
6. Roman Kalvin et al. "Cooling Load Estimation of Auditorium by CLTD Method and its Comparison with HAP and TRACE Software" *Pakistan Journal of Engineering and Technology*, Volume 4, Issue 1, Page # 18-25, March-2021.
7. Roman Kalvin et al. " Investigation of Dissimilar V-Joint of Steel Alloys with Copper and Brass using Tig Welding" *International Journal of Mechanical and Production Engineering*, ISSN(p): 2320-2092, ISSN(e): 2321-2071 Volume-8, Issue-8, Aug.-2020
8. Roman Kalvin "Comparison of ICE's, BEV's, HEV's and FCV's and their Future Prospective" 2nd International Congress on Engineering and

- Architecture, pp. 1035-1055, 22-24 April 2019, Marmaris Turkey.
9. Roman Kalvin "Design and Analysis of Propeller Shaft of an Automobile Using Composite Materials " 2nd International Congress on Engineering and Architecture, pp. 1022-1034, 22-24 April 2019, Marmaris Turkey.
 10. Roman Kalvin "Chip Analysis of Mild Steel Under Different Operating Parameters" 2nd International Congress on Engineering and Architecture, pp. 1011-1021, 22-24 April 2019, Marmaris Turkey.
 11. Roman Kalvin "To Compare Rolling Force, Torque and Power of pure Aluminium and Stainless Steel in Cold Rolling Process" International Journal of Scientific and Engineering Research, Volume 10, Issue 4, April-2019, Page # 1186-1189, ISN 2229-5518.
 12. Roman Kalvin " Fluctuations in Chip Formation with alterations in cutting conditions during turning operation using Aluminium 6061" International Journal of Scientific and Engineering Research, Volume 10, Issue 4, April-2019, Page # 1190-1193, ISN 2229-5518.
 13. Roman Kalvin et. al. "Modification and Performance Analysis of 4 Stroke Engine to 6 Stroke Engine", International Journal of Mechanical and Production Engineering (IJMPE, 2019), pp. 16-20, Volume-7, Issue-2
 14. Roman Kalvin "Stress Analysis of Spider Gear using Structural Steel on ANSYS " International Journal of Aerospace and Mechanical Engineering, Volume 12, Issue 9, 2018, Page # 920-923.
 15. Roman Kalvin " Stress Analysis of Turbine Blades of Turbocharger using Structural Steel" International Journal of Aerospace and Mechanical Engineering, Volume 12, Issue 9, 2018, Page # 929-932.
 16. Roman Kalvin " Design and Implementation of Power Generation Mechanism using Speed Breaker " International Journal of Scientific and Engineering Research, Volume 9, Issue 6, June-2018, Page # 1586-1590, ISN 2229-5518.
 17. Roman Kalvin, et al." Performance Analysis of different configurations of Heating and Cooling for a Multizone Building" International Journal of Renewable Energy Technology, February-2018, IF-1.97
 18. Roman Kalvin, et al." Simulation of Four Stroke IC Engine" International Journal of Scientific and Engineering Research, Volume 7, Issue 2, February-2016, Page # 1212-1219, ISN 2229-5518.
 19. Roman Kalvin et. al. "Impact Analysis Of Cultivation Of Jatropha Tree on Fuel Prices and Environment" International Journal of Energy and Power Engineering, Bangkok Thailand, Vol:12 No:2 ,2018
 20. Roman Kalvin et. al. "Energy Analysis of Seasonal Air Conditioning Demand of all Income Classes using Bottom Up Model in Pakistan " International Journal of Energy and Power Engineering, Bangkok Thailand, Vol:12 No:2 ,2018
 21. Roman Kalvin et al. "Performance analysis and fabrication of power generating shock absorber"," Journal of Expert opinion on Environmental biology" , ISSN: 2325-9655 ,Volume 7, 2018.